Norwegian University
of Life Sciences

Master's Thesis 2021 60 ECTS

Faculty of Environmental Sciences and Natural Resource Management
Ole Christian Lind

Biodistribution of Radionuclides in reindeer from Vågå, Norway

Kaveh Nikouee

Master of Science in Radioecology
Faculty of Environmental Sciences and Natural Resource Management

Contents

List of abbreviations 3
INTRODUCTION 4
OBJECTIVES AND HYPOTHESES 8
Theory 9
Radioactivity 9
Elements 9
^{137}Caesium 9
^{210}Polonium 11
Radiation Dosimetry 12
The ICRP Dosimetric Approach 13
Rangifer tarandus tarandus and physiological traits 14
EXPERIMENTAL 15
Study area 15
Samples and sampling 17
Method and instrumentation 19
Instrumentation 19
UltraClave 19
Scintillation detector 20
Sample preparation for gamma-screening 21
^{137}Cs-analysis 22
Alpha spectrometry 23
Sample preparation for ^{210}Po-measurement 25
^{210}Po-analysis 27
^{210}Pb-analysis 28
DATA TREATMENT 29
Mass estimation 29
Whole body concentration and $CR_{wb:t}$ 29
Internal DCs 30
Estimated absorbed dose rates. 31
QUALITY ASSURANCE 32
^{137}Cs-analysis 33
^{210}Po-analysis 34
RESULTS AND DISCUSSION 34

Radionuclide analyses 35
Comparison with literature 37
Distribution of accumulation and estimated whole body concentration 49
Estimated Dose rates 50
Comparison of external and internal absorbed dose 55
CONCLUSIONS 55
References 55
APPENDIX A 66
APPENDIX B 69
APPENDIX C 75
APPENDIX D 78
APPENDIX E 79
APPENDIX F 82
APPENDIX G 85

ACKNOWLEDGEMENTS

I would like to express an insurmountable amount of gratitude to my main supervisor Ole Christian Lind, for a character with more patience life has yet to prove. A special thanks to my co-supervisors Lavrans Skuterud and Lindis Skipperud as well as Tom Hinton for the feedback and help. Also, a special thanks to Marit Nandrup Pettersen, Karl Andreas Jensen, Solfrid Lohne and Yetneberk Ayalew Kassaye, for support and technical guidance in the laboratory. I would also like to thank Brit Salbu and Knut Hove for assisting in the field work. All seated in my hall of giants, on the shoulders from which this chemist was kept from drowning in the vast ocean that is radioecology. A thanks to Simon Mark Jerome and Estela Reinoso Malet for taking their time to help a panic-stricken soul dealing with the distorted sense of humor alpha-spectrometers occasionally have. And of course, Emil Jarosz, Alexander Sverdrup Aarsand and Halvor Stensrød for the company in the laboratory. Finally, a gratitude which no language to my knowledge can sufficiently express to my friends and family, (you know who you are).

“I love deadlines. I like the whooshing sound they make as they fly by.” – D.A.

ABSTRACT

Purpose: To characterize the biodistribution and internal exposure of ChNPP Cs-137 and the naturally occurring Po-210 in semi-domesticated reindeer in southern Norway.

Materials and method: Semi-domesticated reindeer were gathered during the seasonal autumn slaughter from Vågå herding district. Samples were screened for Cs-137 utilizing NaI-solid scintillation detector before pre-treatment for Po-210 analysis with the use of alpha-spectrometry. Internal exposure was assessed by modelling organs and tissues as aquatic organisms with DCs obtained from BiotaDC software. Internal absorbed doses were compared to external doses given by previous studies from the same herd.

List of abbreviations

CERAD – Center for Environmental Radioactivity

NMBU – Norwegian University of Life Sciences

DSA – Norwegian Radiation and Nuclear Safety Authority

ICRP – The International Comission on Radiological Protection

ChNPP – Chernobyl Nuclear Power Plant

CPS – Counts per second

CPM – Counts per minute

DPM – Disintegrations per minute

MLV – Myocardium, Left Ventricle

MRV – Myocardium, Right Ventricle

LL – Left Lung

RL – Right Lung

RC – Rumen Content

ILN – Intestinal Lymph Node

HT – Hemispheral Tissue

BS – Brain Stem

FT – Fallopian Tube

LV – Lumbar Vertebrae

BM – Bone Marrow

MT – Molar Tooth

QF – Quadriceps Femoris

LD – Longissimus Dorsii

BB – Biceps Brachii

RBC – Red Blood Cells

BP – Blood Plasma

ST – Skeletal Tissue

MM – Muscular Tissue

DUS – The Digestive and Urinary System

CRS – The Circulatory and Respiratory System

EES – The Endocrine and Exocrine System

CNS – The Central Nervous System

RPS – The Reproductive System

MS – The Muscular System

SS – The Skeletal System

IGS – The Integumentary System

INTRODUCTION

Life on earth has evolved under constant exposure to radioactivity, be it from natural sources such as primordial radionuclides in the ground or radionuclides produced in the

atmosphere from bombardment of cosmic radiation (DSA, 2015). The naturally occurring radionuclides ^{210}Pb and ^{210}Po are part of the natural decay chain of the primordial radionuclide ^{238}U. While ^{238}U are primarily trapped in the ground, its progeny ^{222}Rn, being a gas, emanates from the ground releasing its progenies, ^{210}Pb and ^{210}Po, to the atmosphere where inhalation or ingestion from plants with previously deposited ^{210}Pb and ^{210}Po are possible pathways into organisms (Moore et al., 1976; Lavrans Skuterud, Gwynn, et al., 2005). These pathways are dependent on the form or speciation of radionuclides which in turn depends on its release scenario and subsequent interactions with its surroundings along its pathway. This in turn dictates its transport, uptake and biodistribution (B. Salbu et al., 2004).

With the advent of the nuclear technologies, anthropogenic sources include atmospheric nuclear weapon testing as well as accidental or routine release from nuclear fuel cycles (IAEA, 2011). The most notable incident occurred in 1986, Ukraine, where a series of unfortunate events resulted in an explosion and subsequent fires lasting for 10 days at the Chernobyl nuclear power plant (ChNPP) releasing unprecedented amounts of radioactivity into the atmosphere. Through atmospheric transport and subsequent precipitation the severity of the accident were not reserved for the immediate surrounding area, consequently spreading radioactive material throughout Europe reaching as far as the Scandinavian Peninsula (Anspaugh, 2008; Henriksen, 1988).

It was estimated that 6 % of the total ^{137}Cs and ^{134}Cs released from the Chernobyl accident were deposited in Norway (*Backe1987 Fall-out Pattern in Norway after the Chernobyl Accident Estimated from Soil Samples.Pdf*, n.d.). The consequence of this were evident for reindeer herders where ^{137}Cs activity concentrations in reindeer meat far exceeded the intervention limit set by the authorities resulting in the condemnation of several hundred tons of meat in the following years (Brynildsen et al., 1996). Despite the countermeasure initiatives set by the authorities, ^{137}Cs levels still surpass the current intervention limit of 3000 Bq/kg (Lavrans Skuterud, 2005). In addition, ^{137}Cs levels in the ecosystem has been shown to be more persistent than originally hypothesized (Gaare & Staaland, 1994; Lavrans Skuterud, Gaare, et al., 2005). And thus, it has been stated that the reduced decline may lead to reduced seasonal differences which in turn might have

consequences for the ongoing application of countermeasures against ^{137}Cs contamination in reindeers (Lavrans Skuterud, 2005).

It is well established that caribou and reindeer have a high propensity for uptake of anthropogenic and naturally occurring radionuclides, (Tracy, 2012), thought to be partly because of their nomadic lifestyle, diet composition, physiological traits as ruminants and the vulnerable arctic/alpine environment which is their natural habitat (AMAP, 1998). It is believed that lichens are an important dietary factor regarding the transfer of radionuclides to reindeer and caribou. Lacking a root system, absorbing nutrients primarily from the air, having a large surface area to mass ratio, lifetime of decades and the general slow vegetation turnover and short growth season of northern environments make lichen efficient at accumulating and retain pollutants from ambient air over time (Tracy, 2012).

Despite the exposure from anthropogenic nuclear sources, radionuclides derived from natural sources are thought to be the main contributor to internal doses in both humans and animals (F. Carvalho et al., 2017). As a result, the Lichen – Reindeer – Man (L-R-M) pathway has been subject to extensive investigation (Aarkrog, 1994; B. Åhman, 1994; G. Åhman et al., 1990; Allaye-Chan et al., 1990; Aramrun et al., 2019; Beasley & Palmer, 1966; Bergman et al., 1993; Bird, 1968; Blanchard & Kearney, 1967; Gaare, 1987; Gaare & Staaland, 1994; Garner & Comar, 1972; W. C. Hanson, 1967; W. C. Hanson & Palmer, 1965; Wayne C. Hanson, 1966; Fredrik Henricsson & Persson, 2012; Holleman et al., 1971, 1990; Holtzman, 1966; Kauranen & Miettinen, 1969; Lidén & Gustafsson, 1966; C. R. Macdonald et al., 1996; Colin R. Macdonald et al., 2007; Mattsson, 1972; Mattsson & Persson, 1971; Mayes et al., 1996; MIETTINEN & HÄSÄNEN, 1967; O'Hara et al., 1999; Paatero & Salminen-Paatero, 2020; Pálsson et al., 1994; B. R. R. Persson et al., 2018a; R. B. R. Persson, 1969, 1974; Rahola & Miettinen, 1973; Rissanen et al., 1990; Robillard et al., 2002; Salmon et al., 1995; Skogland, 1986; L Skuterud et al., 2016; Lavrans Skuterud, 2005; Lavrans Skuterud et al., 2014; Lavrans Skuterud, Gwynn, et al., 2005; Solatie et al., 2006; Svensson & Lidén, 1965; D. J. Thomas et al., 1992; Patricia A. Thomas & Gates, 1999; White et al., 1986). The main contribution to the vulnerability of this pathway is believed to be the high accumulation of ^{137}Cs and $^{210}Pb/^{210}Po$ in lichen (Sheppard, 2011).

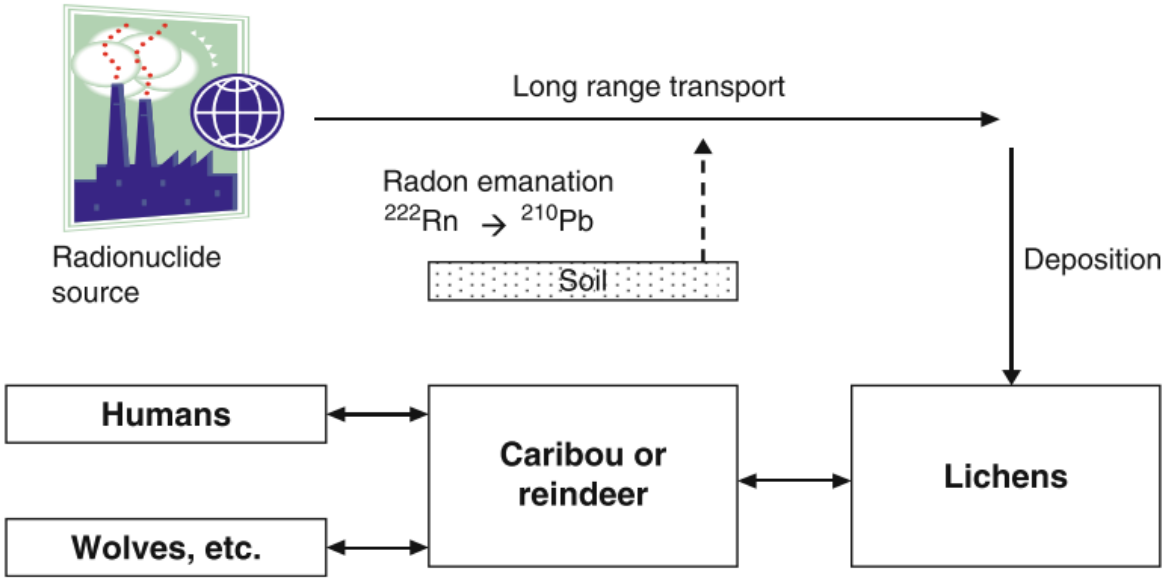

Figure 1: A simplified representation of radionuclide pathways in the reindeer/caribou ecosystem (Tracy, 2012).

Several methods for modelling radionuclide transfer, distribution and dose contribution has been employed for risk assessment purposes, however, estimated components utilized as parameters in models have inherent uncertainties (Brit Salbu, 2016). Dynamic modelling, alleviates some of these uncertainties but are dependent on existing data on radionuclide concentrations for input (B. R. R. Persson et al., 2018b). Also, most assessments are focused on human exposure as an endpoint while relatively few have investigated the potential health effects to non-human biota (C. R. Macdonald et al., 1996).

An understanding of the mechanisms affecting the behavior of radionuclides in animals would contribute to better interpret monitoring results, a more accurate prediction of activity concentration in animal tissues and develop better, flexible and more realistic models (Calmon et al., 2009; Ulanovsky & Pröhl, 2012).

OBJECTIVES AND HYPOTHESES

The present study was conducted to quantify and characterize the distribution of ChNPP derived ^{137}Cs and naturally occurring ^{210}Po within various tissues of semi-domesticated reindeer from Vågå herding district, estimate and compare dose rates in specific tissues and the whole body and contribute to existing data sets, hoping to shed light on potential challenges for future assessments.

The hypotheses are as following:

- The internal absorbed dose from the naturally occurring ^{210}Po exceeds the internal dose from ChNPP derived ^{137}Cs by a factor of 10.
- The biggest contribution of the total dose is from internally incorporated ^{210}Po and ^{137}Cs.

To address the objectives and hypotheses a range of organs and tissues will be extracted from three semi-domesticated reindeers as well as tissues from seven additional reindeeer heads for radionuclide analysis, utilizing Na(Tl)-scintillation detector for screening of ChNPP derived ^{137}Cs, determining ^{210}Po activity levels with isotope dilution alpha spectrometry

(ISAD). Estimation of dose rates will be performed with BiotaDC software to finally estimate and characterize the distribution of investigated radionuclides as well as the distribution of dose contribution within the reindeers.

Theory

Radioactivity

Radioactivity or ionizing radiation is the process where the emission of energy in the form of elementary particles resulting from the spontaneous decay of an unstable atomic nucleus also known as radionuclides. The term 'ionizing' refers to the radiation energy being sufficient to knock an electron out of orbit from an atomic shell, i.e. ionizing an atom. Ionizing radiation may be in the form of α-, β- and γ-particles as well as neutrons emitted directly from the nucleus or auger electrons and x-ray photons from the atomic electron shells. Following a decay event, the radionuclide transforms into another element, a decay product. When the decay product itself is a radionuclide it is said that the radionuclides are part of a decay chain or decay series (Lehto & Hou, 2010).

Elements

The present work focuses on the anthropogenic ChNPP derived radionuclide ^{137}Cs and the naturally occurring radionuclide ^{210}Po internally incorporated in semi-domesticated reindeer from Vågå herding district.

^{137}Caesium

Stable ^{133}Cs, an alkali metal discovered by Robert Bunsen and Gustav Kirchhoff in 1860, it's found in minerals like pollucite and lepidolite. The radioactive isotope ^{137}Cs is produced spontaneously when other radioactive materials such as uranium and plutonium absorb neutrons and undergo fission (Kilde1). It is therefore a common by-product from aboveground testing of nuclear weapons, routine discharges from nuclear installations and nuclear accidents. As illustrated in figure 2, it's a β-emitter, however it's

more practical to measure the γ-emission of its metastable progeny, ^{137m}Ba (Smith & Beresford, 2006). ^{137}Cs has gained a lot of attention in radioecological aspect partly due to its relatively long half-life, persistence in various ecosystems and suggested long-term environmental mobility (Reinoso-Maset et al., 2020; Lavrans Skuterud, Gaare, et al., 2005; D. J. Thomas et al., 1992).

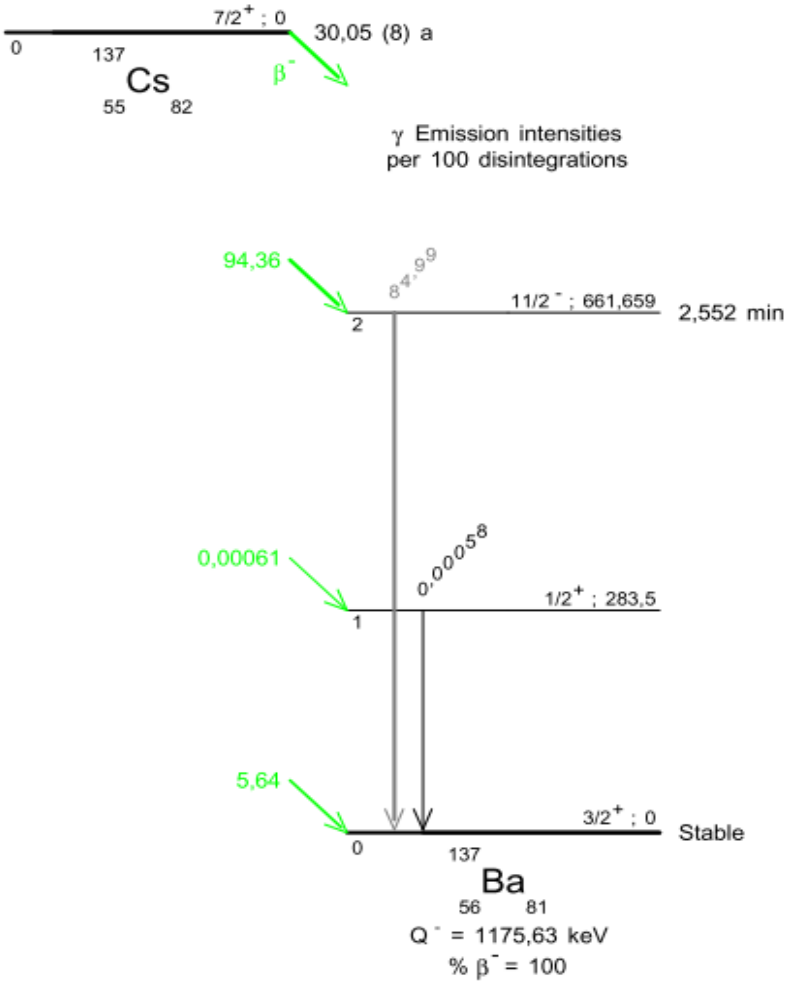

Figure 2: The decay scheme for ^{137}Cs (Helmer & Chechev, 2007).

In the nuclear fuel cycle, it exists as the weakly hydrated cation Cs^+, which is relatively mobile in the environment and highly bioavailable but is readily trapped by fixation in certain sediments and soils through precipitation (Nash & Braley, 2011). Being an alkali metal, its chemical analog is K and are readily taken up by flora and fauna, where it more or less is uniformly distributed throughout the organism (Tracy, 2012).

^{210}Polonium

Polonium was discovered by Marie and Pierre Curie in the late 1800s and was named after Marie's home country, Poland (IAEA, 2006). There are 33 known isotopes of polonium, of which, seven are naturally occurring where ^{210}Po, mainly an α-emitter, is of radioecological interest. It's a silvery-grey soft metal and fairly volatile with a relatively long half-life of 138 days and high specific activity of 1.66 x 10^{14} Bq/g. ^{210}Po exists naturally in trace amounts in both the soil and air, originating from the natural decay series of ^{238}U, figure 3, its distribution to the environment is generally considered in this context. However, several separation processes in nature such as radon migration from the soil or volatilization from volcanic vents, the long term distribution of ^{210}Po is mainly controlled by its parent ^{210}Pb (F. Carvalho et al., 2017).

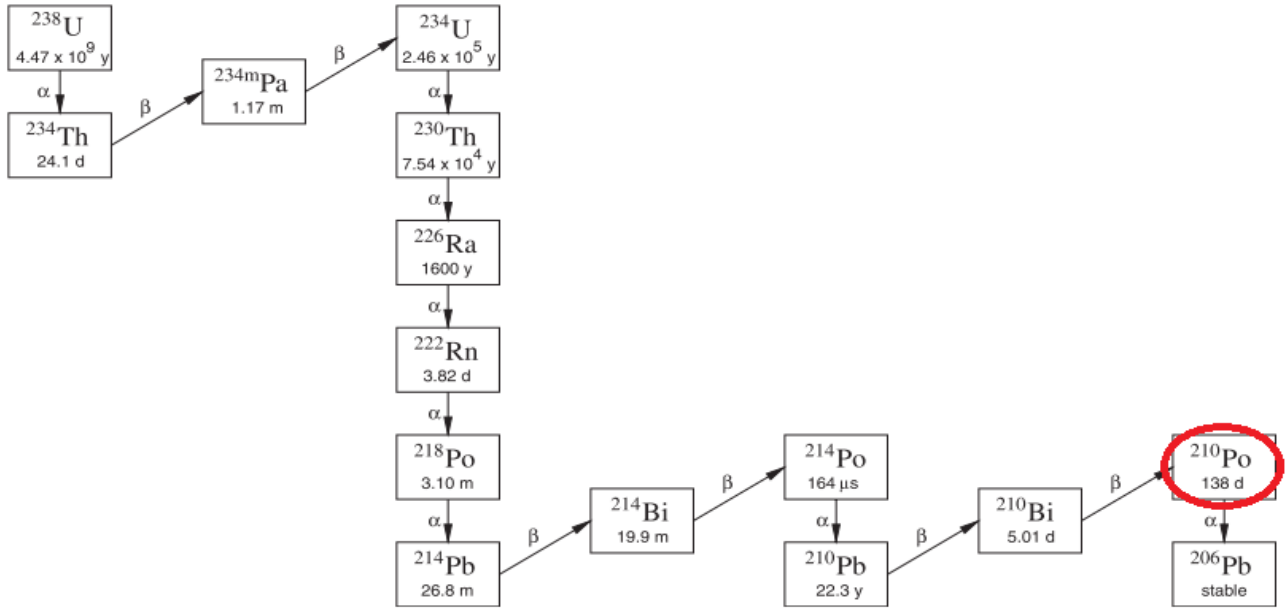

Figure 3: The ^{238}U decay series, ^{210}Po is highlighted with a red circle. (Matthews et al., 2007)

As Po belongs to the chalcogen group, it is considered to have physical and chemical characteristics as the metalloids. Stable oxidation states of -2, +2, +4, +6 have been predicted based on analogy with Selenium (Se) and Tellurium (Te). With +4 being the most stable under oxic freshwater conditions and +2 in reducing conditions (F. Carvalho et al., 2017). Being a pure alpha-emitter, its measurement is not possible without relatively

expensive and time-consuming methods. Consequently, not much is known about the biokinetics of ^{210}Po except that it accumulates in certain soft tissues like kidney and liver. It is, however, believed to have an affinity toward Sulphur (S) containing amino acids like cysteine or cysteine rich proteins like metallothionein. It is also believed to accumulate in a similar fashion as Selenium (Se) as selenocysteine. (Calmon et al., 2009).

Radiation Dosimetry

A key quantity in expressing exposure to ionizing radiation is the absorbed dose defined as the amount of energy absorbed per unit mass of tissue from the ambient radiation field (Copplestone et al., 2001). It is given in units of Gray (Gy), an equivalent of J/kg, and is derived by utilizing dose coefficients (DC) relating activity concentrations in the body or in the environment of an organism to an absorbed dose rate (µGy/h). The DCs are expressed as a dose rate per unit mass (Bq/kg) for internal exposure and for external exposure it can be expressed as either per unit mass (Bq/kg), surface (Bq/m^2) or volume (Bq/L or Bq/m^3) (E. Vano, D.L. Miller, C.J. Martin, M.M. Rehani, 2015).

Depending on radiation type, equal absorbed doses, does not necessarily mean equal effects in biological tissue, where α-radiation deposits its energy over a shorter distance than β- and γ-radiation. It is said that α-particles have a high linear energy transfer (LET), while β and γ-radiation have low LET (Copplestone et al., 2001). There are two categories of effects; deterministic effects are related to cell death leading to organ and or tissue failure as well as stochastic effects, which is the damage of the genetic material from chronic exposure possibly leading to carcinogenesis and mutagenesis. Of the two, the latter has been of main concern with current environmental dose levels regarding exposure to individual humans. While for non-human biota, the radiological protection endpoint is based on effects affecting the population.

In humans, the concept of the equivalent dose was introduced to account for the difference in radiation quality to specific protection endpoints by weighting the absorbed dose with a radiation weighting factor (w_R) (E. Vano, D.L. Miller, C.J. Martin, M.M. Rehani, 2015). For non-human biota the appropriate w_R is still under debate owing to the difference

in radiological protection endpoint, however, a w_R of 10 have been suggested in the assessing deterministic effects for populations, (Chambers et al., 2006; Higley et al., 2012).

The ICRP Dosimetric Approach

The International Commission on Radiological Protection (ICRP) introduced the concept of Reference Animals and Plants (RAP) to gather a consistent data set on the relationship between dose and effects. By using the datasets as reference to the estimated doses of the studied organism, termed as the representative organism (RO), the effects can be assessed in an environmental context. The dose rates are evaluated by comparison to a set of derived consideration reference levels (DCRLs), which are bands of dose rates where there is a probability of detrimental effect in a particular RAP (E. Vano, D.L. Miller, C.J. Martin, M.M. Rehani, 2015).

Complementing this approach is the BiotaDC software tool, developed by A. Ulanovsky and A. Ulanowski, an open-access web-based application performing DC calculations for non-human biota (http://biotadc.icrp.org/). It's related by methodology and data developed in recent projects such as FASSET and ERICA. Originally meant for internal and external exposures of aquatic organisms, the analytical approximation has been extended to estimate DCs for internal exposure of terrestrial animals and plants, treating organs as aquatic organisms (Lecomte et al., 2015; Ulanovsky & Pröhl, 2012). It operates under the assumption of the uniform isotropic model, i.e. elemental composition and density of the organism is close to that of its surrounding medium with the accompanied assumption of homogenously distributed radiation sources throughout the body of the organism (Pröhl et al., 2008). The resulting DCs are accompanied with fraction factors, making it possible to differentiate between radiation types, such as α-particles and spontaneous fission fragments (f1), low energy (<10 keV) electrons and β-particles (f2), as well as high energy (≥10 keV) electrons and photons, (f3). In addition, the internal DCs can be weighted for the absorbed fraction, defined as the fraction of energy absorbed within the target tissue for the various radiation types. A schematic representation of the DC calculation methodology for non-human biota is shown in figure 4.

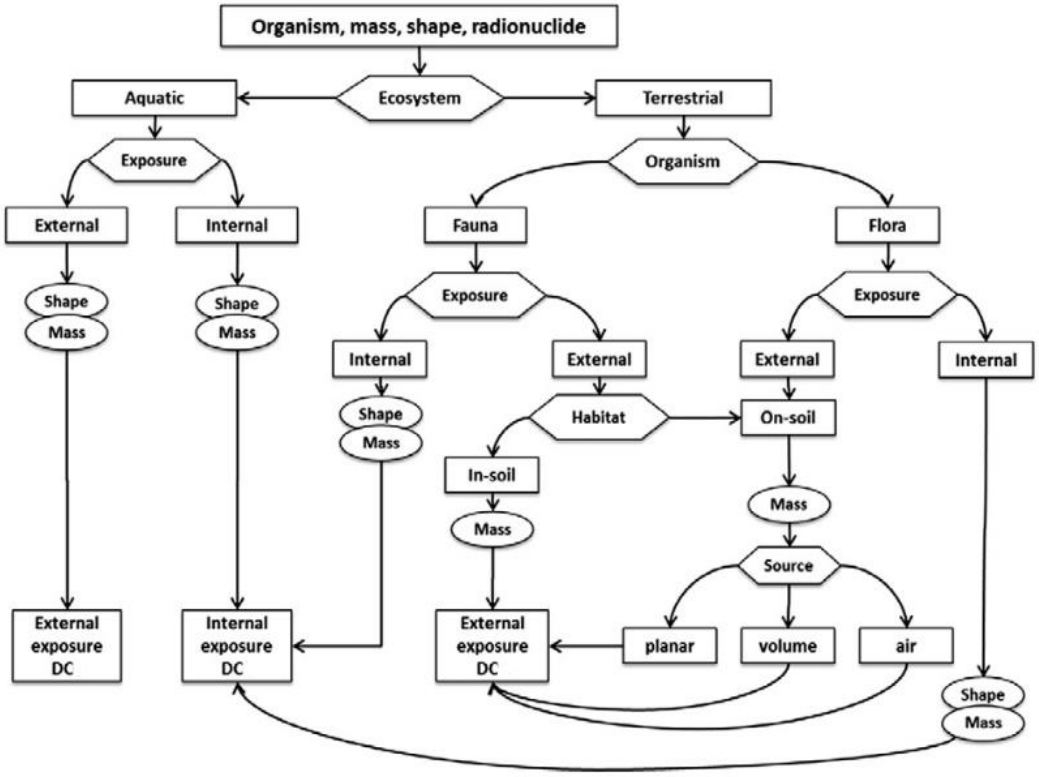

Figure 4: Schematic of computation of DC for non-human biota, depending on organism properties, environment, habitat and radiation source (Ulanovsky & Pröhl, 2012).

Rangifer tarandus tarandus and physiological traits

The Norwegian reindeer, *Rangifer tarandus tarandus*, is a subspecies of *Rangifer tarandus* which is a member of the Cervidae family. They are native to western Fennoscandia where they live a nomadic lifestyle, covering up to 5000 km per year when grazing and or migrating. Their diet is dependent on season and availability. Generally subsisting on lichens, mosses and a wide variety of vascular plants throughout the year, while lichen is usually the main component in the reindeers' diet during winter months (Lavrans Skuterud, 2005; Tracy, 2012). Both male and female reindeer grow antlers which they shed annually. Teeth is regenerated continuously throughout their lifespan which is unique to ruminants as well as their unique digestive anatomy; starting with the mouth and esophagus, feed enters a three-compartment forestomach (rumen, reticulum and omasum) and a true stomach (abomasum). In the first two, masticated vegetation gets fermented by gastrointestinal (GI) microflora in an anaerobic reducing environment, generating volatile

fatty acids (VFA) which is absorbed directly from the rumen. Entering the omasum, water is absorbed, and feed particle size are reduced before continuing into the abomasum where enzymatic digestion takes place. These conditions could potentially result in radionuclide speciation changes and consequently its bioavailability and uptake. Further on, semi-digested feed enters the small intestine which is divided into three parts, duodenum, jejunum and ileum. Pancreatic juices are secreted in duodenum and nutrients are absorbed via enzymatic absorption throughout the small intestine. The large intestine consists of caecum, colon and rectum. Some absorption of VFA takes place in the caecum, while water and salts are absorbed in the colon before being stored in the rectum as feces (Calmon et al., 2009; Underwood et al., 2015).

EXPERIMENTAL

Three reindeer had been previously procured by the Norwegian university of life sciences (NMBU) from the Vågå herding company. The collection and sampling occurred during the seasonal autumn slaughter, 18th-20th of September 2019. Sample containers and vials were prepared at the Isotope laboratory, NMBU prior to sampling.

Study area

Vågå herding district is located in the mountainous parts of southern Norway. It's botanically classified as continental ''indifferent section'' with a total annual precipitation varying between 280- 1200 mm. It's home to a herd of approximately 2000 semi-domesticated reindeer utilizing a grazing area that spans beyond the southern municipal

borders of Vågå, covering approximately 1360 km^2, (61° 18’ 28’’– 61° 51’ 05’’ N, 8° 10’ 44’’- 9° 30’ 42’’ E), between 1000 and 1600 meters above sea level (m.a.s.l). The grazing area is defined to lie in the northern boreal and alpine vegetation zones, the low alpine zone starting at about 1200 m.a.s.l. Most parts of the year they graze in the southern and south-eastern parts except in winter where they migrate to the northern parts where there is less snow and higher availability of lichen. Figure 5 shows deposition densities of ^{137}Cs of Norway highlighting the grazing area (Aramrun et al., 2019; Lavrans Skuterud, Gaare, et al., 2005).

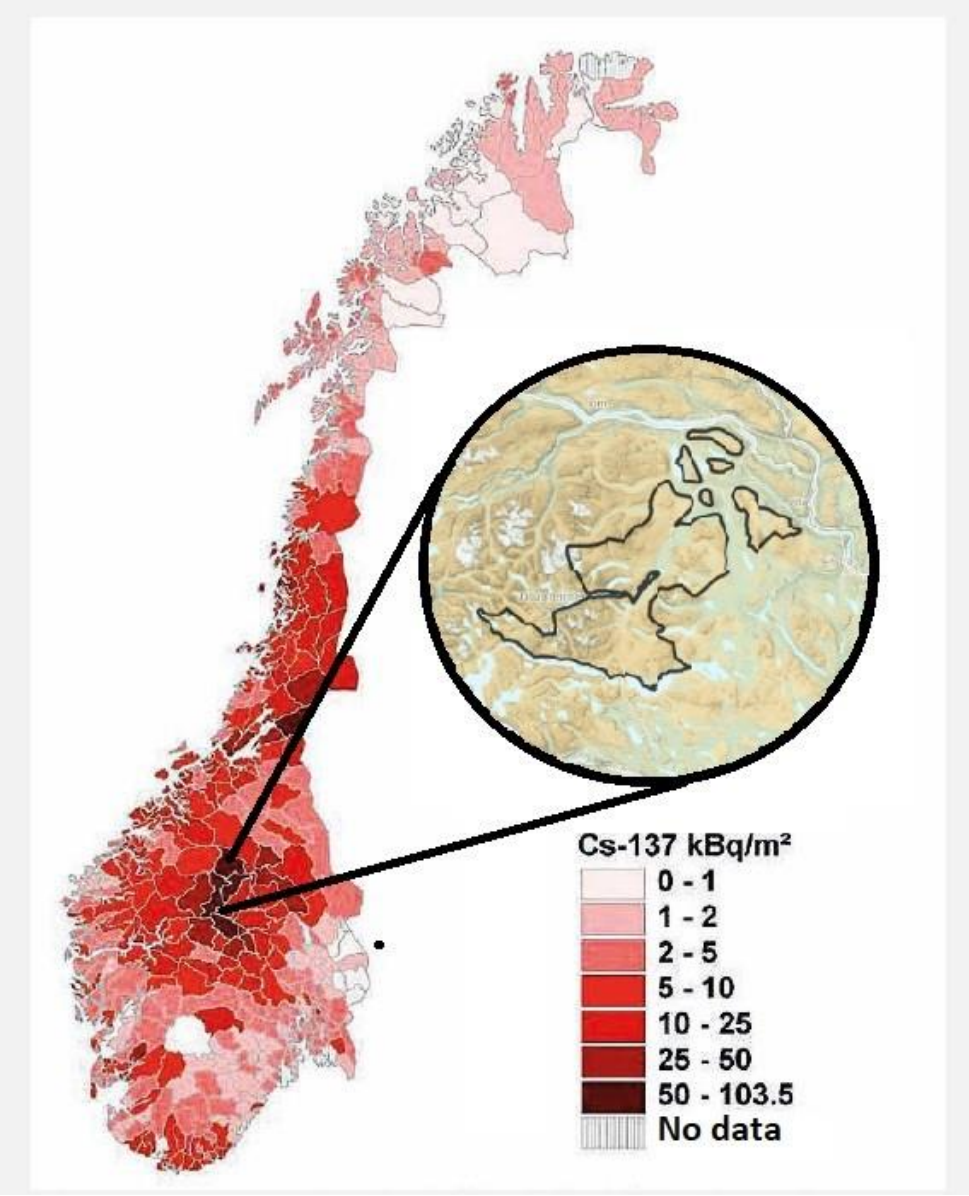

Figure 5: Deposition density map of ^{137}Cs in Norway with emphasis on the grazing area of the semi-domesticated reindeer in Vågå herding district. Source: (NRPA, 2006).

Samples and sampling

Three 10-year old semi-domesticated reindeer cows were picked out of the herd, weighed and monitored for ^{137}Cs by in vivo means with a NaI-probe by the DSA before being guided into a mobile slaughterhouse. The carcasses were collected with the intestines, heads, skins and lower fore and hind legs which were then transported to a nearby garage for dissection. An experienced veterinarian assisted with the extraction and collection of rough tissue samples, which was then transported back to the laboratory at NMBU and stored in a freezer at -30 ˚C prior to sample preparation.

Several organs were weighed as well as the heads and legs. A list of tissues and organs sampled as well as weights are listed in table 1:

Table 1: A list of extracted tissue samples along with weights, given in kg, measured in field, merged cells indicate that the related tissues were collectively weighed. Samples that were not collected are marked nc, missing weights are marked with a hyphen (-). Omasal was not collected but involved in the weighing of the gastrointestinal (GI) tract.

Reindeer:	*A*	*B*	*C*
Live weight:	91.5	-	-
Carcass weight:	44.9	39.3	46.3
Head with Antlers:	5.80	4.70	5.00
Fore- and hind legs:	2.69	2.70	2.80
Hide with fur:	5.4	-	5
The gastrointestinal tract with contents (-esophagus)	13.4	12.5	16.9

Sample #	Extracted tissues	A	B	C
1	**Myocardium, Left Ventricle (MLV)**	**0.8**	**0.72**	**0.70**
2	**Myocardium, Right Ventricle (MRV)**			
3	**Left Lung (LL)**	**0.95**	**1.1**	**0.87**
4	**Right Lung (RL)**			
5	**Blood Plasma (BP)**			
6	**Red blood cells (RBC)**			
7	**Rumen**			

8	**Rumen Content (RC)**			
9	**Omasal (nc)**			
10	**Abomasum**			
11	**Jejunum**			
12	**Caecum**			
13	**Colon**			
14	**Intestinal lymph node (ILN)**	**0.00552**	**0.00573**	**0.00959**
15	**Liver**	**1.95**	**1.39**	**1.53**
16	**Pancreas**	**0.0421**	**0.0318**	**0.0320**
17	**Diaphragm**	**0.0494**	**0.0257**	**0.0385**
18	**Spleen**	**0.155**	**0.141**	**0.141**
19	**Adrenal**	**0.00821**	**0.00286**	**0.00577**
20	**Kidney**	**0.260**	**0.232**	**0.249**
21	**Thyroid**	**0.00770**	**0.00731**	**0.00869**
22	**Ovarium**	**nc**	**0.0033704**	**0.0025565**
23	**Fur**			
24	**Skin**			
25	**Hooves**			
26	**Antler (Tip)**			
27	**Antler (Mid)**			
28	**Tibia**			
29	**Pelvis**			
30	**Costal**			
31	**Lumbar vertebrae (LV)**			
32	**Bone Marrow (BM)**			
33	**Hemispheral tissue (HT)**			
34	**Brain stem (BS)**			
35	**Cerebellum**			
36	**Masseter**	**0.0402**	**0.0296**	**0.0291**
37	**Longissimus dorsii (LD)**			
38	**Quadriceps femoris (QF)**			
39	**Bicephs brachii (BB)**			
40	**Udder**	**0.617**	**0.668**	**0.693**
41	**Tongue**	**0.324**	**0.316**	**0.324**
42	**Mandible**			
43	**Fallopian tube (FT)**	**nc**	**0.0222**	**0.0245**
44	**Cervix**	**nc**	**0.0383**	**0.0468**
45	**Molar Tooth (MT)**			

Method and instrumentation

Sample preparation and instrumental analysis described below was done at the Isotope laboratory and the Soil laboratory of the faculty of Environmental Sciences and Natural Resource Management (MINA), Norwegian University of Life Sciences (NMBU).

Instrumentation

Several instruments were utilized in this study and are listed below:

- Epsilon 2-4 LSC freeze dryer
- MileStone UltraClave
- NaI(Tl)-scintillation detector (PerkinElmer 2480 Automatic Gamma Counter) with complimentary software (WIZARD 2)
- Alpha spectrometer, (Four Canberra 7401 and one 7401VR connected to Canberra ADC model 1520), with complimentary software (ORTECs MAESTRO)
- BiotaDC software

UltraClave

The UltraClave utilizes microwave energy and high pressure for sample digestion. It allows for different sample matrices to be run at the same time and its operation is relatively automated by computer control. The automated steps are shown in Figure 6. Samples in PTFE tubes with loosely fitted caps are put unto a 17-position rotor system, a PTFE vessel is filled with a mixture of water and either 15 mL 67 % HNO_3 or a mixture of H_2O_2 and H_2SO_4, this helps the instrument control the temperature during a run. When the operation starts the reaction-chamber is sealed and pressurized with an inert gas which helps prevent cross-contamination between samples. It has a temperature range up to 300 ˚C and a maximum pressure of up to 200 bars which is controlled by integrated sensors. After completion the system is cooled using an external chiller and pressure is released before the reaction chamber opens (Analysis, n.d.; Automated, n.d.).

Figure 6: The automated steps of the UltraClave process. Source: (Automated, n.d.)

Scintillation detector

A scintillation detector is an instrument for detecting and measuring ionizing radiation by taking advantage of the solid scintillation phenomenon. A general detector setup is shown in figure 7.

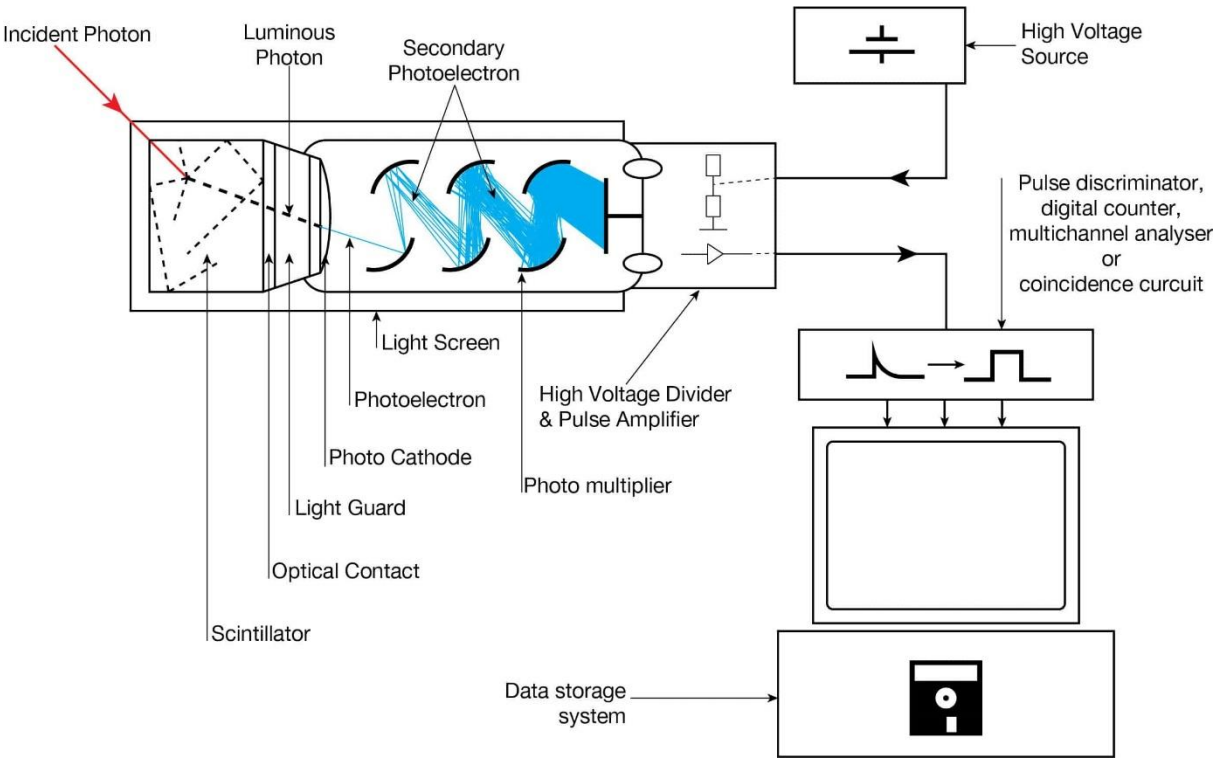

Figure 7: A general scintillation setup with a scintillating crystal, photomultiplier tube and data acquisition components. Source: wikipedia.org License: CC BY-SA 3.0.

Scintillation is a flash of light produced when ionizing radiation passes through a transparent material by excitation and de-excitation of electrons. For this study a NaI-crystal doped with Tl impurities was used, the high density of the crystal gives it more stopping power for γ-rays, hence an increase in counting efficiency compared to other scintillator materials. The scintillator is optically connected to a photomultiplier tube (PMT), which converts light into an electrical current. A high voltage is applied to accelerate the electrons through a dynode chain, where each successive dynode will emit additional electrons amplifying the signal until a measurable voltage pulse is detected at the final dynode. Thus, the PMT has two functions, signal conversion and amplification. Further on, a multichannel analyzer converts the voltage pulse into a digital signal by correlating the height of the voltage pulse with radiation energies and quantifies their intensities which is stored on a computer and displayed as a gamma-spectrum.

The relationship between the voltage pulse and the absorbed γ-ray in the scintillator can be described with the following equation:

$$Pulse\ Height\ (volts) \propto scintillation\ photon\ intensity \propto gamma - ray\ energy\ absorbed$$

(L'Annunziata, 2012)

Sample preparation for gamma-screening

There were a range of different types of tissues all of which required different approaches regarding sample preparation. Samples were treated in a way to minimize contact with metals, as to avoid contamination for future trace metal analysis, also the incision areas from sample collection were avoided where metal tools were utilized for extraction. The only exception being the antlers, which required nippers to break off a piece. Two parts were collected, one from the main beam referred to as antler (Mid) and another from the outer tip of the main beam referred to as antler (Tip).

Soft tissues were cut in a way to get a representative sample. Muscles were clean cut from fat tissue to an extent where this was possible.

A 10x10 cm area of the chin was cut to extract the skin sample, the first batch of hair was collected from the same patch and rinsed in MQ-water, referred to as Fur (A). The second batch was procured later in the procedure and washed according to (Strumińska-Parulska et al., 2015), once with acetone, thrice with water and a final wash with ethanol, referred to as Fur (B).

Bones were cooked in a beaker to remove residual tissue, put in a plastic bag and covered with additional paper prior to being crushed with a hammer. The bone material was collected in a way to get both the surface and internal area. The mandible was also treated this way collecting molar teeth still distinguishable from bone tissue.

Intestinal tissue was shaken in MQ-water and rinsed for residual feces. Rumen content were gathered on site during tissue extraction and was mixed thoroughly before measurement.

The samples were transferred to 20 mL plastic vials and weighed prior to screening on the NaI(Tl)-scintillation detector.

^{137}Cs-analysis

The measurement runs were carried out by Senior Engineer Marit Nandrup Pettersen at MINA, NMBU. The activity concentrations were calculated by subtracting the instrumental background from the obtained counts and corrected for detector efficiency and emission probability as well as incorporating the mass of the sample and a conversion factor, the equation used are given below:

$$Activity\ concentration\ \left(\frac{Bq}{kg}\right) = \frac{(N_s - N_b)}{\varepsilon * \gamma * t * m_s * k}$$

N_s: The net peak area in the sample spectrum.

N_b: corresponding net peak area in the background spectrum.

ε: the efficiency at photopeak energy.

γ: the emission probability of the gamma line corresponding to the peak energy.

t: The live time of the sample spectrum collection in seconds.

m_s: the mass of the sample in kg DW.

k: conversion factor (WW/DW)

Decay corrections were neglected due to the short time-delay between sampling and measurement relative to the half-life of the measured radionuclide.

The efficiency was calculated with the use of a calibration standard with the following equation:

$$\varepsilon = \frac{R_{std}}{A_{std}}$$

R_{std}: The count rate of the calibration standard obtained from the spectrum.

A_{std}: The activity of the calibration standard.

Alpha spectrometry

Alpha-Spectrometry is a sensitive nuclear analytical technique for the determination of alpha emitting nuclides. A typical setup is shown in figure 8. The prepared samples were placed in a vacuum chamber. A distance 5-10 mm from the detector surface is reported to be sufficient for optimal counting efficiency for environmental samples (Matthews et al., 2007).

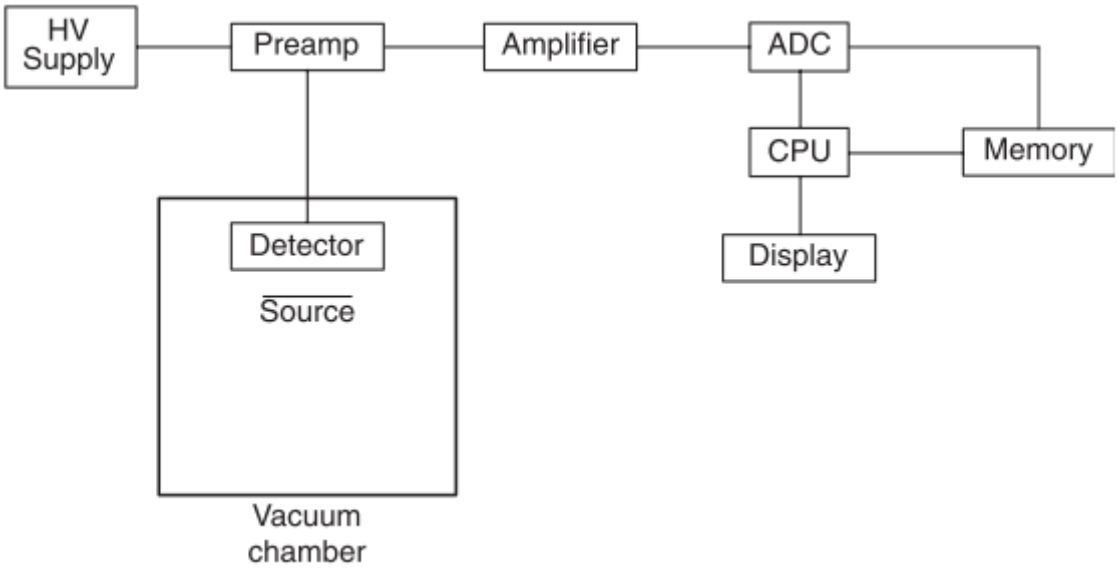

Figure 8: Typical α-particle spectrometry system (Matthews et al., 2007).

This study utilized a Passivated Implanted Planar Silicon detector (PIPS) because of its excellent energy resolution, low background, stability and low sensitivity to γ-radiation. The PIPS detector is a combination of a n-type (electron donating) and p-type (hole donating) silicon. The resulting interaction between these creates a depletion layer at the p-n junction where all the holes are filled with electrons. By applying a voltage over this junction, connecting the negative terminal to the p-type region and the positive terminal to the n-type region, it is said to be reversely biased and the depletion layer thickness increases. In the reverse direction the semiconductor represents a high resistance bypassed by a capacitive component due to the dielectric of the barrier layer. (Choppin et al., 2013)

When an α-particle hits the detector, the particle is stopped in the depletion layer, creating electron-hole pairs. The number of electron-hole pairs created is directly proportional to the energy of the stopped particle, the relationship is described in the equation below:

$$N = \frac{E}{\varepsilon}$$

Where N is the number of electron-hole pairs created, E is the kinetic energy of the stopped particle and ε is the energy gap required to create a single electron-hole pair. (Verplancke et al., 2012). The electron-hole pairs will be separated by an electric field to each of their respective terminals giving a charge pulse which is converted to a voltage pulse in a sensitive preamplifier. Further on, an analog to digital converter (ADC) converts the voltage signal to a digital signal, the height of the voltage pulse is correlated to a channel depending on its energy. The result is an α-spectrum displayed on a computer with the help of complimentary software, a typical spectrum with ^{209}Po as tracer is shown in figure 9.

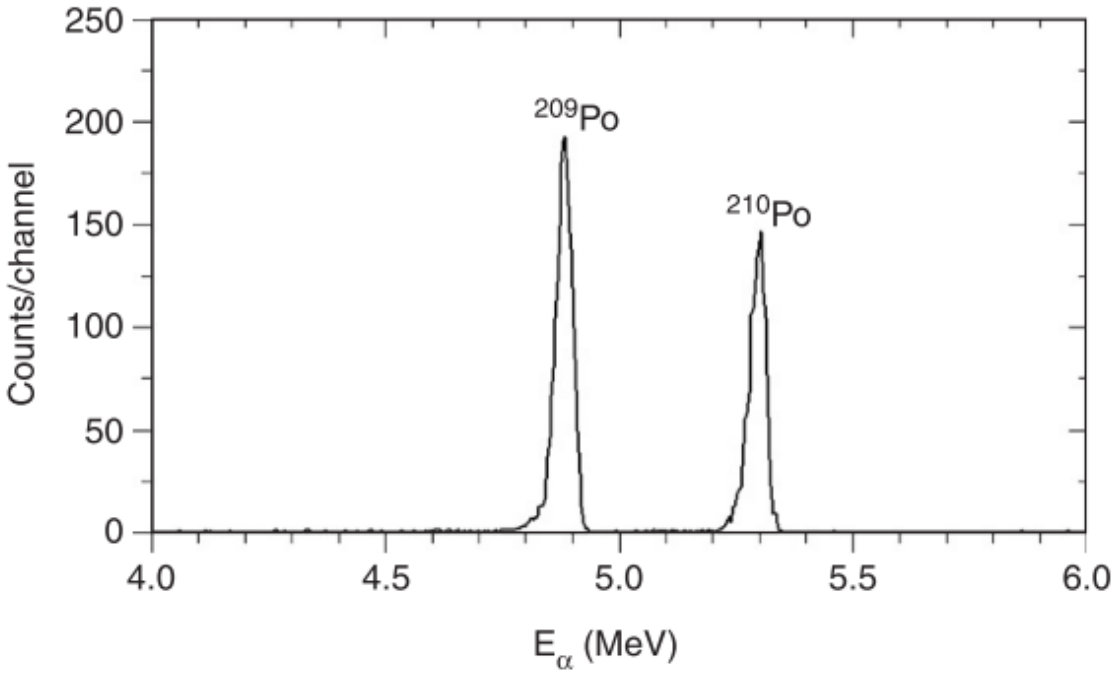

Figure 9: Typical α-spectrum of ^{210}Po with ^{209}Po as yield tracer (Matthews et al., 2007).

Sample preparation for ^{210}Po-measurement

Samples were transferred from 20 mL vials to plastic bags for freeze-drying (Christ EPSILON 2-4 LSC) and then crushed to a powder for homogenization of the samples where this was possible. The tissues containing a lot of fat remained ''elastic'' post freeze-drying

making them difficult to crush. The samples were freeze dried to minimize potential loss of analyte, owing to the volatility of polonium at high temperatures.

The method for radiochemical separation used in this study was developed by (Q. J. Chen et al., 2001) and further modified by the Isotope laboratory at NMBU, a flow chart of the procedure is shown in figure 10.

The method incorporates the use of a radiochemical tracer, (^{209}Po Eckert & Ziegler Isotope Products), added in the early stages of sample preparation allowing corrections for any loss occurring in the proceeding steps of the procedure. It also serves as a quality control of the method in the form of a recovery percentage of the tracer. This is formally known as isotope dilution alpha spectrometry and is valid under the assumption that isotopes have identical chemical properties (Vajda et al., 2020).

Samples were transferred and weighed into PTFE tubes, yield tracer was added as well as 10 mL MQ-water and 5 mL analytical grade 67 % HNO_3 to predigest overnight. This was done to minimize potential exothermic reactions due to fatty acids in the sample matrix in a UC digestion run. After digestion the samples were transferred to glass beakers, the UC PTFE tubes were rinsed with 3x1.5 mL 67 % HNO_3 and transferred to the glass beaker before being left for drying overnight on an electrical sand-bath (LHG) set at 50-60˚C.

The treatment with H_2O_2 and $NH_2OH{\bullet}HCl$ is to improve the source quality, the former can remove potential elemental sulfur in the solution by oxidation to H_2SO_3, which then can decompose to $H_2O + SO_2$ in an acidic medium. Elemental Sulfur can deposit on the source during polonium deposition, increasing the thickness of the source surface. With the addition of $NH_2OH{\bullet}HCl$, the color of the solution changes from yellow to colorless, allowing polonium to deposit unto metal surfaces in this reducing system, it also helps suppressing potential interference of iron during spontaneous deposition by reducing Fe^{3+} (Q. J. Chen et al., 2001; F. Carvalho et al., 2017).

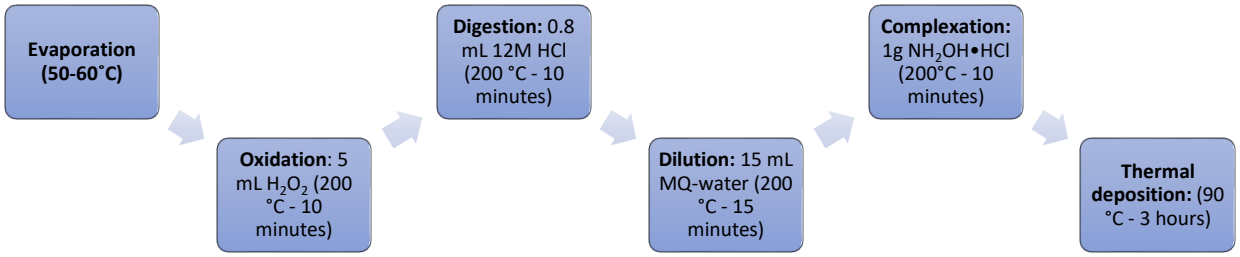

Figure 10: Flow chart of the radiochemical separation method for measurement on α-detector.

The Ni-discs (TRISKEM International) were washed with soap (JIF Scouring cream with microgranules) to remove residues and the columns were assembled. The samples were transferred to columns, rinsed 3x3 mL of 1.0 mg NaCl in 0.3 M HCl through a filtered funnel conditioned with MQ-water (Whatman analytical filter). The columns were then left in a rocking water bath (Julabo SW22) set at 90 °C for 3 hours.

After thermal deposition, the Ni-discs were removed from the columns, rinsed with MQ-water, dried on a heated sand bath at 50°C for 10 minutes and stored in plastic bags awaiting measurement on the alpha-spectrometer.

Equipment for deposition and UC digestion were rinsed with MQ-water and put in an acid bath in between runs, where a 20 % HNO_3 solution was used for former and a separate 50 % HNO_3 solution was used for the UC medium-sized PTFE tubes. An exception being the bottom part of the columns along with the rubber O-rings, which was only rinsed in MQ-water.

^{210}Po-analysis

When evaluating the spectrum; the gross count rates are determined by integrating regions of interest (ROI) set asymmetrically around the two peaks divided by the counting time.

The activity can then be determined with the given equations:

$$Activity\ (Bq) = A_T * \frac{R_{GA} - R_{BA}}{R_{GT} - R_{BT}}$$

A_T: The specific activity of the tracer. **R_{GA}**: Rate of gross analyte, s^{-1}.

R_{BA}: Rate of instrumental blank analyte, s^{-1}. **R_{GT}**: Rate of gross tracer, s^{-1}.

R_{BT}: Rate of instrumental blank tracer, s^{-1}

$$Activity\ concentration\ \left(\frac{Bq}{kg}\right) = \frac{Activity\ (Bq)}{m_s * k} * \ e^{\lambda*(t_S - t_E)}$$

m_S: Mass of sample (DW). **k**: Conversion factor DW to WW. **λ**: Decay constant of analyte.

t_S: Beginning of measurement time. **t_E**: End of sampling time.

Decay corrections of the analyte and tracer during counting times were neglected in these calculations owing to the relatively large radionuclide half-life compared to counting times.

The recovery from the tracer blank were calculated with:

$$Chemical\ recovery\ (\%) = \frac{R_{NT}}{\varepsilon * A_T}$$

ε: The efficiency of the detector, estimated from measurements with certified reference standard.

R_{NT}: Net count rate of yield-tracer obtained by subtracting the background.

^{210}Pb-analysis

Ideally, ^{210}Pb activity determinations should have been done for ^{210}Po-analysis. For one, the evolution of ^{210}Po is very much affected by the presence of its parent ^{210}Pb, having contrasting affinities for different tissues within biological systems, may lead to fractionation creating either an excess or deficiency of ^{210}Po which over time grows into secular equilibrium with the parent. Understanding these systematics yields better interpretations of the resulting dose received over time from ^{210}Po. Also, it is useful to determine the unsupported fraction of ^{210}Po i.e. ^{210}Po not originating from in situ decay ^{210}Pb. The analysis is done by retaining the solution from thermal deposition for an ingrowth period of 6 months, where at the end another round deposition would be done, and the ^{210}Po from the ingrowth of ^{210}Pb decay would be measured on the alpha-detector, reflecting how much

^{210}Pb that was left in the solution, assuming adsorption effects are negligible (Matthews et al., 2007). From the determined ^{210}Pb activity, the unsupported fraction of ^{210}Po can be estimated by using Batesman's equation. (F. Carvalho et al., 2017; Lavrans Skuterud, 2005)

DATA TREATMENT

Data were treated in Microsoft Excel, version 2008 (Build 13127.21064). Missing data on biomass of tissue compartments were estimated with data obtained from literature. Missing data from radionuclide analyses were ignored if its contribution to the resulting estimation were thought negligible.

Mass estimation

Live weights, bone and muscular tissue were estimated data given by (Ringberg et al., 1981b). The brain and tibia were estimated with data from (Ringberg et al., 1981a). LD was estimated with data given by (Eva Wiklund, 2017). Total GI tract were estimated as well as associated component tissues were estimated with data given by (Staaland et al., 1979). RBC, BP and antlers were estimated with data given by (Gaare & Staaland, 1994).

Fur and skin were estimated from the total weight of skin and fur obtained in this study with the ratio of the weights between the 10x10 cm patch of skin and its associated fur obtained in sample preparation. Hooves were estimated by subtracting the estimated tibia weight from the weight of the lower hind and forelegs obtained in this study. Molar teeth were estimated based on an average of intact teeth extracted in this study (appendix A, table 1A).

Whole body concentration and $CR_{wb:t}$

Whole-body concentrations were reconstructed based on data from radionuclide analyses and weights obtained in the field. Substituting missing data were evaluated based on its contribution to the whole body.

$$C_{wb} = \sum A_n * F_n$$

Where Wb_c = the estimated whole-body concentration. A_n = average activity concentration in compartment n. F_n = Fractional fresh biomass of compartment n relative to the whole-body.

Concentration ratio to whole body, $C_{Wb:t}$, were estimated in accordance with the standards of Yankovich et al., (Yankovich et al., 2010).

$$CR_{wb:t} = \frac{\sum(C_t * F_t)}{C_t}$$

Where $CR_{wb:t}$ is the dimensionless whole-body to tissue concentration ratio, C_t is the concentration of a given radionuclide in each tissue (Bq/kg) and F_t is the fractional fresh biomass of the whole-body.

Internal DCs

DCs were attained from BiotaDC software with the biomass of the sampled tissues and organs. The input parameters are shown in table 2. Organs and tissues were treated as aquatic organisms with a spherical shape (sphericity = 1) and 'transient-activities ratio' was the selected method to account for radioactive progeny and time was set to 0.

Table 2: Input parameters in the BiotaDC software for estimation of tissue specific internal DCs.

Input parameters	**Input**

Ecosystem:	Aquatic
Exposure:	Internal
Mass of organism:	Kg
Shape of organism:	1:1:1
Radionuclide:	^{137}Cs / ^{137m}Ba / ^{210}Po
Effect of radioactive progeny:	transient-activities ratio
Time (d):	0

Absorbed fractions were obtained with data given by, (Ulanovsky & Pröhl, 2006) for 0.03 and 0.5 MeV photons as well as 0.5 MeV and 1 MeV electrons for a range of different masses, given in appendix E.

Estimated absorbed dose rates.

Tissue specific dose rates were estimated based on data from radionuclide analysis and the obtained internal DCs obtained. The DCs were weighted for fraction of radiation type, radiation weighting factor as well as the absorbed fraction.

$$D_n = \sum A_n * DC_{n,r} * f_r * w_{R,r} * \varphi_{n,r}$$

Where D = Absorbed dose rate (uGy/h), A = Activity concentration (Bq/kg), DC = Dose Coefficient, f = fraction of radiation type, w_R=radiation quality factor, ϕ = absorbed fraction. n = tissue compartment. r = radiation type.

Whole-body dose rates were obtained by taking the weighted average of localized tissue doses. Fur and RC was excluded.

$$D_{wb} = \sum_{n} D_n * F_n$$

Where D_{wb} = Absorbed dose rate (uGy/h), D = Absorbed dose rate (µGy/h). f = Relative biomass of to the whole body. n = tissue compartment

Relative distribution of dose contribution was calculated by weighting relative compartment masses to dose rates in the same compartment:

$$\%\ Dose\ contribution = \frac{D_n * F_n}{\sum_n D_n * F_n} * 100\ \%$$

Where D_n = Estimated dose rate in compartment n. F = Relative biomass to whole body. n = tissue compartment.

QUALITY ASSURANCE

In general, every measurement is accompanied with some uncertainty which needs to be considered when interpreting the result or assuring the quality of the method. These uncertainties are classified as systematic and random errors. Systematic errors can emerge from methodological flaws, equipment faults or contaminated reagents which can be corrected if discovered. Random errors are exactly what the name implies, errors originating from uncontrollable factors and thus unavoidable, though not unmanageable. Precision and accuracy are concepts used to describe the consistency and ‘’trueness’’ of a measurement method.

To account for the uncertainties introduced throughout the measurement process, the combined standard uncertainty (CSU) is calculated using summation in quadrature:

$$CSU(x) = \sqrt{(u_1(x))^2 + (u_2(x))^2 + (u_3(x))^2 + \cdots + (u_n(x))^2}$$

Where CSU(x) is the combined standard uncertainty of x and $u_n(x)$ is the uncertainty component n introduced in the measurement process of x.

Uncertainty components incorporated in the estimation of CSU in ^{210}Po-analysis:

- Count of tracer and analyte.
- Count of the background measurement.
- Concentration of yield tracer at calibration date.
- Volume of tracer used.

Uncertainty components incorporated in the estimation of CSU in ^{137}Cs-analysis:

- Efficiency calibration
- Background measurement
- Emission intensity

Utilization of certified reference materials (CRM), internal standards and/or blank samples are useful sanity checks when evaluating the measurement process and the quality of the results (C. C. Chen et al., 2010). Further on, every detector has some level of noise in a signal domain of interest and must be considered to avoid false negatives and false positives when evaluating a signal on the detector. Detection and quantification limits are statistical concepts derived from samples containing no analyte to establish the lowest detectable signal significantly distinguishable from detector noise or blank signal or the lowest apparent signal one can quantify with a certain accuracy (C. C. Chen et al., 2010).

^{137}Cs-analysis

Samples were analyzed for 30 minutes with a counting uncertainty of <10%. Several blanks were run to determine background contribution in the region of interest. The efficiency calibration was done with IAEA 373 CRM.

The instrumental detection (LoD) and quantification limit (LoQ) were calculated based on a method given by (Currie, 1968):

$$LoD = 4.65 * \sigma_b$$

$$LoQ = 14.1 * \sigma_b$$

σ_b: The uncertainty of the arithmetic mean of the background measurement.

Achieving a LoD of 0.39 Bq and LoQ of 1.2 Bq.

^{210}Po-analysis

Instrument calibration and efficiency determination were done with a certified calibration source, (Standard Radionuclide Source, 67976-121, Analytics, USA), consisting of four alpha-emitters, (U^{238}, U^{234}, Pu^{239}, Am^{241}), in the energy range of 3700-7950 keV.

A counting uncertainty of ≤10% were achieved, only a few had counting uncertainties 10%>13%. Procedural blanks (PB) and analytical blanks (AB) were run with every radiochemical separation procedure, recovery % of the AB varied between 25-45%, see appendix C, table C1-C3.

The detection limit was estimated based on a method given by (Armbruster & Pry, 2008), using the limit of the blank (LoB), i.e. the average apparent concentration measured in the procedural blanks (n=20) across detectors:

$$LoD = LoB + 3 * \sigma_{LoB}$$

$$LoD = LoQ$$

Achieving a LoD of 2.69 mBq.

RESULTS AND DISCUSSION

Presentation of the results begins with some comments on the radionuclide analysis method, before presenting the determined activity concentrations from ^{137}Cs and ^{210}Po analyses. Followed by body burden distribution as pie charts given as a percentage, then a comparison of estimated dose rates from the investigated radionuclides. Leading to pie-charts showing distribution of dose contribution are presented of ^{137}Cs and ^{210}Po. Finally, an

estimated whole-body tissue concentration as well as whole-body dose are presented for both radionuclides.

Radionuclide analyses

Activity measurements of ^{137}Cs and ^{210}Po in various tissues of semi-domesticated reindeer yielded results, table 2, uncensored data are given in appendix B, table B1. A total of 171 and 148 samples were prepared for analysis for ^{137}Cs and ^{210}Po determination, respectively, however, only 115 samples were measured due to time restrictions regarding the latter. ^{137}Cs results from the additional heads are given in appendix B, table B2.

Table 3: Determined ^{137}Cs and ^{210}Po activity concentrations in samples tissues from three semi-domesticated reindeer, given as Bq/kg (w.w.) with the analytical uncertainty given in parentheses. Samples that were below the detection or quantification limit, not collected or not analyzed are marked <LoD, <LoQ, nc and na respectively. ^{210}Po that were close to LoD evaluated from signal to noise ratio >10 are marked with an asterisk.

	^{137}Cs, Bq/kg (RSD%) (w.w.)			**^{210}Po, Bq/kg (RSD%) (w.w.)**		
Tissues:	A	B	C	A	B	C
MLV	1564 (2)	1275 (2)	1595 (2)	<LoD	11 (14)	6 (20)*
MRV	1581 (2)	1282 (2)	1685 (2)	<LoD	13 (10)*	<LoD
LL	890 (2)	980 (2)	903 (2)	9 (14)*	20 (22)*	16 (29)
RL	955 (2)	950 (2)	954 (2)	9 (11)*	28 (9)	22 (19)
BP	<LoD	<LoQ	<LoD	na	na	na
RBC	326 (8)	423 (7)	325 (8)	<LoD	<LoD	18 (8)*
Rumen	715 (3)	369 (4)	654 (2)	14 (9)	19 (12)	28 (15)
RC	516 (2)	340 (2)	344 (3)	59 (12)	27 (11)	65 (15)
Fur (B)	nc	nc	nc	56 (6)	65 (4)	73 (7)*
Abomasum	1151 (2)	719 (2)	852 (2)	13 (5)	83 (14)	17 (12)
Jejunum	2078 (1)	1698 (2)	1144 (2)	28 (13)	29 (13)	19 (5)
Caecum	422 (3)	335 (3)	375 (3)	8 (7)	20 (13)	8 (15)
Colon	475 (3)	700 (2)	1048 (2)	5 (9)	16 (14)	7 (10)
ILN	1140 (3)	1096 (4)	854 (2)	51 (10)	134 (14)	178 (7)
Liver	1286 (2)	1241 (2)	1275 (2)	50 (7)	36 (12)	76 (8)
Pancreas	2401 (1)	1997 (1)	2290 (1)	21 (11)	23 (12)	20 (10)
Diaphragm	1996 (2)	1834 (1)	2113 (1)	6 (8)	10 (16)*	5 (15)*
Spleen	1209 (2)	1160 (2)	1323 (2)	6 (13)*	10 (16)*	8 (7)
Adrenal	1263 (2)	1280 (4)	1329 (2)	13 (11)*	50 (13)	7 (9)*
Kidney	2899 (1)	3004 (1)	2797 (1)	65 (7)	58 (17)	68 (4)
Thyroid	732 (3)	601 (4)	679 (3)	53 (9)	61 (13)	54 (5)
Ovary	Nc	766 (6)	958 (6)	nc	12 (19)*	12 (9)*
Fur (A)	534 (8)	<LoQ	<LoD	95 (15)*	68 (16)	75 (11)*
Skin	908 (3)	784 (4)	722 (6)	13 (10)*	19 (16)*	16 (12)
Hoof	206 (9)	<LoQ	199 (13)	112 (11)	107 (9)	134 (7)*

Antler (Tip)	470 (5)	281 (7)	365 (5)		52 (12)	109 (13)	158 (10)
Antler (Mid)	95 (10)	79 (12)	<LoQ		131 (21)	157 (11)	na
Tibia	<LoQ	<LoQ	<LoQ		358 (26)	331 (11)	521 (7)
Pelvis	<LoQ	<LoQ	389 (11)		179 (11)	425 (15)	849 (5)
Costal	<LoQ	284 (10)	258 (8)		302 (13)	382 (15)	na
LV	538 (4)	418 (5)	365 (6)		311 (13)	375 (11)	na
BM	<LoD	<LoQ	<LoQ		<LoD	na	na
HT	384 (4)	410 (3)	312 (4)		<LoD	na	na
BS	675 (2)	894 (2)	744 (3)		5 (13)*	13 (14)*	na
Cerebellum	556 (4)	605 (3)	369 (3)		<LoD	15 (16)*	na
Masseter	3205 (1)	2486 (1)	3053 (1)		5 (12)*	7 (13)*	na
LD	1874 (1)	2160 (1)	1740 (1)		6 (17)*	7 (11)*	17 (8)
QF	2012 (1)	2039 (1)	2118 (1)		<LoD	na	na
BB	2099 (1)	2186 (1)	2203 (1)		9 (14)*	3 (12)*	5 (11)*
Udder	1363 (1)	1621 (1)	1384 (1)		26 (12)	56 (14)	28 (10)
Tongue	1394 (2)	987 (2)	1259 (2)		<LoD	na	<LoD
Mandible	268 (5)	224 (7)	226 (6)		271 (14)	356 (13)	656 (4)
FT	nc	759 (2)	756 (2)		nc	16 (13)	21 (13)
Cervix	nc	639 (2)	671 (2)		nc	10 (11)	na
MT	189 (10)	<LoQ	196 (9)		507 (18)	581 (12)	na

Quality on ^{137}Cs data were generally better than for ^{210}Po with an analytical uncertainty ranging from 1-13 % and 4-20 % respectively. From a signal-to-noise ratio evaluation, a considerable amount of tissues in ^{210}Po-analysis were close to detection limit, i.e. S/N > 10. In addition, the procedural blanks from ^{210}Po-analysis indicated cross-contamination with an RSD of 51 %, appendix A, table A5. A possible explanation might be the use of a single acid bath for the radiochemical separation equipment, where the use of separate acid baths for expected high activity samples and low activity samples might reduce cross-contamination. Another reason could be the lack of coating on the rubber O-rings used in the column setup, preventing direct contact between the rubber and the solution. Leaching has been observed, (Langford & Brodzinski, 1974), regarding rubber. Further on, the rubber O-rings were only rinsed with MQ-water in between runs, where a more thorough method of washing might be necessary considering low activity determination. In the end, when considering signal detection, the decision was made to use a conservative detection limit based on the average signal from the procedural blanks across detectors and evaluated on counts per second basis as to avoid uncertainties in the efficiency of the instrument. Also, the poor recovery from the analytical blanks could in part be attributed to

the use of UC-digestion where loss of volatile Po species has been observed by (F. Henricsson et al., 2011) in closed microwave digestion systems. However, as stated by (Matthews et al., 2007), the lack of information available regarding the extent of loss due to Po volatility in different sample matrices and sample preparation procedures makes it difficult to pinpoint the exact reason for the poor recovery. Finally, regarding the choice of Ni-discs, co-deposition of both Pb and Bi with Po has been observed in the production of alpha sources on different metals, (F. Henricsson et al., 2011), where Ni-discs proved to be the most efficient at depositing Pb. Therefore, if a significant fraction of ^{210}Pb is co-deposited and a considerable time delay between deposition and measurement occurs there would be a risk of overestimating ^{210}Po in the sample. This is especially relevant for organs and tissues that has been shown to readily accumulate Pb. The considerable time delay is referred to as weeks or more, (F. Henricsson et al., 2011), which was avoided for most samples in this study, but due to the 2020 Covid-19 pandemic and the consequent quarantine rules, this overestimation might be true for some of the samples. For future reference, Ag-discs was demonstrated to be the better choice for Po-analysis to avoid co-deposition of Pb (F. Henricsson et al., 2011).

The two different sample preparation methods regarding fur for ^{210}Po-analysis yielded indistinguishable results for reindeer B and C, Appendix B, figure B1 , while Fur (A) seemed to have higher levels than Fur (B) for reindeer A. Further presentation use data from Fur (A), referred to as 'Fur', since the time delay between sampling and measurement were considerably less compared to Fur (B).

Comparison with literature

The results from ^{137}Cs and ^{210}Po analyses are presented as column graphs, given as an arithmetic mean (AM) of the activity concentrations with the associated standard deviation (SD) as error bars on a wet weight basis (w.w.). Data with n≠3 are marked and elaborated in footnotes. Data with n=1 are presented as an activity concentration (A) with the combined standard uncertainty (CSU). For data with n=2, the SD reflects the variation between the reindeers if it was larger than any one of the analytical uncertainties, if not the largest analytical uncertainty were carried over to reflect the SD.

.

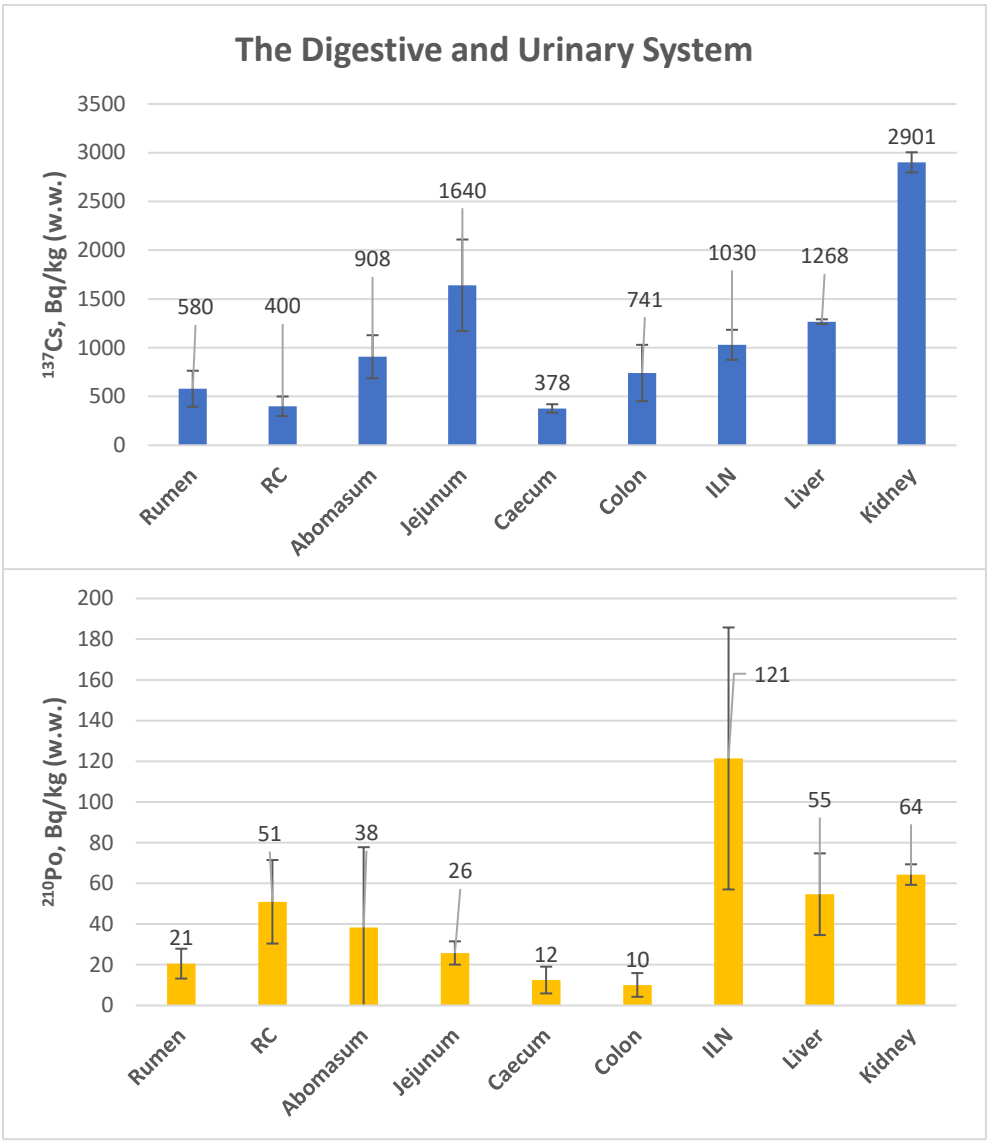

Figure 11: Activity concentrations of ^{137}Cs (top) and ^{210}Po (bottom), Bq/Kg (w.w.), in the digestive and urinary system. Given as AM ± SD with n=3. Note the different scales of the y-axes.

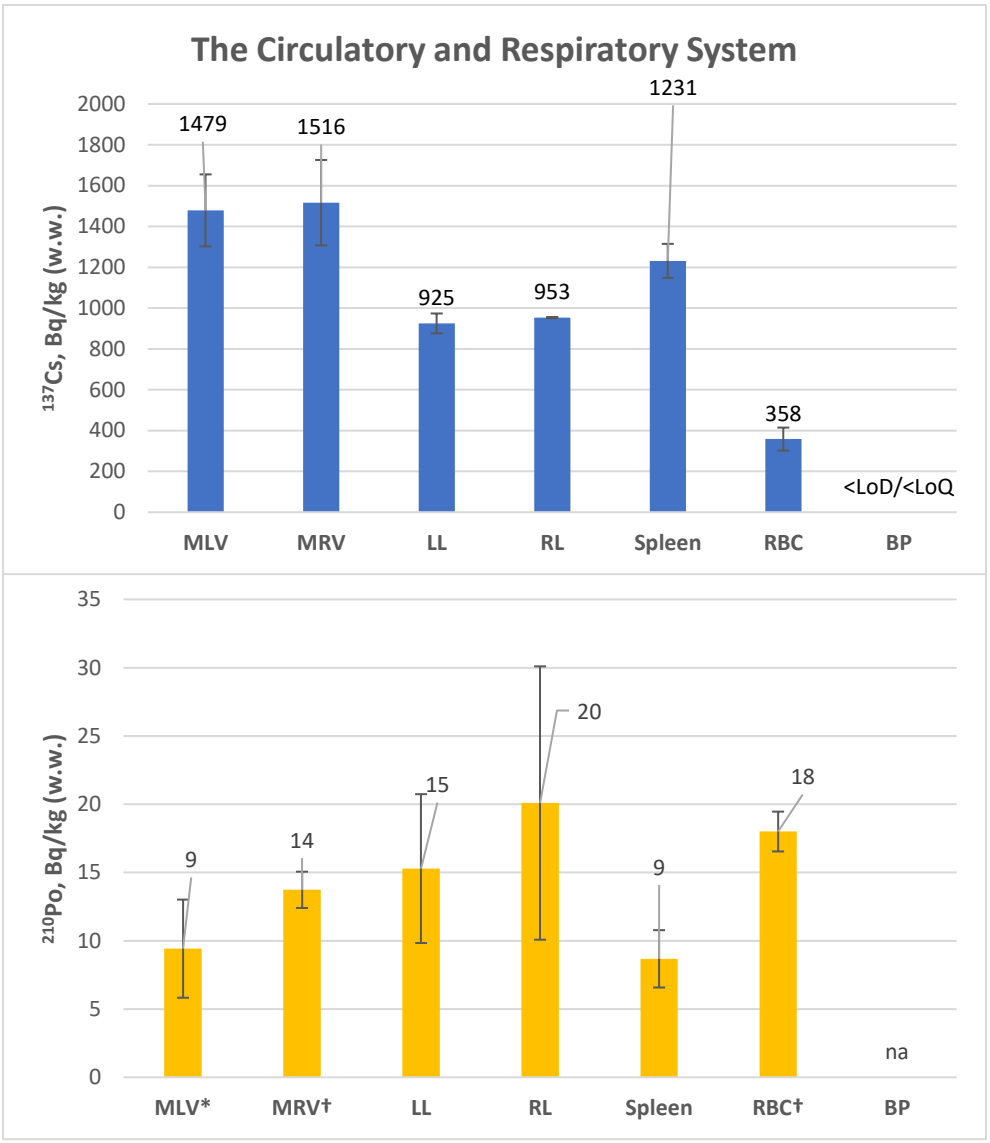

Figure 12: Activity concentrations of ^{137}Cs (top) and ^{210}Po (bottom), Bq/Kg (w.w.), in the circulatory and respiratory system. Given as AM ± SD with n=3. *Given as AM ± SD with n=2. †Given as A ± CSU with n=1. Note the different scales of the y-axes.

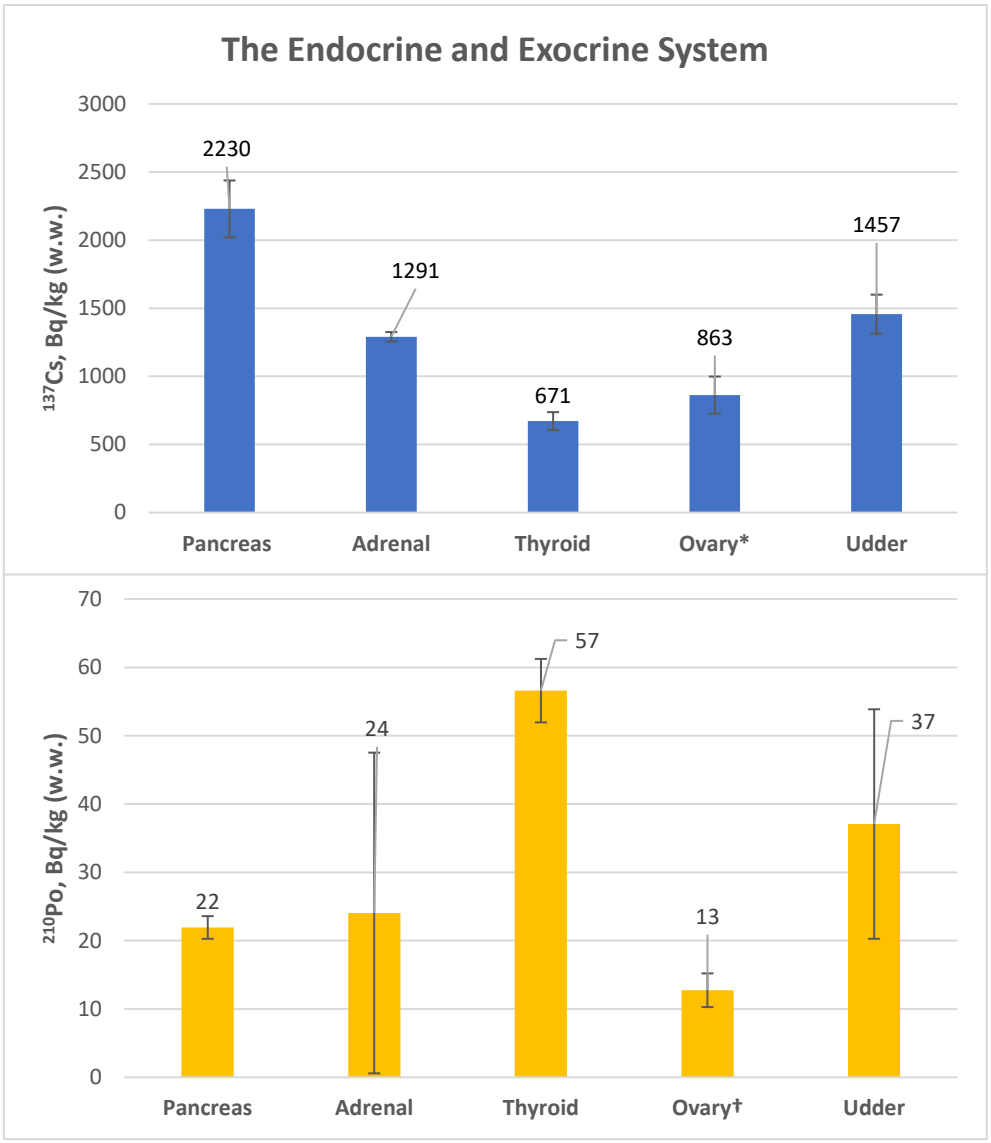

Figure 13: Activity concentrations of ^{137}Cs (top) and ^{210}Po (bottom), Bq/Kg (w.w.), in the endocrine and exocrine system. Given as AM ± SD with n=3. *Given as AM ± SD with n=2. †Given as AM ± CSU with n=2. Note the different scales of the y-axes.

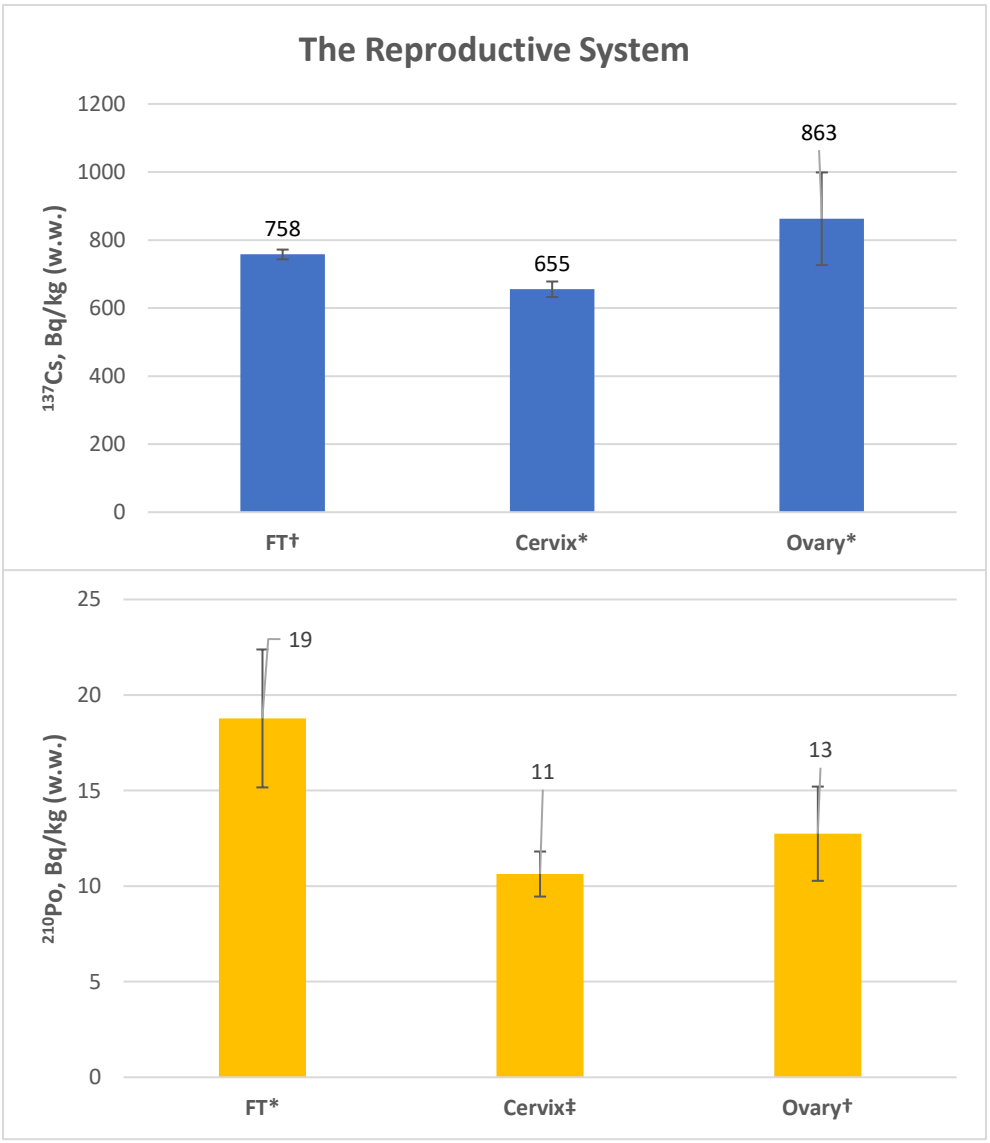

Figure 14: Activity concentrations of ^{137}Cs (top) and ^{210}Po (bottom), Bq/Kg (w.w.), in the reproductive system. Given as AM ± SD with n=3. *Given as AM ± SD with n=2. †Given as AM ± CSU with n=2. ‡Given as A ± CSU with n=1. Note the different scales of the y-axes.

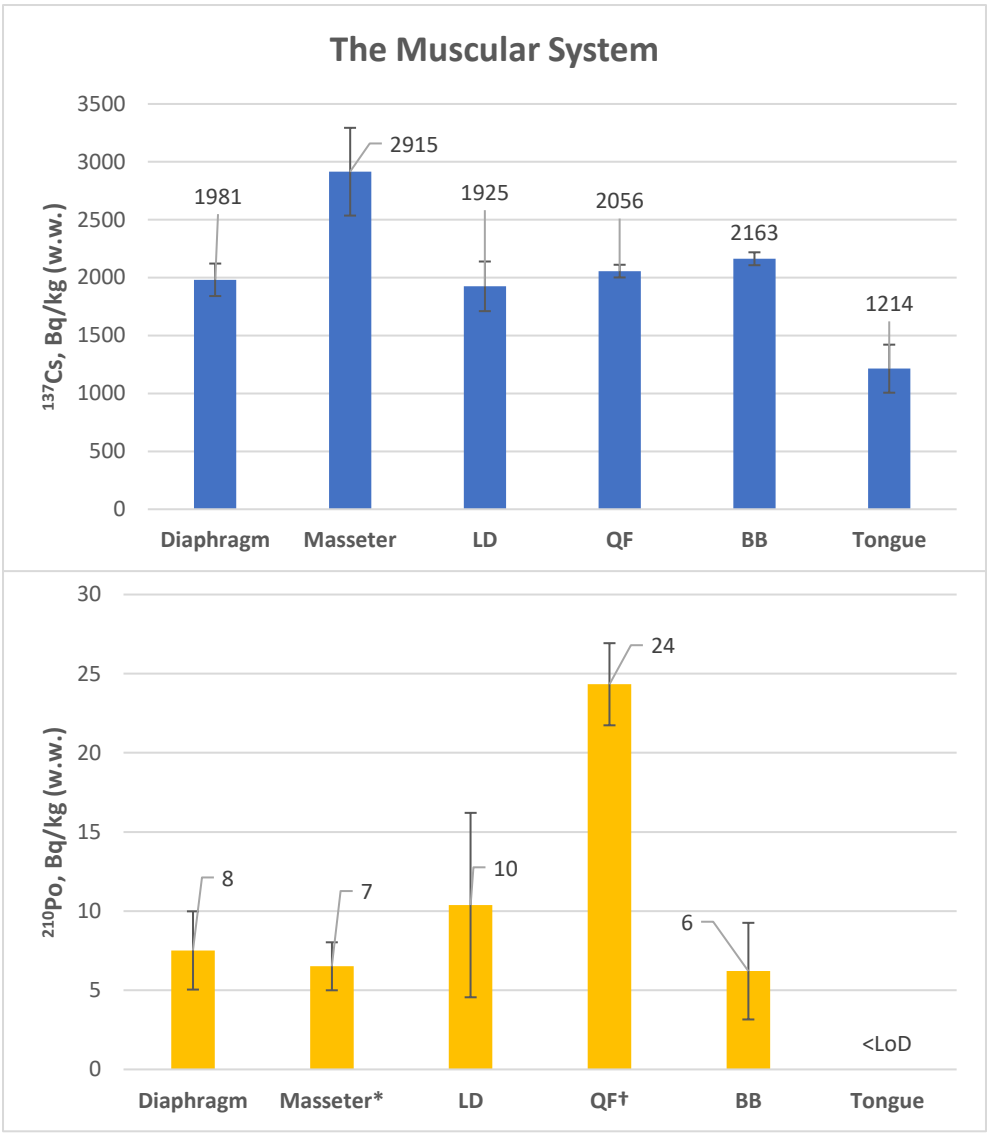

Figure 15: Activity concentrations of ^{137}Cs (top) and ^{210}Po (bottom), Bq/Kg (w.w.), in the muscular system. Given as AM ± SD with n=3. *Given as AM ± SD with n=2. †Given as A ± CSU with n=1. Note the different scales of the y-axes.

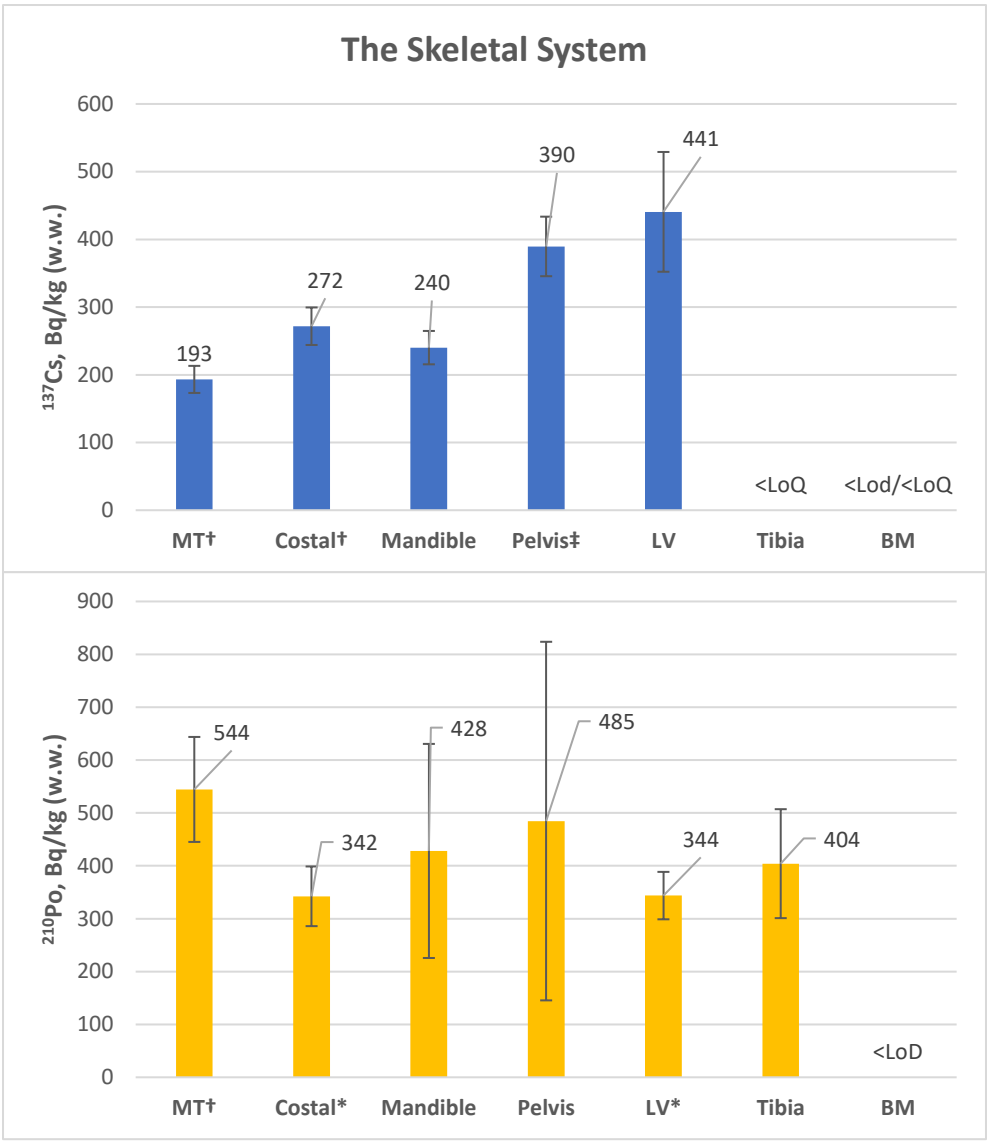

Figure 16: Activity concentrations of ^{137}Cs (top) and ^{210}Po (bottom), Bq/Kg (w.w.), in the skeletal system. Given as AM ± SD with n=3. *Given as AM ± SD with n=2. †Given as AM ± CSU with n=2. ‡Given as A ± CSU with n=1. Note the different scales of the y-axes.

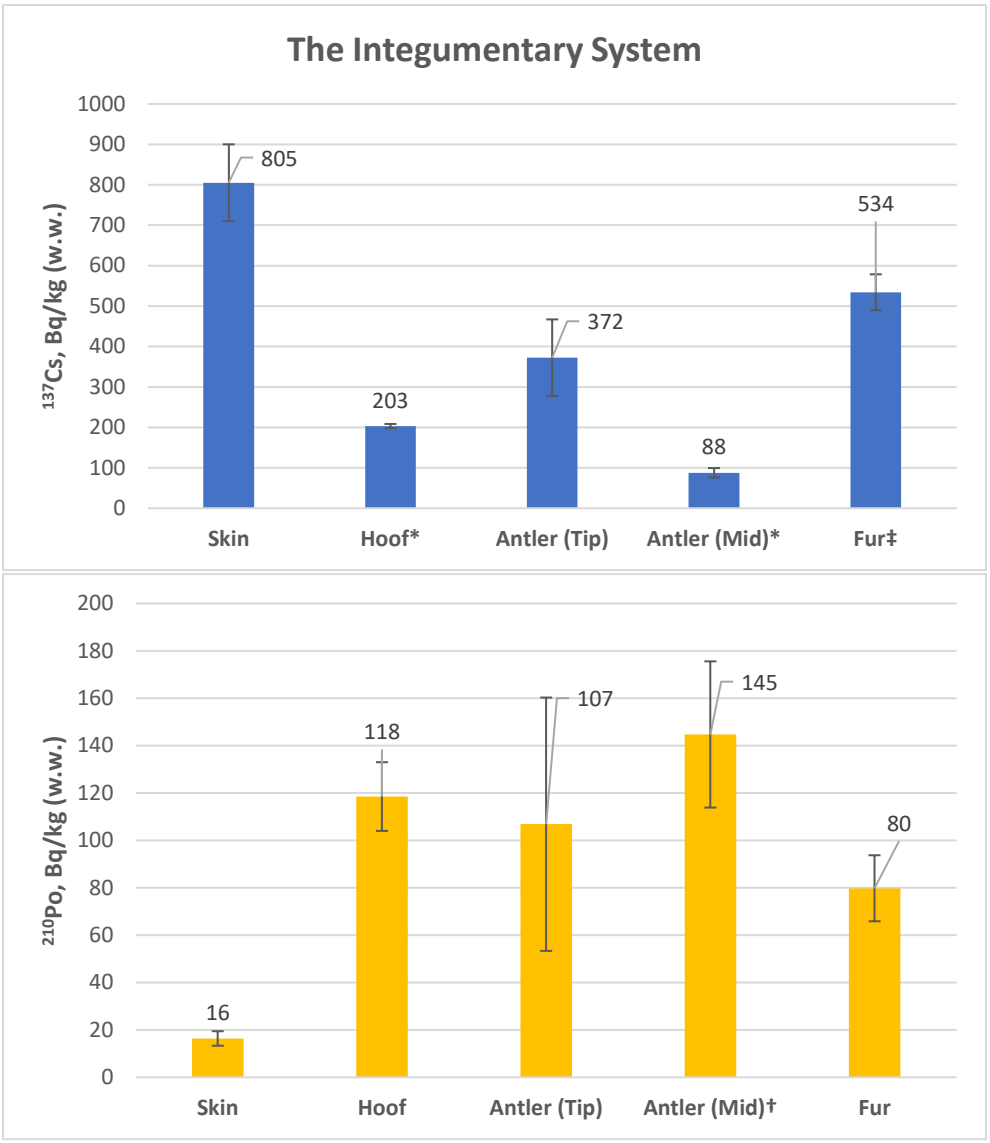

Figure 17: Activity concentrations of ^{137}Cs (top) and ^{210}Po (bottom), Bq/Kg (w.w.), in the integumentary system. Given as AM ± SD with n=3. *Given as AM ± SD with n=2. †Given as AM ± CSU with n=2. ‡Given as A ± CSU with n=1. Note the different scales of the y-axes.

Average ^{137}Cs concentrations differed 33-fold between the lowest and highest quantifiable value, fig. 11-17, with the highest average values observed in masseter and kidney, 2915 ± 379 and 2901 ± 103 Bq/kg respectively, followed by pancreas 2230 ± 208 Bq/kg fig. 11 and 13. Including the additional heads average ^{137}Cs concentration in masseter was 2735 ± 972 Bq/kg (n=10), with the highest value observed in reindeer F, 4883 ± 336 Bq/kg (appendix B, table B2). Average ^{137}Cs concentrations in muscular tissue was 2208 ± 58 Bq/kg (w.w.), fig 15. The variation between different parts of muscular tissue within a single reindeer ranged from 11 – 22 % owing to the comparably higher levels observed in the

masseter. Excluding masseter, the variation was more in line with previous studies (B. Åhman, 1994; Gaare & Staaland, 1994). The masseter has been shown to have a different fiber type composition in humans, (Österlund et al., 2011), drawing an analogy between the physiology of mammals, might explain the seemingly higher activity level in masseter compared to other muscular tissues. However, being beyond the scope of this study, this won't be speculated further. In addition, the relatively higher levels in masseter to muscular tissue is expected to be of little significance in the resulting dose to the reindeer considering the size of the tissue compartment relative to the whole body. ^{137}Cs concentration ratios in RBC relative to muscular tissue, (0.14 -0.20), was comparable to reported values from earlier studies on reindeer, (Gaare & Staaland, 1994; L. Skuterud et al., 2004). Excluding skeletal tissue, the skin and the GI tract, average ^{137}Cs levels differed 8-fold with relatively lower levels, by decreasing order, in the heart, udder, adrenal, liver, spleen, tongue, ILN, lungs, ovarium, BS, uterus, cerebellum, HT and RBC.

Average ^{137}Cs levels in the skeletal system ranged from <LoD to 441 ± 88 Bq/kg for, fig. 16, for BM and LV respectively. A difference ^{137}Cs concentration was observed in tibia (<LoQ for all three reindeer, table 2) compared to other hard skeletal tissue. Average ^{137}Cs concentration in tissues in the integumentary system ranged from 88 ± 18 to 805 ± 95 Bq/kg for antler (Mid) and skin respectively, fig. 17. With consistently higher ^{137}Cs concentrations observed in antler (Tip) in relation to antler (Mid) in individual reindeer, including the additional heads (except reindeer E and H where both were <LoQ).

Average ^{137}Cs levels in tissues of the GI tract ranged from 378 ± 43 to 1640 ± 470 Bq/kg in caecum and jejunum respectively, fig. 11. Jejunum containing the highest concentrations amongst the tissues of the GI tract is expected since soluble compounds of Cs are highly bioavailable, and a majority of monovalent ion absorption takes place in the jejunum (Sjaastad et al., 2016). Average ^{137}Cs concentration in RC was 400 ± 100 Bq/kg. It should be noted that reindeer A was slaughtered the same day the herd was guided into an enclosed area with limited forage availability and no access to water while reindeer B and C were slaughtered the next day. A fact that might contribute to the variability observed in ^{137}Cs concentrations between the reindeer in addition to the varying retention times of the different compartments of the GI tract.

In general, results from ^{137}Cs-analysis was in agreement with earlier studies, distributing preferably to certain soft tissues such as kidney, pancreas and muscular tissue (B. Åhman, 1994; C. R. Macdonald et al., 1996; Rissanen et al., 1990; L. Skuterud et al., 2004; Lavrans Skuterud, Gaare, et al., 2005; Patricia A. Thomas & Gates, 1999). ^{137}Cs levels in muscular tissue, liver and kidney were comparable to those reported by Lavrans et al., (Lavrans Skuterud, Gwynn, et al., 2005), from the same herd in September 2001. Confirming the previously stated persistence of ^{137}Cs in the environment (Lavrans Skuterud, Gaare, et al., 2005). The higher variation observed in masseter including the additional heads suggests that the variation between reindeer A, B and C isn't sufficient to reflect the variability within the herd.

^{210}Po-levels differed 88-fold among the tissues sampled, owing mainly to the consistently higher levels measured in skeletal tissue as opposed to soft tissues in agreement with earlier studies done on caribou and reindeer (Beasley & Palmer, 1966; Kauranen & Miettinen, 1969; P A Thomas et al., 1989). ^{210}Po levels in skeletal tissue were generally higher in reindeer C compared to the rest reindeer, with the highest ^{210}Po concentrations were observed in pelvis pelvis 849 ± 44 Bq/kg. Of the internal organs the highest ^{210}Po levels were observed in ILN, 119 (54 ± 5 – 178 ± 13) Bq/kg, the large variation owing to relatively lower activity measured in reindeer A for the lower end, and for reindeer C in the upper end. Average ^{210}Po-levels in muscular tissue 10 ± 5 Bq/kg, with highest individual measurement done in reindeer C, QF, 24 ± 3 Bq/kg. The distribution relative to kidney and liver, were comparable to the ones reported in Deer in Northern Poland, (Skwarzec & Prucnal, 2007). ^{210}Po in RBC 18 ± 1,5 Bq /kg was more comparable caribou measured in Finland December, (Kauranen & Miettinen, 1969). It should be noted that RBC was prepared and measured approximately one year after field work and the unsupported fraction of ^{210}Po were not estimated. While average ^{210}Po activity concentrations in muscular tissue were comparable to values reported by Lavrans et al., (Lavrans Skuterud, Gwynn, et al., 2005) from the same herd in December, activity concentrations in liver were lower in this study. Kauranen et al., (Kauranen & Miettinen, 1969) indicated a seasonal variation in reindeer ^{210}Po activity levels in reindeer, with a relatively lower liver activity concentration in early autumn compared to the rest of the year.

In addition, a model given by Persson et al., (B. R. R. Persson et al., 2018b), predicts ^{210}Po activity levels in reindeer liver and muscle throughout the year based on data from kauranen et al., (Kauranen & Miettinen, 1969), predicting a liver activity concentration minima in September, while activity concentrations in meat was lowest in august and on the rise by September, reaching a maxima in winter which is in agreement with the differences observed in this study. The comparable ^{210}Po levels in muscular tissue might be partly explained by differing retention times between various tissues in the body as well as the fact that these are the supported ^{210}Po-levels. Further on, the following periods were defined by Gaare & Staaland, (Gaare & Staaland, 1994), for reindeer ^{137}Cs accumulation in Vågå herding district; 1: Autumn accumulation period (August/early September). 2: Winter maximum period, 3: Spring decontamination and 4: Summer minimum period. ^{137}Cs levels with season is partly due to migration to different metabolic rate in various seasons of the year, new grazing area with differing diet composition. Regarding the higher ^{210}Pb/^{210}Po activity levels in lichen, (Lavrans Skuterud, Gwynn, et al., 2005) a seasonal variation in ^{210}Po wouldn't be that unthinkable.

Distribution of accumulation and estimated whole body concentration

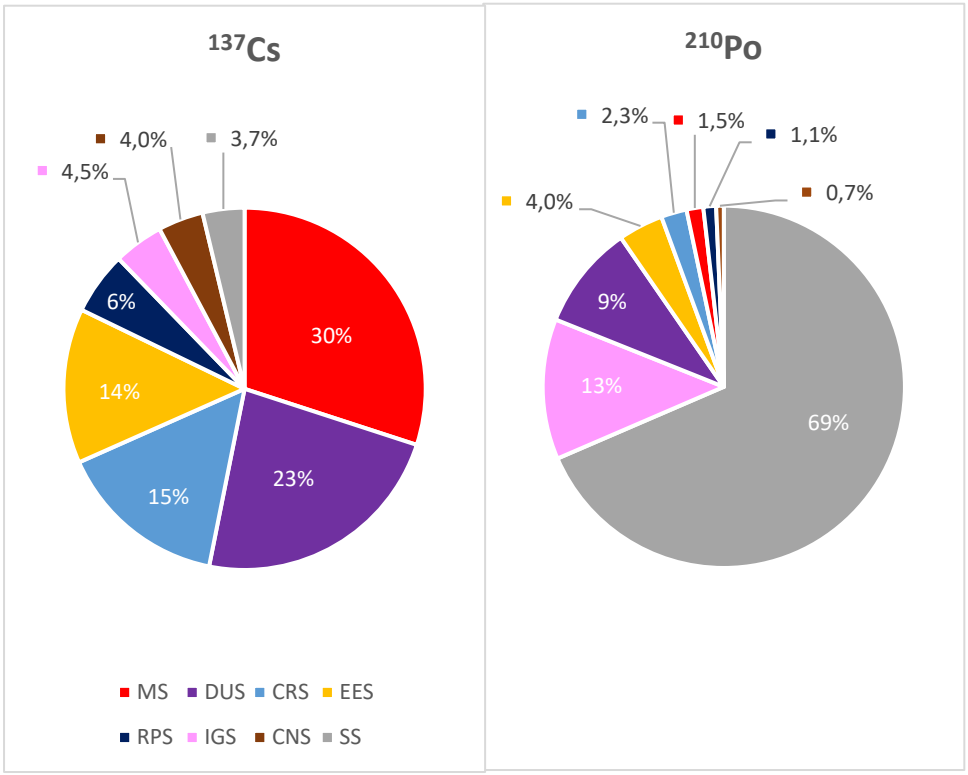

Figure 18: The relative accumulation in various organ systems given as a percentage of ^{137}Cs (left) and ^{210}Po (right) based on measured activity concentrations of different tissues in three semi-domesticated reindeer from Southern-Norway.

Table 4: Estimated whole-body concentration (C_{WB}) for ^{137}Cs and ^{210}Po in the three semi-domesticated reindeer. Given as Bq/kg for each reindeer and AM with the associated SD and RSD (%).

C_{WB}	A	B	C	AM	SD	RSD (%)
^{137}Cs	905	956	899	920	31	3 %
^{210}Po	43	57	95	65	27	42 %

Estimated Dose rates

Dose rates for internal exposure were estimated with DCs attained from BiotaDC software with weights, estimated weights and activity concentrations of the investigated radionuclides for each reindeer. ^{210}Po dose rates were weighted with a factor of 10 based on recommendations by (Chambers et al., 2006; Higley et al., 2012) to account for the relative biological effectiveness of alpha radiation. Absorbed fraction were gamma radiation, an absorption fraction was multiplied for Cs-137 dose rates based on data given by (Ulanovsky & Pröhl, 2006), consistent with the assumptions of the uniform isotropic model for 0.5 MeV photons. MLV and MRV as well as LL and RL were compartmentalized as the heart and lungs respectively. ^{137}Cs and ^{210}Po dose rates are presented collectively in column graphs, AM ± SD (mGy/d) as blue and yellow columns respectively.

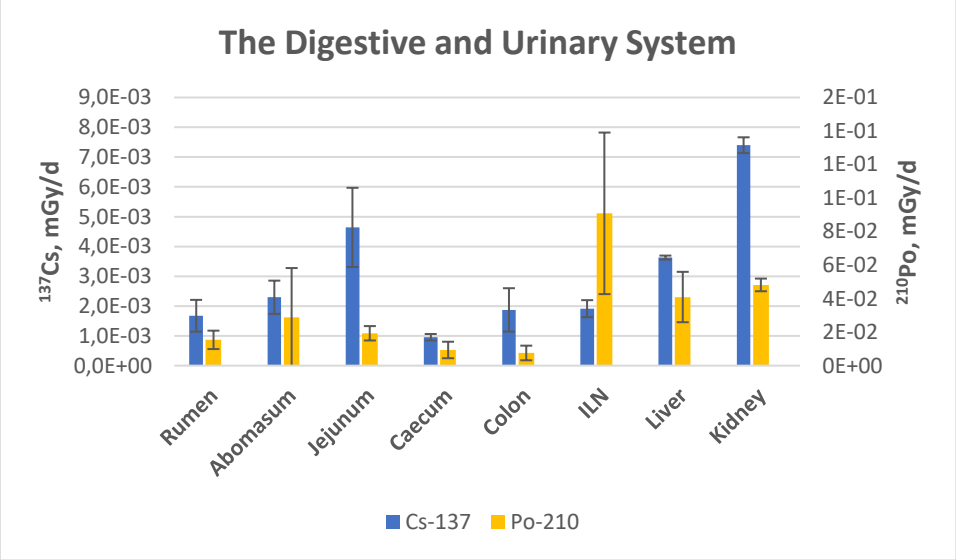

Figure 19: Estimated weighted dose rates (mGy/d) of ^{137}Cs and ^{210}Po, respectively, in the digestive and urinary system organs. Given as AM ± SD with n=3. Note the different scales of the y-axes.

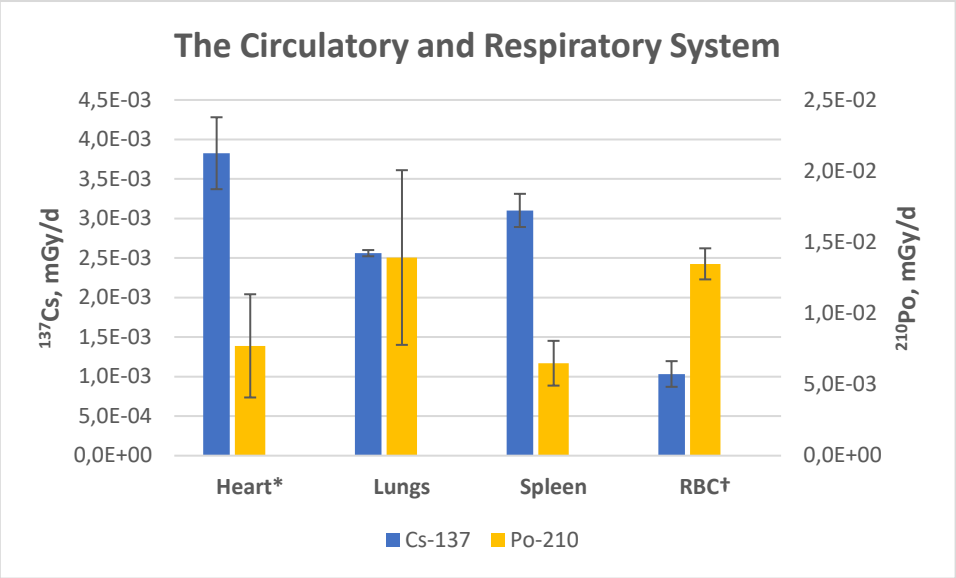

Figure 20: Estimated weighted dose rates (mGy/d) of ^{137}Cs and ^{210}Po, respectively, in the circulatory and respiratory system. Given as AM ± SD with n=3. *^{210}Po: Given as AM ± SD with n=2. †^{210}Po: Given as an absorbed dose rate ± SD with n=1. Note the different scales of the y-axes.

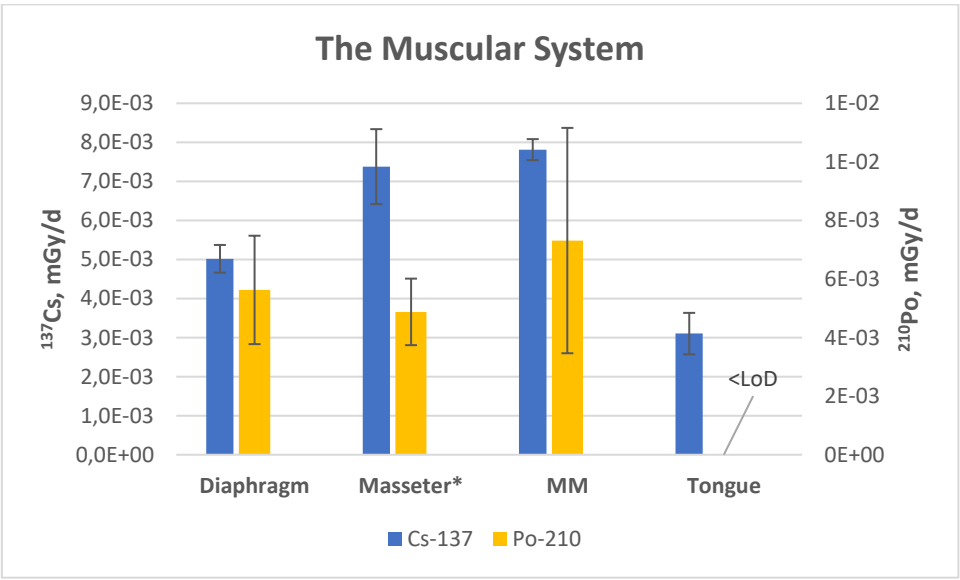

Figure 21: Estimated weighted dose rates (mGy/d) of ^{137}Cs and ^{210}Po, respectively, in the muscular system. Given as AM ± SD with n=3. *^{210}Po: AM ± CSU with n=2. Note the different scales of the y-axes.

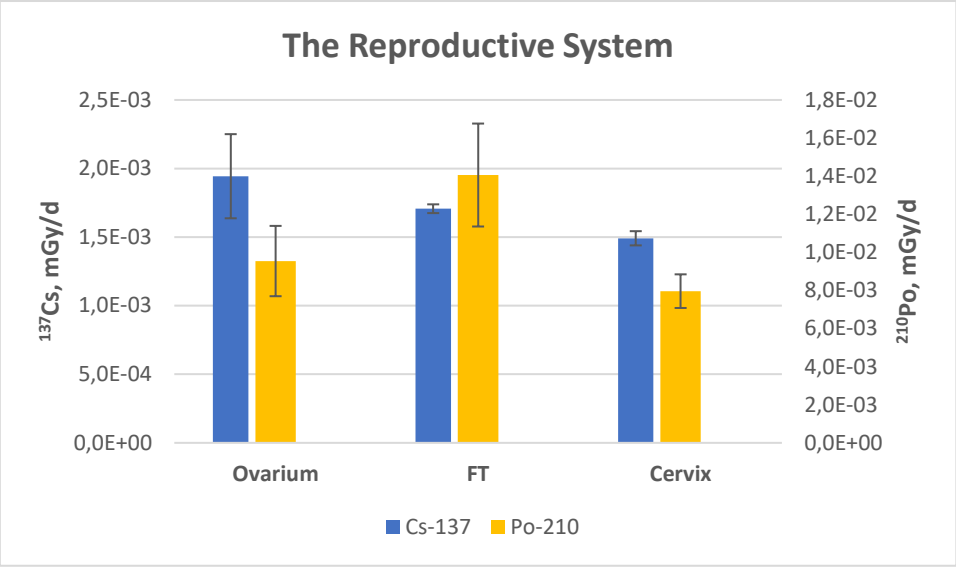

Figure 22: Estimated weighted dose rates (mGy/d) of ^{137}Cs and ^{210}Po, respectively, in the reproductive system. Given as AM ± SD with n=2. Note the different scales of the y-axes.

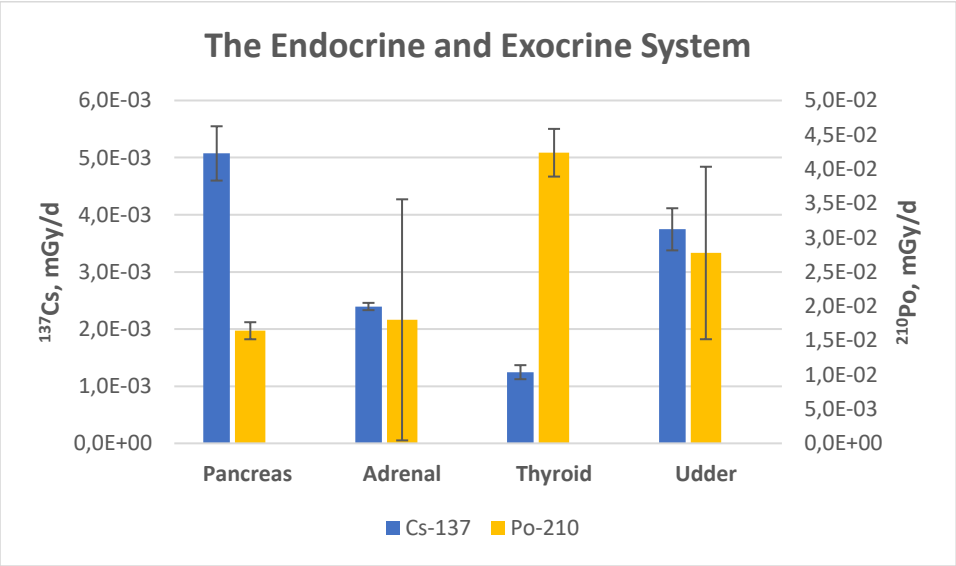

Figure 23: Estimated weighted dose rates (mGy/d) of ^{137}Cs and ^{210}Po, respectively, in the endocrine and exocrine system. Given as AM ± SD with n=3. Note the different scales of the y-axes.

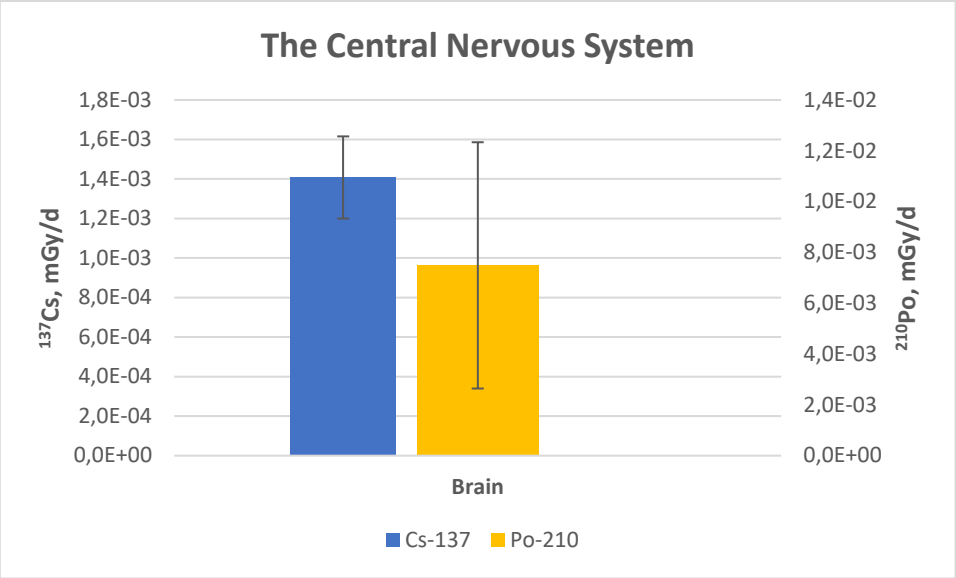

Figure 23: Estimated weighted dose rates (mGy/d) of ^{137}Cs and ^{210}Po, respectively, in the central nervous system. Given as AM ± SD with n=3. Note the different scales of the y-axes.

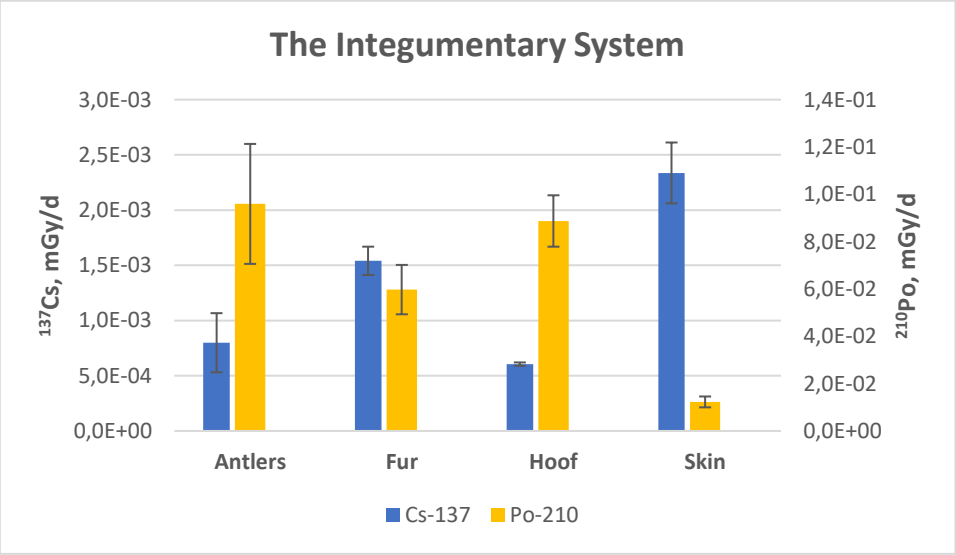

Figure 24: Estimated weighted dose rates (mGy/d) of ^{137}Cs and ^{210}Po, respectively, in the integumentary system. Given as AM ± SD with n=3. Note the different scales of the y-axes.

Estimated whole body dose and distribution of dose contribution from Cs-137 and Po-210

The pie-charts presents an estimated distribution of contributed dose of Cs-137 and Po-210 respectively. The estimation was by taking the weighted average of the estimated dose rates with the relative weight of the related tissue compartment to the live weight.

Table 4: Estimated whole-body dose (Wbd) from three semi-domesticated reindeer, given as mGy/d for each reindeer, AM with the associated SD and range as well as a ratio of the two investigated radionuclides.

Wbd (mGy/d)	A	B	C	AM	RSD (%)	Po/Cs
Cs-137	3.2E-03	3.4E-03	3.3E-03	3.3E-03	5.1	14
Po-210	3.1E-02	4.1E-02	7.0E-02	4.7E-02	43	

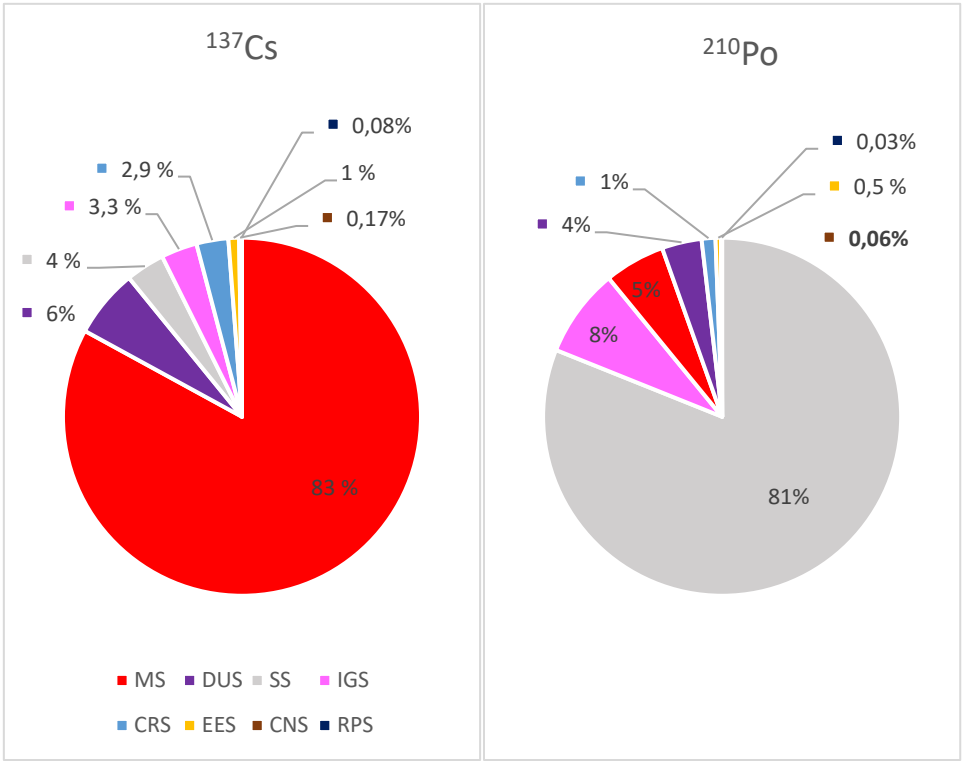

Figure 22: Pie-charts of estimated contributed dose distribution from ^{137}Cs and ^{210}Po respectively, in three semi-domesticated reindeer from Norway. Based on the estimated dose rates and given as a percentage.

Comparison of external and internal absorbed dose

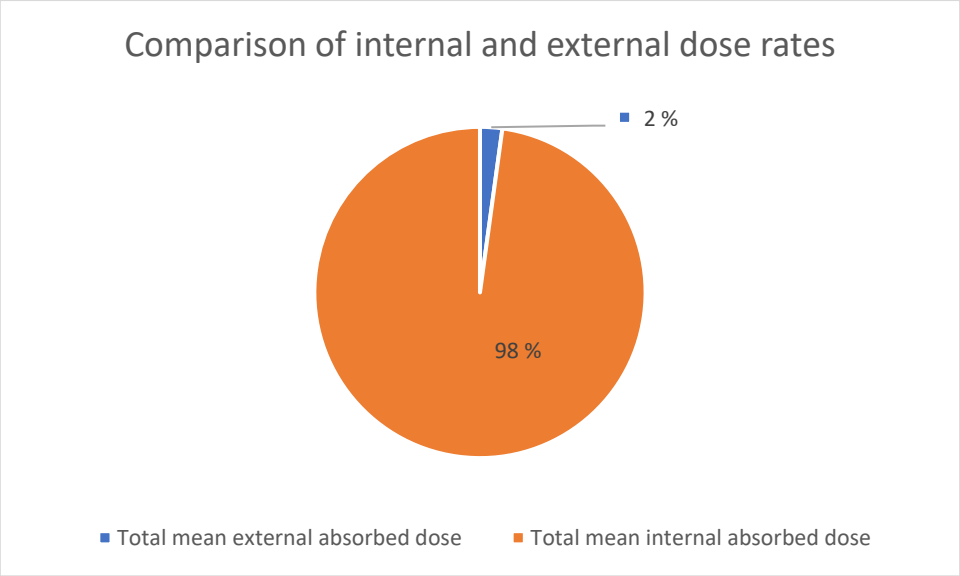

CONCLUSIONS

The dose arising from naturally occurring ^{210}Po were

References

Aarkrog, A. (1994). Radioactivity in Polar Regions Main Sources. *Water*, *25*, 21–35.

Åhman, B. (1994). Body burden and distribution of 137Cs in reindeer. *Rangifer*, *14*(1), 23. https://doi.org/10.7557/2.14.1.1129

Åhman, G., Åhman, B., & Rydberg, A. (1990). Consequences of the Chernobyl accident for reindeer husbandry in Sweden. *Rangifer*, *10*(3), 83. https://doi.org/10.7557/2.10.3.835

Allaye-Chan, A. C., White, R. G., Holleman, D. F., & Russell, D. E. (1990). Seasonal concentrations of cesium-137 in rumen content, skeletal muscles and feces of caribou from the Porcupine herd: lichen ingestion rates and implications for human consumption. *Rangifer*, *10*(3), 17. https://doi.org/10.7557/2.10.3.816

AMAP. (1998). Chapter 4: Ecological Characteristics of the Arctic. *AMAP Assessment Report: Arctic Pollution Issues*, 117–140.

Analysis, I. N. E. (n.d.). *IN ELEMENTAL ANALYSIS BEGINS WITH*.

Anspaugh, L. R. (2008). Chernobyl: Looking Back to Go Forward. *Environmental Consequences of the Chernobyl Accident and Their Remediation: 20 Years of Experience*, *September*, 47–76. https://www-pub.iaea.org/MTCD/Publications/PDF/Pub1312_web.pdf

Aramrun, K., Beresford, N. A., Skuterud, L., Hevrøy, T. H., Drefvelin, J., Bennett, K., Yurosko, C., Phruksarojanakun, P., Esoa, J., Yongprawat, M., Siegenthaler, A., Fawkes, R., Tumnoi, W., & Wood, M. D. (2019). Measuring the radiation exposure of Norwegian reindeer under field conditions. *Science of the Total Environment*, *687*, 1337–1343. https://doi.org/10.1016/j.scitotenv.2019.06.177

Armbruster, D. A., & Pry, T. (2008). Limit of blank, limit of detection and limit of quantitation. *The Clinical Biochemist. Reviews*, *29 Suppl 1*(October), S49-52. http://www.ncbi.nlm.nih.gov/pubmed/18852857%0Ahttp://www.pubmedcentral.nih.gov/articlerender.fcgi?artid=PMC2556583

Automated, F. (n.d.). *Simultaneous, Fully Automated Microwave Digestion System*.

backe1987 Fall-out pattern in Norway after the Chernobyl accident estimated from soil samples.pdf. (n.d.).

Beasley, T. M., & Palmer, H. E. (1966). Lead-210 and polonium-210 in biological samples from Alaska. *Science*, *152*(3725), 1062–1064. https://doi.org/10.1126/science.152.3725.1062

Bergman, R., Nelin, P., & Palo, T. (1993). *Caesium-137 in a boreal forest ecosystem*. *November*.

Bird, P. M. (1968). Studies of Fallout 137Cs in the Canadian North. *Archives of Environmental Health*, *17*(4), 631–638. https://doi.org/10.1080/00039896.1968.10665294

Blanchard, R. L., & Kearney, J. W. (1967). *Natural Radioactivity and NORM*. 1–45.

Brynildsen, L. I., Selnaes, T. D., Strand, P., & Hove, K. (1996). *Countermeasures for radiocesium in animal products in Norway after the Chernobyl accident - Techniques, effectiveness, and costs*. *5*.

Calmon, P., Fesenko, S., Voigt, G., & Linsley, G. (2009). Quantification of radionuclide transfer in terrestrial and freshwater environments. *Journal of Environmental Radioactivity*, *100*(9), 671–674. https://doi.org/10.1016/j.jenvrad.2009.06.021

Chambers, D. B., Osborne, R. V., & Garva, A. L. (2006). Choosing an alpha radiation weighting factor for doses to non-human biota. *Journal of Environmental Radioactivity*, *87*(1), 1–14. https://doi.org/10.1016/j.jenvrad.2005.10.009

Chen, C. C., Chyau, C. C., Liao, C. C., Hu, T. J., & Kuo, C. F. (2010). Harris Quantitative analytical chemistry. In *Journal of agricultural and food chemistry* (Vol. 58, Issue 22). https://doi.org/10.1021/jf103070m

Chen, Q. J., Hou, X. L., Dahlgaard, H., Nielsen, S. P., & Aarkrog, A. (2001). A rapid method for the separation of Po-210 from Pb-210 by TIOA extraction. *Journal of Radioanalytical and Nuclear Chemistry*, *249*(3), 587–593.

Choppin, G., Liljenzin, J.-O., Rydberg, J., & Ekberg, C. (2013). Detection and Measurement Techniques. In *Radiochemistry and Nuclear Chemistry*. https://doi.org/10.1016/b978-0-12-405897-2.00009-4

Copplestone, D., Bielby, S., Jones, S., Patton, D., Daniel, P., & Gize, I. (2001). *Impact assessment of ionising radiation on wildlife R&D Publication 128*.

Currie, L. A. (1968). Limits for Qualitative Detection and Quantitative Determination: Application to Radiochemistry. *Analytical Chemistry*, *40*(3), 586–593. https://doi.org/10.1021/ac60259a007

DSA. (2015). *Stråledoser fra miljøet*.

E. Vano, D.L. Miller, C.J. Martin, M.M. Rehani, et al. (2015). *Annals o f the ICRP* (Vol. 44, Issue 1).

F. Carvalho et al. (2017). The environmental behaviour of Polonium. *International Atomic Energy Agency*, *7*(6), 585. https://doi.org/10.1016/0883-2927(92)90073-c

Gaare, E. (1987). The Chernobyl accident: Can lichens be used to characterize a radiocesium contaminated range? *Rangifer*, *7*(2), 46. https://doi.org/10.7557/2.7.2.716

Gaare, E., & Staaland, H. (1994). Pathways of fallout radiocaesium via reindeer to man. *Conservation, Nature*.

Garner, R. J., & Comar, C. L. (1972). Transfer of radioactive materials from the terrestrial environment to animals and man. *C R C Critical Reviews in Environmental Control*, *2*(1–4), 337–385. https://doi.org/10.1080/10643387109381585

Hanson, W. C. (1967). Cesium-137 in alaskan lichens, caribou and eskimos. *Health Physics*, *13*(4), 383–389. https://doi.org/10.1097/00004032-196704000-00007

Hanson, W. C., & Palmer, H. E. (1965). Seasonal cycle of 137Cs in some alaskan natives and animals. *Health Physics*, *11*(12), 1401–1406. https://doi.org/10.1097/00004032-196512000-00018

Hanson, Wayne C. (1966). Cesium-137 body burdens in Alaskan Eskimos during the summer of 1965. *Science*, *153*(3735), 525–526. https://doi.org/10.1126/science.153.3735.525

Helmer, R. G., & Chechev, V. P. (2007). Cs 137. *Table de Radionucleides*, *0015*(2), 1–8.

Henricsson, F., Ranebo, Y., Holm, E., & Roos, P. (2011). Aspects on the analysis of 210Po. *Journal of Environmental Radioactivity*, *102*(5), 415–419. https://doi.org/10.1016/j.jenvrad.2010.09.010

Henricsson, Fredrik, & Persson, B. R. R. (2012). Polonium-210 in the bio-sphere: Bio-kinetics and biological effects. *Radionuclides: Sources, Properties and Hazards*, 33–60.

Henriksen, T. (1988). *Fallout and Radiation Doses in Norway*. *14*, 157–163.

Higley, K. A., Kocher, D. C., Real, A. G., & Chambers, D. B. (2012). Relative biological

effectiveness and radiation weighting factors in the context of animals and plants. *Annals of the ICRP*, *41*(3–4), 233–245. https://doi.org/10.1016/j.icrp.2012.06.014

Holleman, D. F., Luick, J. R., & Whicker, F. W. (1971). Transferof radiocesium from lichen to reindeer. *Health Physics*, *21*(5), 657–666. https://doi.org/10.1097/00004032-197111000-00006

Holleman, D. F., White, R. G., & Allaye-Chan, A. C. (1990). Modelling of radiocesium transfer in the lichen-reindeer / caribou-wolf food chain Key words : The computer program - SAAM and The model - A description and the output. *Rangifer*, *No. 3*, 39–42.

Holtzman, R. B. (1966). Natural levels of Lead-210, Polonium-210 and Radium-226 in humans and biota of the arctic. *Nature*.

IAEA. (2006). Polonium-210. *Polonium-210*, *210*(Factsheets & FAQs).

IAEA. (2011). Radioactive Particles in the Environment: Sources, Particle Characterization and Analytical Techniques - IAEA TECDOC No. 1663. In *IAEA TECDOC No. 1663*. https://doi.org/IAEA-TECDOC-1663

Kauranen, P., & Miettinen, J. K. (1969). 210Po and 210Pb in the Arctic food chain and the natural radiation exposure of lapps. *Health Physics*, *16*(3), 287–295. https://doi.org/10.1097/00004032-196903000-00004

L'Annunziata, M. F. (2012). Solid Scintillation Analysis. In *Handbook of Radioactivity Analysis* (Third Edit, Issue 2004). Elsevier. https://doi.org/10.1016/B978-0-12-384873-4.00016-5

Langford, J. C., & Brodzinski, B. L. (1974). Contamination Problems and the Measurement of Low-Level Polonium-210. *Radiochimica Acta*, *21*(1–2), 117–118. https://doi.org/10.1524/ract.1974.21.12.117

Lecomte, J.-F., Solomon, S., Takala, J., Jung, T., Strand, P., Murith, C., Kiselev, S., Zhuo, W., Shannoun, F., & Janssens, A. (2015). *Annals o f the ICRP* (Vol. 44, Issue 1).

Lehto, J., & Hou, X. (2010). Chemistry and Analysis of Radionuclides. In *Chemistry and Analysis of Radionuclides*. https://doi.org/10.1002/9783527632770

Lidén, K., & Gustafsson, M. (1966). 137 Cs levels of different population groups in Sweden. *Acta Radiologica: Diagnosis*, 38–46. https://doi.org/10.1177/0284185166004s25407

Macdonald, C. R., Ewing, L. L., Elkin, B. T., & Wiewel, A. M. (1996). Regional variation in radionuclide concentrations and radiation dose in caribou (Rangifer tarandus) in the Canadian Arctic; 1992-94. *Science of the Total Environment*, *182*(1–3), 53–73. https://doi.org/10.1016/0048-9697(95)05037-X

Macdonald, Colin R., Elkin, B. T., & Tracy, B. L. (2007). Radiocesium in caribou and reindeer in northern Canada, Alaska and Greenland from 1958 to 2000. *Journal of Environmental Radioactivity*, *93*(1), 1–25. https://doi.org/10.1016/j.jenvrad.2006.11.003

Matthews, K. M., Kim, C. K., & Martin, P. (2007). Determination of 210Po in environmental materials: A review of analytical methodology. *Applied Radiation and Isotopes*, *65*(3), 267–279. https://doi.org/10.1016/j.apradiso.2006.09.005

Mattsson, L. J. S. (1972). *Cs-137 in the reindeer lichen cladonia alpestris; deposition, retention and internal distribution, 1961-1970.* 1961–1970.

Mattsson, L. J. S., & Persson, R. B. R. (1971). *Radioecology of Na-22, Po-210 and Pb-210 in the unique foodchain Lichen -Reindeer - Man*.

Mayes, R. W., Beresford, N. A., Howard, B. J., Vandecasteele, C. M., & Stakelum, G. (1996). Use of the true absorption coefficient as a measure of bioavaitability of radiocaesium in ruminants. *Radiation and Environmental Biophysics*, *35*(2), 101–109. https://doi.org/10.1007/BF02434032

MIETTINEN, J. K., & HÄSÄNEN, E. (1967). 137Cs IN FINNISH LAPPS AND OTHER FINNS IN 1962–6. *Radioecological Concentration Processes*, 221–231. https://doi.org/10.1016/b978-0-08-012122-2.50028-1

Moore, H. E., Martell, E. A., & Poet, S. E. (1976). Sources of Polonium-210 in Atmosphere. *Environmental Science and Technology*, *10*(6), 586–591. https://doi.org/10.1021/es60117a005

Nash, K. L., & Braley, J. C. (2011). Chemistry of radioactive materials in the nuclear fuel cycle. In *Advanced Separation Techniques for Nuclear Fuel Reprocessing and Radioactive Waste Treatment*. Woodhead Publishing Limited. https://doi.org/10.1533/9780857092274.1.3

NRPA. (2006). NRPA Bulletin. *Distribution*, *November*, 0–1.

O'Hara, T. M., Dasher, D., George, J. C., & Woshner, V. (1999). Radionuclide levels in caribou of Northern Alaska in 1995-96. *Arctic*, *52*(3), 279–288. https://doi.org/10.14430/arctic933

Österlund, C., Thornell, L. E., & Eriksson, P. O. (2011). Differences in fibre type composition between human masseter and biceps muscles in young and adults reveal unique masseter fibre type growth pattern. *Anatomical Record*, *294*(7), 1158–1169. https://doi.org/10.1002/ar.21272

Paatero, J., & Salminen-Paatero, S. (2020). Transfer of transuranium elements along the food chain lichen-reindeer-man – A review of investigations in Finnish Lapland. *Journal of Environmental Radioactivity*, *212*(November 2019), 106126. https://doi.org/10.1016/j.jenvrad.2019.106126

Pálsson, S. E., Egilsson, K., Pórisson, S., Magnússon, S. M., Ólafsdóttir, E. D., & Indriason, K. (1994). Transfer of radiocaesium from soil and plants to reindeer in Iceland. *Journal of Environmental Radioactivity*, *24*(2), 107–125. https://doi.org/10.1016/0265-931X(94)90048-5

Persson, B. R. R., Gjelsvik, R., & Holm, E. (2018a). Radioecological modelling of Polonium-210 and Caesium-137 in lichen-reindeer-man and top predators. *Journal of Environmental Radioactivity*, *186*, 54–62. https://doi.org/10.1016/j.jenvrad.2017.08.006

Persson, B. R. R., Gjelsvik, R., & Holm, E. (2018b). Radioecological modelling of Polonium-210 and Caesium-137 in lichen-reindeer-man and top predators. *Journal of Environmental Radioactivity*, *186*, 54–62. https://doi.org/10.1016/j.jenvrad.2017.08.006

Persson, R. B. R. (1969). Iron-55 in northern Sweden; relationships and annual variation from 1956 until 1967 in lichen and reindeer as well as uptake and metabolism in man. *Health Physics*, *16*(1), 69–78. https://doi.org/10.1097/00004032-196901000-00008

Persson, R. B. R. (1974). Stable lead and 210Pb in the food chain lichen → reindeer → man. *Int.Atom.Energy Agency Vienna*, *January 1974*, 231–247.

Pröhl, G., Golikov, S., Doi, M., Brown, J., Kamboj, S., Battle, V. i, Ulanovsky, J. A., & Beaugelin-

Seiller, K. (2008). ICRP Publication 108: Environmental Protection: the Concept and Use of Reference Animals and Plants. In *ICRP Publication 108* (p. 247). Elsevier Ltd.

Rahola, T., & Miettinen, J. K. (1973). Accumulation of 137cs in finnish lapps. *Archives of Environmental Health*, *26*(2), 67–69. https://doi.org/10.1080/00039896.1973.10666225

Reinoso-Maset, E., Brown, J., Pettersen, M. N., Steenhuisen, F., Tetteh, A., Wada, T., Hinton, T. G., Salbu, B., & Lind, O. C. (2020). Linking heterogeneous distribution of radiocaesium in soils and pond sediments in the Fukushima Daiichi exclusion zone to mobility and potential bioavailability. *Journal of Environmental Radioactivity*, *211*(October 2019), 106080. https://doi.org/10.1016/j.jenvrad.2019.106080

Ringberg, T. M., White, R. G., Holleman, D. F., & Luick, J. R. (1981a). Body growth and carcass composition of lean reindeer (Rangifer tarandus tarandus L.) from birth to sexual maturity . *Canadian Journal of Zoology*, *59*(6), 1040–1044. https://doi.org/10.1139/z81-145

Ringberg, T. M., White, R. G., Holleman, D. F., & Luick, J. R. (1981b). Prediction of carcass composition in reindeer (Rangifer tarandus tarandus L.) by use of selected indicator bones and muscles . *Canadian Journal of Zoology*, *59*(4), 583–588. https://doi.org/10.1139/z81-086

Rissanen, K., Rahola, T., & Aro, P. (1990). Distribution of cesium-137 in reindeer. *Rangifer*, *10*(2), 57. https://doi.org/10.7557/2.10.2.795

Robillard, S., Beauchamp, G., Paillard, G., & Bélanger, D. (2002). Levels of cadmium, lead, mercury and 137caesium in caribou (Rangifer tarandus) tissues from Northern Québec. *Arctic*, *55*(1), 1–9. https://doi.org/10.14430/arctic686

Salbu, B., Lind, O. C., & Skipperud, L. (2004). Radionuclide speciation and its relevance in environmental impact assessments. *Journal of Environmental Radioactivity*, *74*(1–3), 233–242. https://doi.org/10.1016/j.jenvrad.2004.01.008

Salbu, Brit. (2016). Environmental impact and risk assessments and key factors contributing to the overall uncertainties. *Journal of Environmental Radioactivity*, *151*, 352–360. https://doi.org/10.1016/j.jenvrad.2015.09.001

Salmon, P. L., Henshaw, D. L., Bondarenko, O. A., Thomas, P. A., Macdonald, C. R., & Goodall, C. (1995). Distribution of 210pb at endosteal surfaces of bone from canadian arctic caribou. *International Journal of Radiation Biology*, *68*(6), 655–661. https://doi.org/10.1080/09553009514551661

Salmon, P. L., Henshaw, D. L., Keitch, P. A., Allen, J. E., & Fews, A. P. (1994). TASTRAK spectroscopy of polonium-210 alpha-particle activity at bone surfaces: Evidence for a concentrated surface deposit less than 3 µm deep. *Radiation Research*, *140*(1), 63–71. https://doi.org/10.2307/3578569

Sheppard, S. C. (2011). Review of "Handbook of Parameter Values for the Prediction of Radionuclide Transfer in Terrestrial and Freshwater Environments." *Journal of Environmental Radioactivity*, *102*(2), 217. https://doi.org/10.1016/j.jenvrad.2010.10.004

Sjaastad, Ø., Sand, O., & Hove, K. (2016). *Physiology of Domestic Animals. Third edition*. Scandinavian Veterinary Press.

Skogland, T. (1986). *High radio-cesium contamination of wild reindeer from southern Norway following the Chernobyl accident*. 1986.

Skuterud, L., Pedersen, Staaland, H., Røed, K. H., Salbu, B., Liken, A., & Hove, K. (2004). Absorption, retention and tissue distribution of radiocaesium in reindeer: Effects of diet and radiocaesium source. *Radiation and Environmental Biophysics*, *43*(4), 293–301. https://doi.org/10.1007/s00411-004-0257-4

Skuterud, L, Hevrøy, T. H., & Thørring, H. (2016). *Caesium-137 in Norwegian reindeer and Sámi herders – 50 years of studies*. *April 2018*.

Skuterud, Lavrans. (2005). *Investigation of selected natural and anthropogenic radionuclides in reindeer (Rangifer tarandus tarandus) and lynx (Lynx lynx)*.

Skuterud, Lavrans, Gaare, E., Eikelmann, I. M., Hove, K., & Steinnes, E. (2005). Chernobyl radioactivity persists in reindeer. *Journal of Environmental Radioactivity*, *83*(2), 231–252. https://doi.org/10.1016/j.jenvrad.2005.04.008

Skuterud, Lavrans, Gwynn, J. P., Gaare, E., Steinnes, E., & Hove, K. (2005). 90Sr, 210Po and

210Pb in lichen and reindeer in Norway. *Journal of Environmental Radioactivity*, *84*(3), 441–456. https://doi.org/10.1016/j.jenvrad.2005.04.016

Skuterud, Lavrans, Radiation, N., & Authority, N. S. (2014). *Radioactive contamination in reindeer herders and other people in Radioaktiv forurensning i befolkningen Reindriftsutøvere og andre personer i Kautokeino 1965 – 2010*. *January 2013*.

Skwarzec, B., & Prucnal, M. (2007). Accumulation of polonium 210Po in tissues and organs of deer carvidae from Northern Poland. *Journal of Environmental Science and Health - Part B Pesticides, Food Contaminants, and Agricultural Wastes*, *42*(3), 335–341. https://doi.org/10.1080/03601230701229346

Smith, J. T., & Beresford, N. A. (2006). Radioactive fallout and environmental transfers. *Chernobyl — Catastrophe and Consequences*, 35–80. https://doi.org/10.1007/3-540-28079-0_2

Solatie, D., Junttila, M., & Vesterbacka, P. (2006). 210Po and 210Pb in the food chain lichen-reindeer-human. *Radiochemistry*, *48*(6), 632–633. https://doi.org/10.1134/S106636220606018X

Staaland, H., Jacobsen, E., & White, R. G. (1979). Comparison of the Digestive Tract in Svalbard and Norwegian Reindeer. *Arctic and Alpine Research*, *11*(4), 457. https://doi.org/10.2307/1550563

Strumińska-Parulska, D. I., Szymańska, K., & Skwarzec, B. (2015). Determination of 210Po in hair of domestic animals from Poland and Norway. *Journal of Radioanalytical and Nuclear Chemistry*, *306*(1), 71–78. https://doi.org/10.1007/s10967-015-4062-0

Svensson, G. K., & Lidén, K. (1965). The transport of 137Cs from lichen to animal and man. *Health Physics*, *11*(12), 1393–1400. https://doi.org/10.1097/00004032-196512000-00017

Thomas, D. J., Tracey, B., Marshall, H., & Norstrom, R. J. (1992). Arctic terrestrial ecosystem contamination. *Science of the Total Environment, The*, *122*(1–2), 135–164. https://doi.org/10.1016/0048-9697(92)90247-P

Thomas, P A, Sheard, J. W., & Swanson, S. (1989). *TRANSFER OF 210Po and 210Pb THROUGH*

THE LICHEN-CARIBOU-WOLF FOOD CHAIN OF NORTHERN CANADA.

Thomas, Patricia A., & Gates, T. E. (1999). Radionuclides in the lichen-caribou-human food chain near uranium mining operations in northern Saskatchewan, Canada. *Environmental Health Perspectives*, *107*(7), 527–537. https://doi.org/10.1289/ehp.99107527

Tracy, B. L. (2012). Encyclopedia of Sustainability Science and Technology. In *Radiation Effects on Caribou and Reindeer*. https://doi.org/10.1007/978-1-4419-0851-3

Ulanovsky, A., & Pröhl, G. (2006). A practical method for assessment of dose conversion coefficients for aquatic biota. *Radiation and Environmental Biophysics*, *45*(3), 203–214. https://doi.org/10.1007/s00411-006-0061-4

Ulanovsky, A., & Pröhl, G. (2012). Dosimetry for Reference Animals and Plants: Current state and prospects. *Annals of the ICRP*, *41*(3–4), 218–232. https://doi.org/10.1016/j.icrp.2012.06.034

Underwood, W. J., Blauwiekel, R., Delano, M. L., Gillesby, R., Mischler, S. A., & Schoell, A. (2015). Chapter 15 - Biology and Diseases of Ruminants (Sheep, Goats, and Cattle). In *Laboratory Animal Medicine: Third Edition* (Third Edit). Elsevier Inc. https://doi.org/10.1016/B978-0-12-409527-4.00015-8

Vajda, N., Pöllänen, R., Martin, P., & Kim, C.-K. (2020). Alpha spectrometry. In *Handbook of Radioactivity Analysis* (Vol. 1). https://doi.org/10.1016/b978-0-12-814397-1.00005-4

Verplancke, J., Fettweis, P. F., Venkataraman, R., Young, B. M., & Schwenn, H. (2012). Semiconductor Detectors. In *Handbook of Radioactivity Analysis* (Third Edit). Elsevier Inc. https://doi.org/10.1016/B978-0-12-384873-4.00005-0

White, R. G., Holleman, D. F., & Allaye-Chan, A. C. (1986). Radiocesium concentrations in the lichen-reindeer/caribou food chain: Before and after Chernobyl. *Rangifer*, *6*(1), 24. https://doi.org/10.7557/2.6.1-app.579

Wiklund, E., Finstad, G., Johansson, L., Aguiar, G., & Bechtel, P. J. (2008). Carcass composition and yield of Alaskan reindeer (Rangifer tarandus tarandus) steers and effects of electrical stimulation applied during field slaughter on meat quality. *Meat*

Science, *78*(3), 185–193. https://doi.org/10.1016/j.meatsci.2007.06.004

Wiklund, Eva. (2017). *Composition and quality of reindeer (Rangifer tarandus L) carcasses*. *August*.

Yankovich, T. L., Beresford, N. A., Wood, M. D., Aono, T., Andersson, P., Barnett, C. L., Bennett, P., Brown, J. E., Fesenko, S., Fesenko, J., Hosseini, A., Howard, B. J., Johansen, M. P., Phaneuf, M. M., Tagami, K., Takata, H., Twining, J. R., & Uchida, S. (2010). Whole-body to tissue concentration ratios for use in biota dose assessments for animals. *Radiation and Environmental Biophysics*, *49*(4), 549–565. https://doi.org/10.1007/s00411-010-0323-z

APPENDIX A

This section contains data on background measurements and analytical and procedural blanks utilized in ^{137}Cs-analysis, (table A1-A2), and ^{210}Po-analysis (table A3-A5).

Table A1: Separate blank runs on the NaI-scintillation detector to determine the background contribution in ^{137}Cs-analysis. Given as counts per minute (CPM) with the related counting uncertainty (%) and the estimated background contribution given as AM ± ASD utilized in ^{137}Cs-activity determination as well as in estimating the detection and quantification limits.

Blank #	CPM	u(%)
Blank 1	14,39	26,36
Blank 2	14,94	25,87
Blank 3	16,53	24,59
Blank 4	14,6	26,17
Blank 5	16,38	24,71
Blank 6	16,52	24,61
Blank 7	16,54	24,59

Blank 8	14,5	26,26
Blank 9	16,2	24,84
Blank 10	15,46	25,43
Blank 11	15,74	25,2
Blank 12	16,47	24,64
Blank 13	15,24	25,61
Blank 14	15,5	25,4
Blank 15	16,6	24,54
Blank 16	17,53	23,89
AM ± ASD	15,8 ± 0,915	

Table A2: Reference materials utilized in estimating the efficiency of the NaI-scintillation detector, achieving an estimated counting efficiency of 16.9 ± 0.7 %.

Reference materials	CPM	u(%)	Count eff. (%)	Certified Activity (DPM)	Estimated Efficiency
^{137}Cs-test low	384,71	5,1	17,8	2167	0,177531
^{137}Cs-test high	2953,52	1,84	17,0	17394	0,169801
IAEA 373 6,812g	430,74	4,82	16,1	2670	0,161326
^{137}Cs-test low	385,37	5,09	17,8	2167	0,177836
^{137}Cs-test high	2935,96	1,85	16,9	17394	0,168792
IAEA 373	429,32	4,83	16,1	2670	0,160794
AM ± ASD					0,169 ± 0,007

Table A3: Background measurement on the alpha-spectrometer, used for calculation of activity concentrations of ^{210}Po.

Detector	Counts			CPS	
	^{209}Po	^{210}Po	Live time	^{209}Po	^{210}Po
1	34	27	692220	4.91E-05	3.90E-05
2	58	25	692244	8.38E-05	3.61E-05
3	62	32	692453	8.95E-05	4.62E-05
4	63	15	692489	9.10E-05	2.17E-05
6	21	5	692553	3.03E-05	7.22E-06

Table A4: Data on Analytical blanks, counts of tracer and analyte with counting uncertainty (%) as well as duration of measurement given in seconds, detector # and counts per second (CPS).

AB #	Counts				Time	Detector	CPS	
	209	u(%)	210	u(%)			209	210
3	138	9	32	18	263309	1	0.000524099	0.00012153
4	365	5	168	8	939249	2	0.000388608	0.000178866
2	673	4	217	7	1379595	3	0.000487824	0.000157293
7	446	5	21	22	94567	3	0.004716233	0.000222065
3	105	10	22	21	262094	4	0.00040062	8.39394E-05
5	219	7	111	9	343498	4	0.000637558	0.000323146
6	441	5	17	24	87383	4	0.005046748	0.000194546
8	5132	1	111	9	938228	4	0.005469886	0.000118308
1	100	10	223	7	344636	6	0.000290161	0.00064706
3	476	5	128	9	1157624	6	0.000411187	0.000110571

Table A5: Data on procedural blanks, counts of tracer and analyte with counting uncertainty (%) as well as duration of measurement given in seconds, detector and counts per second (CPS). *The measurement of PB2 in detector 2 were involved in electrical blackout mid-measurement, while the measurement of PB7 at detector 2 were not found when looking through specter data, these were still involved in calculating the limit of detection, resulting in a more conservative estimate.

PB #	Counts				Time (seconds)	Detector	CPS	
	^{209}Po	u(%)	^{210}Po	u(%)			^{209}Po	^{210}Po
1	161	8	103	10	2338326	1	6.88527E-05	4.40486E-05
4	61	13	144	8	940258	1	6.48758E-05	0.000153149
7	74	12	40	16	441894	1	0.000167461	9.05194E-05
8	126	9	58	13	418773	1	0.000300879	0.0001385
1	233	7	80	11	2415779	2	9.64492E-05	3.31156E-05
3	80	11	156	8	1032722	2	7.74652E-05	0.000151057
5	39	16	119	9	418900	2	9.3101E-05	0.000284077
8	165	8	66	12	441984	2	0.000373317	0.000149327
2	36	17	62	13	442065	3	8.1436E-05	0.000140251
4	49	14	68	12	419045	3	0.000116933	0.000162274

5	108	10	276	6	940536.92	3	0.000114828	0.000293449
2	34	17	63	13	419139	4	8.11187E-05	0.000150308
4	46	15	58	13	442177	4	0.000104031	0.000131169
7	239	6	128	9	1157620	4	0.000206458	0.000110572
2	54	14	374	5	1898681	6	2.84408E-05	0.000196979
6	40	16	38	16	263399	6	0.000151861	0.000144268
7	83	11	30	18	419265	6	0.000197965	7.15538E-05
8	285	6	158	8	936689.9	6	0.000304263	0.000168679
2*	38	16	47	15	1157560	2	3.27E-05	4.06E-05
7*	56	13	23	21	262005	2	2.14E-04	8.78E-05

APPENDIX B

The tables given below show the determined activity concentrations for the radionuclides, given as Bq/kg ± SD, on a wet weight (w.w.) and dry weight (d.w.) basis. The SD reflects the total propagated uncertainty through the measurement procedure. Table B1 contains the determined ^{137}Cs activity concentrations in various tissues from reindeer A, B and C. Table B2 contains determined ^{137}Cs activity concentrations from the additional seven reindeer heads. Table B4 contains the determined ^{210}Po activity concentrations in various tissues from reindeer A, B and C. Table B4-B5 contains the determined ^{210}Po activity concentrations from replicate measurements in reindeer A and C respectively. Samples that were not collected or not analyzed are marked nc and na, respectively. Data below the detection or quantification limits are left uncensored but marked and elaborated in the related table text.

Table B1: Determined ^{137}Cs activity concentrations from reindeer A, B and C. Given as Bq/kg ± SD on wet weight (w.w.) and dry weight (d.w.) basis. With the associated relative standard deviation (RSD) as a percentage. The SD reflects the total propagated uncertainty from the analysis. Samples that were <LoD are colored blue and marked with an asterisk. Samples that were <LoQ are colored purple and marked with a double asterisk.

	A			B			C		
Tissues	**Bq/kg (w.w.)**	**Bq/kg (d.w.)**	**RSD (%)**	**Bq/kg (w.w.)**	**Bq/kg (d.w.)**	**RSD (%)**	**Bq/kg (w.w.)**	**Bq/kg (d.w.)**	**RSD (%)**
MLV	1565 ± 29	7324 ± 134	2 %	1276 ± 23	5816 ± 107	2 %	1595 ± 28	7271 ± 127	2 %
MRV	1581 ± 27	7145 ± 123	2 %	1282 ± 22	5367 ± 91	2 %	1686 ± 32	7502 ± 143	2 %

LL	891 ± 22	3997 ± 99	2 %	981 ± 20	4125 ± 86	2 %	904 ± 22	3977 ± 96	2 %
RL	956 ± 23	4151 ± 100	2 %	950 ± 22	4071 ± 93	2 %	954 ± 21	4188 ± 91	2 %
BP	45 ± 24*	477 ± 253*	53 %	89 ± 24**	882 ± 239**	27 %	35 ± 27*	351 ± 270*	77 %
RBC	326 ± 25	955 ± 74	8 %	423 ± 29	1192 ± 83	7 %	325 ± 27	962 ± 80	8 %
Rumen	715 ± 22	4513 ± 141	3 %	370 ± 13	2989 ± 107	4 %	655 ± 16	5373 ± 130	2 %
RC	516 ± 10	4964 ± 100	2 %	340 ± 8	3611 ± 88	2 %	345 ± 9	6091 ± 155	3 %
Abomasum	1151 ± 22	6643 ± 125	2 %	720 ± 14	3458 ± 67	2 %	853 ± 15	3117 ± 54	2 %
Jejunum	2078 ± 31	9914 ± 148	1 %	1699 ± 26	7259 ± 113	2 %	1144 ± 18	4816 ± 75	2 %
Caecum	422 ± 13	2590 ± 80	3 %	336 ± 10	2482 ± 77	3 %	376 ± 10	2252 ± 62	3 %
Colon	475 ± 13	2746 ± 77	3 %	701 ± 15	3578 ± 75	2 %	1048 ± 19	4389 ± 79	2 %
ILN	1141 ± 38	4283 ± 144	3 %	1096 ± 43	4271 ± 167	4 %	854 ± 19	2605 ± 59	2 %
Liver	1287 ± 22	4195 ± 72	2 %	1241 ± 21	4159 ± 70	2 %	1276 ± 23	4323 ± 76	2 %
Pancreas	2402 ± 31	8563 ± 110	1 %	1997 ± 26	9265 ± 123	1 %	2290 ± 31	8761 ± 118	1 %
Diaphragm	1996 ± 30	7796 ± 119	2 %	1834 ± 27	7251 ± 108	1 %	2114 ± 30	8109 ± 114	1 %
Spleen	1210 ± 21	5485 ± 95	2 %	1161 ± 20	5125 ± 88	2 %	1323 ± 22	5723 ± 94	2 %
Adrenal	1263 ± 25	4582 ± 89	2 %	1280 ± 53	5634 ± 232	4 %	1329 ± 32	5232 ± 124	2 %
Kidney	2899 ± 37	14752 ± 189	1 %	3005 ± 36	13497 ± 163	1 %	2797 ± 36	13593 ± 177	1 %
Thyroid	733 ± 22	2631 ± 78	3 %	601 ± 21	2100 ± 75	4 %	680 ± 19	2266 ± 65	3 %
Ovary	nc			766 ± 42	4419 ± 245	6 %	959 ± 56	4962 ± 287	6 %
Fur	534 ± 44	974 ± 81	8 %	348 ± 66**	553 ± 105**	19 %	133 ± 83*	151 ± 95*	63 %
Skin	909 ± 32	3267 ± 114	3 %	784 ± 29	3054 ± 112	4 %	722 ± 46	2024 ± 130	6 %
Hoof	207 ± 18	262 ± 23	9 %	122 ± 25**	149 ± 30**	20 %	200 ± 26	257 ± 33	13 %
Antler (Tip)	470 ± 23	566 ± 28	5 %	282 ± 20	337 ± 25	7 %	365 ± 20	435 ± 23	5 %
Antler (Mid)	96 ± 10	114 ± 12	10 %	79 ± 10	93 ± 11	12 %	63 ± 13**	76 ± 16**	21 %
Tibia	46 ± 14**	51 ± 16**	31 %	39 ± 12**	44 ± 13**	30 %	51 ± 11**	56 ± 12**	22 %
Pelvis	314 ± 59**	486 ± 91**	19 %	198 ± 30**	266 ± 40**	15 %	390 ± 44	540 ± 61	11 %
Costal	195 ± 30**	256 ± 40**	16 %	285 ± 29	357 ± 36	10 %	259 ± 21	322 ± 27	8 %
LV	538 ± 23	751 ± 32	4 %	418 ± 21	597 ± 30	5 %	365 ± 23	523 ± 34	6 %
BM	90 ± 46*	112 ± 58*	52 %	28 ± 6**	34 ± 8**	23 %	27 ± 7**	32 ± 8**	25 %
HT	385 ± 14	1753 ± 62	4 %	410 ± 13	1985 ± 63	3 %	313 ± 11	1656 ± 61	4 %
BS	675 ± 15	2796 ± 62	2 %	895 ± 19	3117 ± 68	2 %	745 ± 21	2778 ± 78	3 %
Cerebellum	557 ± 20	2969 ± 108	4 %	606 ± 21	2555 ± 89	3 %	369 ± 10	1931 ± 52	3 %
Masseter	3205 ± 40	13063 ± 163	1 %	2486 ± 28	9698 ± 109	1 %	3053 ± 34	12222 ± 135	1 %
LD	1874 ± 27	7297 ± 106	1 %	2160 ± 27	8105 ± 103	1 %	1741 ± 24	6723 ± 91	1 %
QF	2012 ± 29	8483 ± 123	1 %	2039 ± 25	8151 ± 100	1 %	2118 ± 27	8546 ± 109	1 %
BB	2099 ± 30	9055 ± 128	1 %	2186 ± 29	8907 ± 120	1 %	2204 ± 30	9423 ± 126	1 %
Udder	1363 ± 20	4737 ± 69	1 %	1621 ± 21	5762 ± 76	1 %	1385 ± 20	4689 ± 68	1 %
Tongue	1395 ± 21	3287 ± 50	2 %	987 ± 19	1866 ± 35	2 %	1260 ± 21	2508 ± 41	2 %
Mandible	269 ± 14	305 ± 16	5 %	225 ± 15	260 ± 18	7 %	227 ± 14	260 ± 16	6 %
FT	nc			759 ± 14	4293 ± 80	2 %	757 ± 13	4296 ± 76	2 %
Cervix	nc			639 ± 13	2955 ± 59	2 %	671 ± 13	3265 ± 64	2 %
MT	189 ± 20	221 ± 23	10 %	129 ± 26**	149 ± 29**	20 %	197 ± 18	231 ± 21	9 %

Table B2: Determined ^{137}Cs Activity concentration from the additional seven reindeer heads. Given as Bq/kg ± SD on wet weight (w.w.) and dry weight (d.w.) basis. The SD reflects the total propagated uncertainty from the analysis. Samples that were <LoD are colored blue and marked with an asterisk. Samples that were <LoQ are colored purple and marked with a double asterisk.

Tissue	Bq/kg (w.w.)	Bq/kg (d.w.)	RSD (%)	
Mandible	262 ± 18	325 ± 23	7 %	D
Masseter	2234 ± 32	9197 ± 131	1 %	
Antler (Tip)	61 ± 10**	72 ± 12**	17 %	
Antler (Mid)	27 ± 11*	32 ± 13*	41 %	
Skin	458 ± 14	1427 ± 45	3 %	
MT	199 ± 19	230 ± 22	10 %	
Mandible	194 ± 16	240 ± 20	8 %	E
Masseter	1711 ± 24	7113 ± 99	1 %	
Antler (Tip)	57 ± 12**	67 ± 14**	22 %	
Antler (Mid)	37 ± 10**	44 ± 11**	26 %	
Skin	387 ± 13	1157 ± 37	3 %	
MT	204 ± 14	247 ± 17	7 %	
Mandible	298 ± 15	333 ± 16	5 %	F
Masseter	4883 ± 48	17966 ± 178	1 %	
Antler (Tip)	47 ± 10**	57 ± 12**	22 %	
Antler (Mid)	28 ± 10*	35 ± 13*	37 %	
Skin	1174 ± 27	3766 ± 85	2 %	
MT	245 ± 16	283 ± 19	7 %	
Mandible	293 ± 16	332 ± 18	5 %	G
Masseter	3377 ± 38	13281 ± 148	1 %	
Antler (Tip)	245 ± 19	303 ± 23	8 %	
Antler (Mid)	79 ± 10**	98 ± 13**	13 %	
Skin	807 ± 23	2577 ± 75	3 %	
MT	199 ± 14	233 ± 16	7 %	
Mandible	151 ± 12	170 ± 14	8 %	H
Masseter	2359 ± 27	9202 ± 105	1 %	
Antler (Tip)	97 ± 13**	117 ± 15**	13 %	
Antler (Mid)	66 ± 13**	80 ± 16**	20 %	
Skin	524 ± 30	1638 ± 95	6 %	
MT	143 ± 14	169 ± 17	10 %	

Mandible	121 ± 16**	141 ± 18**	13 %	I
Masseter	2057 ± 29	7750 ± 108	1 %	
Antler (Tip)	292 ± 22	357 ± 27	8 %	
Antler (Mid)	68 ± 11**	85 ± 13**	15 %	
Skin	467 ± 27	1497 ± 85	6 %	
MT	190 ± 19	236 ± 24	10 %	
Mandible	168 ± 15	193 ± 17	9 %	J
Masseter	3294 ± 37	12390 ± 138	1 %	
Antler (Tip)	144 ± 15	178 ± 19	11 %	
Antler (Mid)	71 ± 11**	83 ± 13**	15 %	
Skin	740 ± 28	2298 ± 88	4 %	
MT	166 ± 17	191 ± 20	10 %	

Table B3: Determined ^{210}Po activity concentrations from reindeer A, B and C. Given as Bq/kg ± SD on wet weight (w.w.) and dry weight (d.w.) basis, with the associated relative standard deviation (RSD) as a percentage. The SD reflects the total propagated uncertainty from the analysis. Samples that were <LoD are colored blue and marked with an asterisk.

	A			B			C		
Tissue	**Bq/kg (w.w.)**	**Bq/kg (d.w.)**	**RSD (%)**	**Bq/kg (w.w.)**	**Bq/kg (d.w.)**	**RSD (%)**	**Bq/kg (w.w.)**	**Bq/kg (d.w.)**	**RSD (%)**
MLV	5,7 ± 0,6*	27 ± 3*	11 %	12 ± 2	55 ± 8	14 %	7 ± 1	31 ± 6	20 %
MRV	6,9 ± 0,8*	31 ± 4*	11 %	14 ± 1	57 ± 6	10 %	19 ± 2*	84 ± 10*	12 %
LL	9 ± 1	42 ± 6	14 %	20 ± 4	84 ± 18	22 %	17 ± 3	73 ± 14	19 %
RL	9 ± 1	40 ± 4	11 %	29 ± 3	124 ± 11	9 %	22 ± 4	97 ± 18	19 %
BP	na			na			na		
RBC	27 ± 3*	79 ± 8*	11 %	23 ± 2*	65 ± 5*	8 %	18 ± 1	53 ± 4	8 %
Rumen	14 ± 1	88 ± 8	9 %	19 ± 2	155 ± 19	12 %	28 ± 4	234 ± 35	15 %
RC	59 ± 7	570 ± 66	12 %	28 ± 3	292 ± 31	11 %	66 ± 10	1165 ± 177	15 %
Fur (B)	56 ± 3	102 ± 6	6 %	66 ± 3	105 ± 5	4 %	73 ± 5	84 ± 6	7 %
Abomasum	13,7 ± 0,7	79 ± 4	5 %	84 ± 12	403 ± 56	14 %	18 ± 2	64 ± 8	12 %
Jejunum	29 ± 4	138 ± 17	13 %	29 ± 4	125 ± 17	13 %	19 ± 1	81 ± 4	5 %
Caecum	8,4 ± 0,6	52 ± 3	7 %	20 ± 3	148 ± 19	13 %	9 ± 0,5	54 ± 3	5 %
Colon	5,8 ± 0,5	33 ± 3	9 %	17 ± 2	85 ± 12	14 %	7,7 ± 0,8	32 ± 3	10 %
ILN	51 ± 5	193 ± 18	10 %	135 ± 18	525 ± 72	14 %	178 ± 13	543 ± 40	7 %
Liver	51 ± 4	166 ± 12	7 %	37 ± 4	123 ± 15	12 %	76 ± 6	259 ± 21	8 %
Pancreas	22 ± 2	77 ± 9	11 %	24 ± 3	110 ± 14	12 %	20 ± 2	78 ± 8	10 %

Diaphragm	6,2 ± 0,5	24 ± 2	8 %	10 ± 2	41 ± 6	16 %	6 ± 0,9	23 ± 3	15 %
Spleen	6,8 ± 0,9	31 ± 4	13 %	11 ± 2	48 ± 8	16 %	8,3 ± 0,6	36 ± 3	7 %
Adrenal	13 ± 1	49 ± 5	11 %	51 ± 7	224 ± 30	13 %	7,7 ± 0,7	30 ± 3	9 %
Kidney	66 ± 5	335 ± 25	7 %	59 ± 10	263 ± 44	17 %	68 ± 3	332 ± 14	4 %
Thyroid	53 ± 5	190 ± 17	9 %	62 ± 8	216 ± 29	13 %	55 ± 3	183 ± 9	5 %
Ovary	nc			13 ± 2	72 ± 14	19 %	13 ± 1	67 ± 6	9 %
Fur (A)	95 ± 14	174 ± 26	15 %	68 ± 11	109 ± 17	16 %	76 ± 8	86 ± 9	11 %
Skin	13 ± 1	47 ± 5	10 %	19 ± 3	75 ± 12	16 %	17 ± 2	47 ± 6	12 %
Hoof	113 ± 12	143 ± 15	11 %	108 ± 10	132 ± 12	9 %	135 ± 9	174 ± 12	7 %
Antler (Tip)	52 ± 6	62 ± 7	12 %	109 ± 14	128 ± 17	13 %	159 ± 16	191 ± 19	10 %
Antler (Mid)	132 ± 28	159 ± 34	21 %	158 ± 17	189 ± 20	11 %	na		
Tibia	359 ± 92	401 ± 103	26 %	331 ± 37	373 ± 42	11 %	522 ± 36	580 ± 40	7 %
Pelvis	179 ± 20	277 ± 30	11 %	425 ± 62	572 ± 84	15 %	849 ± 44	1177 ± 60	5 %
Costal	302 ± 40	398 ± 53	13 %	382 ± 57	479 ± 72	15 %	na		
LV	312 ± 40	435 ± 55	13 %	375 ± 40	536 ± 58	11 %	na		
BM	10 ± 2*	12 ± 2*	19 %	na			na		
HT	9 ± 1*	39 ± 6*	16 %	na			na		
BS	5,4 ± 0,7	22 ± 3	13 %	13 ± 2	47 ± 7	14 %	na		
Cerebellum	3 ± 0,4*	16 ± 2*	14 %	16 ± 2	67 ± 10	16 %	na		
Masseter	5,4 ± 0,7	22 ± 3	12 %	8 ± 1	30 ± 4	13 %	na		
LD	7 ± 1	26 ± 4	17 %	7,3 ± 0,8	28 ± 3	11 %	17 ± 1	66 ± 6	8 %
QF	4,5 ± 0,6*	19 ± 2*	13 %	na			24 ± 3	98 ± 10	11 %
BB	10 ± 1	42 ± 6	14 %	3,9 ± 0,4	16 ± 2	12 %	5,1 ± 0,5	22 ± 2	11 %
Udder	27 ± 3	93 ± 11	12 %	56 ± 8	201 ± 28	14 %	28 ± 3	95 ± 9	10 %
Tongue	4 ± 0,4*	9 ± 1*	10 %	na			4,8 ± 0,7*	10 ± 1*	14 %
Mandible	271 ± 37	308 ± 42	14 %	357 ± 47	411 ± 54	13 %	657 ± 29	751 ± 9	4 %
FT	nc			16 ± 2	92 ± 12	13 %	21 ± 3	121 ± 15	13 %
Cervix	nc			11 ± 1	49 ± 5	11 %	na		
MT	508 ± 93	593 ± 108	18 %	581 ± 68	670 ± 78	12 %	na		

Table B4: Replicate measurements from reindeer A for ^{210}Po-analysis. Given as Bq/kg ± SD on wet weight (w.w.) and dry weight (d.w.) basis, with the associated relative standard deviation (RSD) as a percentage. The SD reflects the total propagated uncertainty from the analysis

Tissue	Bq/kg (w.w.)	Bq/kg (d.w.)	RSD (%)
Liver	64 ± 7	208 ± 22	11 %
Fur (A)	56 ± 7	103 ± 14	13 %

Table B5: Replicate measurements from reindeer C for ^{210}Po-analysis. Given as Bq/kg ± SD on wet weight (w.w.) and dry weight (d.w.) basis with the associated relative standard deviation (RSD) as a percentage. The SD reflects the total propagated uncertainty from the analysis. Samples that were <LoD are colored blue and marked with an asterisk.

Tissue	Bq/kg (w.w.)	Bq/kg (d.w.)	RSD (%)
RC	2,3 ± 0,2	36 ± 3	9 %
ILN	163 ± 8	496 ± 25	5 %
Liver	76 ± 6	259 ± 21	8 %
Diaphragm	9 ± 2*	35 ± 7*	20 %

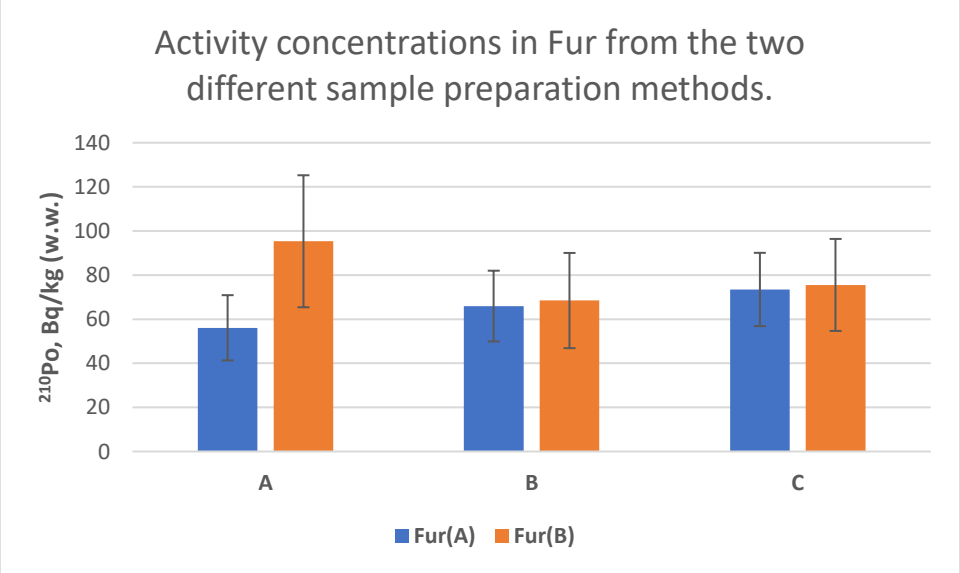

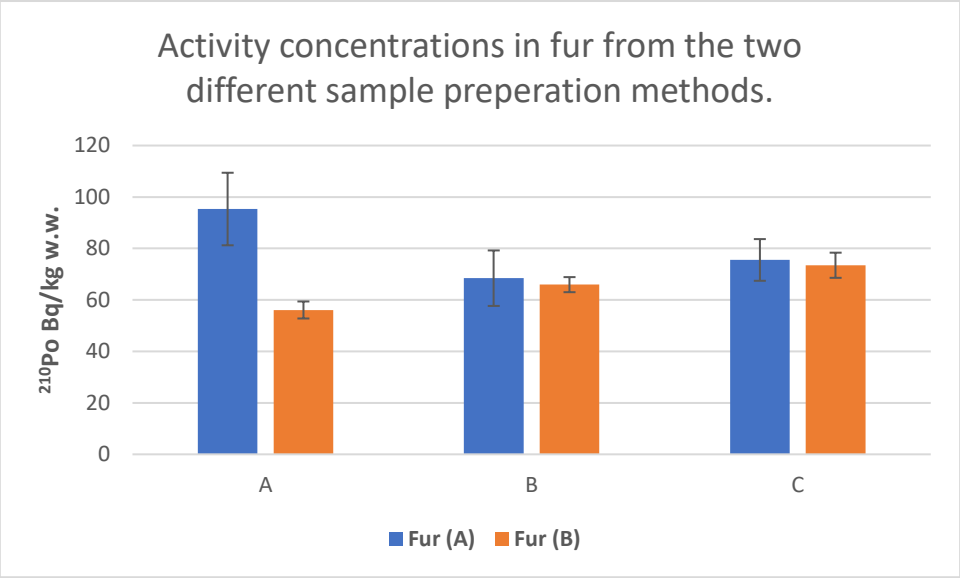

Figure B1: ^{210}Po activity concentrations in fur from the two different sample preparation methods in three semi-domesticated reindeer

APPENDIX C

This section contains data on live weights and biomass of tissue compartments, (table C1), as well as the estimated dry weight to wet weight ratio for each tissue sampled in this study, (table C2). Missing data on biomass and live weights were estimated from data found in literature, these are marked and elaborated in the table text.

Table C1: Reindeer weights measured in field, as well as estimated weights of missing data. *Estimated with data from (Staaland et al., 1979). **Estimated with data from (Ringberg et al., 1981a). ***Estimated with data from (Ringberg et al., 1981b), tibia was assumed to be the same weight as metatarsus. ****Estimated with data from (E. Wiklund et al., 2008). *****Estimated with data from (Gaare & Staaland, 1994) †Estimated based on data gathered in this study. ‡Estimated based on data gathered in this study, as well as data from (Ringberg et al., 1981b).

Reindeer	A	B	C
Live Weight	91.5	76.7**	90.3**
Carcass weight	44.9	39.3	46.3
Head with antlers	5.8	4.7	5
Hind and front legs	2.7	2.7	2.8
Hide with fur	5.4	5.3	5
GI tract with contents (without the esophagus)	13.4	12.477	16.9
Diaphragm	0.049	0.026	0.038

Masseter	0.040	0.030	0.029
ILN	0.0055	0.0057	0.0096
Heart	0.80	0.72	0.70
Lungs	0.95	1.1	0.87
Pancreas	0.042	0.032	0.032
Adrenal	0.0082	0.0029	0.0058
Thyroid	0.0077	0.0073	0.0092
Udder	0.62	0.67	0.69
Spleen	0.16	0.14	0.14
Liver	2.0	1.4	1.5
Kidney	0.26	0.23	0.25
Tongue	0.32	0.32	0.32
FT	nc	0.022	0.025
Cervix	nc	0.038	0.047
Ovary	nc	0.0034	0.0026
Uterus without ovaries	nc	0.060	0.071
Estimated weights			
GI tract*	4.8	4.1	4.9
Rumen*	2.6	2.2	2.6
Abomasum*	0.24	0.20	0.25
Jejunum*	1.0	0.87	1.1
Caecum*	0.18	0.16	0.19
Colon*	0.18	0.16	0.19
RC*	12.7	11.2	12.8
Brain**	0.36	0.31	0.36
MM***	30.8016	26.9712	31.7592
LD****	2.2	2.0	2.3
ST***	10.0	8.8	10.3
Tibia***	0.49	0.42	0.50
MT†	0.0086	0.0086	0.0086
Antlers*****	2.9	2.4	2.5
Hooves‡	1.6	1.7	1.7
Skin†	2.4	3.7	2.7
Fur†	3.0	1.7	2.3
RBC*****	2.4	2.0	2.4
BP*****	4.9	4.2	5.0

Table C2: Estimated DW/WW conversion factor, given as AM ± SD (RSD%) with number of sampled animals n.

For n=2, given as (min – max).

Tissue	DW/WW	n

MLV	2.17E-01 ± 3.32E-03 (1.52%)	3
MRV	2.28E-01 ± 9.36E-03 (4.10%)	3
LL	2.29E-01 ± 7.63E-03 (3.33%)	3
RL	2.30E-01 ± 2.81E-03 (1.22%)	3
BP	9.75E-02 ± 3.68E-03 (3.78%)	3
RBC	3.45E-01 ± 9.12E-03 (2.64%)	3
Rumen	1.35E-01 ± 2.06E-02 (15.33%)	3
RC	8.49E-02 ± 2.50E-02 (29.45%)	3
Abomasum	2.18E-01 ± 5.09E-02 (23.30%)	3
Jejunum	2.27E-01 ± 1.52E-02 (6.70%)	3
Caecum	1.55E-01 ± 1.72E-02 (11.09%)	3
Colon	2.03E-01 ± 3.34E-02 (16.49%)	3
ILN	2.84E-01 ± 3.87E-02 (13.66%)	3
Liver	3.00E-01 ± 5.96E-03 (1.99%)	3
Pancreas	2.52E-01 ± 3.34E-02 (13.21%)	3
Diaphragm	2.57E-01 ± 3.87E-03 (1.51%)	3
Spleen	2.26E-01 ± 5.36E-03 (2.37%)	3
Adrenal	2.52E-01 ± 2.42E-02 (9.61%)	3
Kidney	2.08E-01 ± 1.32E-02 (6.36%)	3
Thyroid	2.88E-01 ± 1.08E-02 (3.76%)	3
Ovarium	(1.73E-1 – 1.93E-1)	2
Fur	6.84E-01 ± 1.70E-01 (24.90%)	3
Skin	3.13E-01 ± 2.78E-02 (8.89%)	10
Hoof	7.94E-01 ± 2.08E-02 (2.62%)	3
Antler (Tip)	8.26E-01 ± 1.65E-02 (1.99%)	10
Antler (Mid)	8.34E-01 ± 2.09E-02 (2.51%)	10
Tibia	8.94E-01 ± 5.94E-03 (0.67%)	3
Pelvis	7.04E-01 ± 5.12E-02 (7.27%)	3
Costal	7.87E-01 ± 2.31E-02 (2.94%)	3
LV	7.05E-01 ± 9.84E-03 (1.39%)	3
BM	8.29E-01 ± 2.54E-02 (3.06%)	3
HT	2.05E-01 ± 1.53E-02 (7.49%)	3
BS	2.66E-01 ± 2.29E-02 (8.62%)	3
Cerebellum	2.05E-01 ± 2.76E-02 (13.45%)	3
Masseter	2.55E-01 ± 1.05E-02 (4.11%)	10
LD	2.61E-01 ± 5.10E-03 (1.96%)	3
QF	2.45E-01 ± 6.90E-03 (2.81%)	3
BB	2.37E-01 ± 7.32E-03 (3.09%)	3
Udder	2.88E-01 ± 6.98E-03 (2.42%)	3
Tongue	4.85E-01 ± 5.44E-02 (11.21%)	3
Mandible	8.63E-01 ± 3.17E-02 (3.67%)	10
FT	(1.76E-1 – 1.77E-01)	2
Cervix	(2.06E-1 – 2.16E-1)	2
MT	8.51E-01 ± 2.04E-02 (2.40%)	10

APPENDIX D

The following tables contain whole body to tissue concentration, $C_{Wb:t,}$ estimated with the method given (Yankovich et al., 2010).

Table D1: Estimated whole body to tissue concentration ratios with data from radionuclide analyses. Given as AM ± SD with the associated RSD (%), min – max and the number of data points (n).

$CR_{wb:t}$	^{137}Cs				^{210}Po			
	AM ± SD	RSD (%)	(min-max)	n	AM ± SD	RSD (%)	(min – max)	n
Rumen	1,8 ± 0,8	43 %	(1,3 - 2,7)	3	3,1 ± 0,2	6 %	(3 - 3,4)	3
Abomasum	1,1 ± 0,3	26 %	(0,8 - 1,4)	3	3 ± 2	77 %	(0,7 - 5,4)	3
Jejunum	0,6 ± 0,2	30 %	(0,5 - 0,8)	3	3 ± 2	68 %	(1,5 - 5)	3
Caecum	2,6 ± 0,4	15 %	(2,3 - 3)	3	6 ± 4	65 %	(2,8 - 10,7)	3
Colon	1,5 ± 0,6	38 %	(0,9 - 2)	3	7,7 ± 4,5	58 %	(3,4 - 12,4)	3
ILN	1 ± 0,1	14 %	(0,8 - 1,1)	3	0,6 ± 0,2	36 %	(0,4 - 0,8)	3
Liver	0,76 ± 0,04	6 %	(0,7 - 0,8)	3	1,2 ± 0,4	28 %	(0,9 - 1,5)	3
Kidney	0,334 ± 0,005	2 %	(0,3 - 0,3)	3	1 ± 0,4	37 %	(0,7 - 1,4)	3
Heart	0,7 ± 0,1	18 %	(0,6 - 0,8)	3	9 ± 7	73 %	(4,4 - 13,9)	2
Lungs	1,03 ± 0,02	2 %	(1 - 1)	3	4 ± 1	36 %	(2,3 - 5)	3
Spleen	0,79 ± 0,08	10 %	(0,7 - 0,9)	3	8 ± 3	44 %	(5,2 - 11,5)	3
RBC	2,7 ± 0,3	11 %	(2,4 - 2,9)	3	5 ± 1	0 %	(5,3 - 5,3)	1
Pancreas	0,44 ± 0,06	14 %	(0,4 - 0,5)	3	3 ± 2	73 %	(0,9 - 4,7)	3
Adrenal	0,75 ± 0,04	5 %	(0,7 - 0,8)	3	5,6 ± 6	108 %	(1,1 - 12,4)	3
Thyroid	1,6 ± 0,2	14 %	(1,3 - 1,7)	3	1,2 ± 0,5	44 %	(0,8 - 1,7)	3
Udder	0,67 ± 0,04	6 %	(0,6 - 0,7)	3	2 ± 1	62 %	(1 - 3,4)	3
Brain	1,8 ± 0,2	11 %	(1,6 - 2)	3	6 ± 3	49 %	(3,9 - 8)	2
FT	1,29 ± 0,06	5 %	(1,2 - 1,3)	2	4 ± 0,7	17 %	(3,5 - 4,5)	2
Cervix	1,5 ± 0,1	8 %	(1,4 - 1,6)	2	5 ± 2	0 %	(5,3 - 5,3)	1
Ovarium	1,2 ± 0,2	21 %	(1 - 1,3)	2	6 ± 2	34 %	(4,5 - 7,4)	2
Diaphragm	0,49 ± 0,05	11 %	(0,4 - 0,6)	3	9 ± 7	60 %	(5,5 - 16)	3
Masseter‡	0,34 ± 0,06	18 %	(0,3 - 0,4)	3	7,7 ± 0,3	4 %	(7,5 - 8)	2
LD	0,51 ± 0,04	7 %	(0,5 - 0,5)	3	7 ± 1	16 %	(5,6 - 7,7)	3

MM	0,473 ± 0,005	1 %	(0,5 - 0,5)	3	7 ± 2,6	36 %	(5,3 - 10,1)	3
Tongue	0,8 ± 0,2	22 %	(0,7 - 1)	3				
Tibia					0,16 ± 0,03	21 %	(0,1 - 0,2)	3
ST	2,9 ± 0,5	16 %	(2,4 - 3,3)	3	0,148 ± 0,006	4 %	(0,1 - 0,2)	3
MT	4,9 ± 0,2	3 %	(4,8 - 5)	2	0,091 ± 0,009	10 %	(0,1 - 0,1)	2
Antlers	4 ± 2	41 %	(2,6 - 5,6)	3	0,49 ± 0,09	18 %	(0,4 - 0,6)	3
Fur	1,78 ± 0,09	5 %	(1,8 - 1,8)	1	1 ± 0,3	29 %	(0,8 - 1,3)	3
Hoof	4,66 ± 0.09	2 %	(4,6 - 4,7)	2	0,5 ± 0,2	30 %	(0,4 - 0,7)	3
Skin	1,2 ± 0,1	12 %	(1 - 1,3)	3	4 ± 1	37 %	(3 - 5,7)	3

APPENDIX E

Internal dose coefficients (DC) obtained from BiotaDC software are presented in table E1.

Absorbed fractions utilized in organ dose estimation are given in table E2.

Table E1: Unweighted internal DCs obtained from BiotaDC (µGy/h per Bq/kg) for ^{137}Cs, ^{137m}Ba and ^{210}Po with the associated fraction of radiation type (f2/f3) utilized in dose estimation.

Tissue	^{137}Cs	f2	f3	^{137m}Ba	f2	f3	^{210}Po
Rumen	1.1E-04	9.1E-04	1.0E+00	1.0E-04	2.9E-03	1.0E+00	3.1E-03
Abomasum	1.1E-04	9.1E-04	1.0E+00	6.8E-05	4.4E-03	1.0E+00	3.1E-03
Jejunum	1.1E-04	9.1E-04	1.0E+00	8.7E-05	3.4E-03	1.0E+00	3.1E-03
Caecum	1.1E-04	9.1E-04	1.0E+00	6.5E-05	4.5E-03	1.0E+00	3.1E-03
Colon	1.1E-04	9.1E-04	1.0E+00	6.5E-05	4.5E-03	1.0E+00	3.1E-03
Diaphragm	1.1E-04	9.2E-04	1.0E+00	5.3E-05	5.6E-03	9.9E-01	3.1E-03
Masseter	1.1E-04	9.2E-04	1.0E+00	5.2E-05	5.7E-03	9.9E-01	3.1E-03
LD	1.1E-04	9.1E-04	1.0E+00	1.0E-04	2.9E-03	1.0E+00	3.1E-03
MM	1.1E-04	9.1E-04	1.0E+00	1.7E-04	1.7E-03	1.0E+00	3.1E-03
ILN	1.1E-04	9.3E-04	1.0E+00	4.4E-05	6.7E-03	9.9E-01	3.1E-03
Heart	1.1E-04	9.11E-04	1.0E+00	8.2E-05	3.6E-03	1.0E+00	3.1E-03
Lungs	1.1E-04	9.1E-04	1.0E+00	8.6E-05	3.4E-03	1.0E+00	3.1E-03

Pancreas	1.1E-04	9.2E-04	1.0E+00	5.2E-05	5.6E-03	9.9E-01	3.1E-03
Adrenal	1.1E-04	9.4E-04	1.0E+00	4.3E-05	6.8E-03	9.9E-01	3.1E-03
Thyroid	1.1E-04	9.3E-04	1.0E+00	4.5E-05	6.6E-03	9.9E-01	3.1E-03
Udder	1.1E-04	9.1E-04	1.0E+00	8.1E-05	3.7E-03	1.0E+00	3.1E-03
Spleen	1.1E-04	9.2E-04	1.0E+00	6.3E-05	4.7E-03	1.0E+00	3.1E-03
Liver	1.1E-04	9.1E-04	1.0E+00	9.5E-05	3.1E-03	1.0E+00	3.1E-03
Kidney	1.1E-04	9.1E-04	1.0E+00	6.8E-05	4.3E-03	1.0E+00	3.1E-03
Tongue	1.1E-04	9.1E-04	1.0E+00	7.1E-05	4.1E-03	1.0E+00	3.1E-03
Brain	1.1E-04	9.1E-04	1.0E+00	7.2E-05	4.1E-03	1.0E+00	3.1E-03
Uterus	1.1E-04	9.2E-04	1.0E+00	5.6E-05	5.2E-03	9.9E-01	3.1E-03
FT	1.1E-04	9.2E-04	1.0E+00	5.0E-05	5.9E-03	9.9E-01	3.1E-03
Cervix	1.1E-04	9.2E-04	1.0E+00	5.3E-05	5.5E-03	9.9E-01	3.1E-03
Ovarium	1.1E-04	9.2E-04	1.0E+00	5.6E-05	5.2E-03	9.9E-01	3.1E-03
Tibia	1.1E-04	9.1E-04	1.0E+00	7.1E-05	4.1E-03	1.0E+00	3.1E-03
ST	1.1E-04	9.1E-04	1.0E+00	1.4E-04	2.1E-03	1.0E+00	3.1E-03
Antler	1.1E-04	9.1E-04	1.0E+00	1.0E-04	2.8E-03	1.0E+00	3.1E-03
MT	1.1E-04	9.3E-04	1.0E+00	4.5E-05	6.5E-03	9.9E-01	3.1E-03
Fur	1.1E-04	9.1E-04	1.0E+00	1.0E-04	2.9E-03	1.0E+00	3.1E-03
Hoof	1.1E-04	9.1E-04	1.0E+00	7.5E-05	3.9E-03	1.0E+00	3.1E-03
Skin	1.1E-04	9.1E-04	1.0E+00	1.1E-04	2.8E-03	1.0E+00	3.1E-03
RBC	1.1E-04	9.1E-04	1.0E+00	1.0E-04	2.9E-03	1.0E+00	3.1E-03

Table E2: Absorbed fractions utilized in organ dose estimations. Based on data given by Ulanovsky et al.,, (Ulanovsky & Pröhl, 2006), 0.5 MeV and 1 MeV electrons (β) as well as 0,03 MeV and 0.5 MeV photons (γ). Alpha-particles were assumed to be 1.

Mass (Kg)	**β (MeV)**		**γ (MeV)**	
	0,5	**1**	**0.03**	**0,5**
1E-06	0,21	0,0082	6E-03	9E-04
1E-05	0,52	0,19	1E-02	3E-03

1E-04	0,76	0,47	3E-02	6E-03
1E-03	0,89	0,73	6E-02	1E-02
1E-02	0,95	0,87	1E-01	3E-02
1E-01	0,97	0,94	3E-01	7E-02
1E+00	0,99	0,97	5E-01	2E-01
1E+01	0,99	0,99	7E-01	3E-01
1E+02	1	0,99	9E-01	5E-01
1E+03	1	1	9E-01	8E-01

Table E3: Unweighted absorbed dose rates for ^{137}Cs, ^{137m}Ba and ^{210}Po respectively for the three semi-domesticated reindeer, given as µGy/h. The dose rates are multiplied by the absorbed fractions given by Ulanovsky et al., (Ulanovsky & Pröhl, 2006) with its associated radiation type.

µGy/h	^{137}Cs			^{137m}Ba			^{210}Po		
	A	**B**	**C**	**A**	**B**	**C**	**A**	**B**	**C**
Rumen	7,5E-02	3,9E-02	6,9E-02	1E-02	6E-03	1E-02	4,4E-02	6,0E-02	8,9E-02
Abomasum	1,2E-01	7,2E-02	8,6E-02	5E-03	3E-03	4E-03	4,3E-02	2,6E-01	5,5E-02
Jejunum	2,2E-01	1,8E-01	1,2E-01	3E-02	2E-02	2E-02	9,0E-02	9,2E-02	6,0E-02
Caecum	4,2E-02	3,4E-02	3,8E-02	2E-03	2E-03	2E-03	2,6E-02	6,3E-02	2,8E-02
Colon	4,8E-02	7,0E-02	1,1E-01	2E-03	3E-03	5E-03	1,8E-02	5,2E-02	2,4E-02
ILN	8,7E-02	8,4E-02	6,6E-02	7E-04	7E-04	5E-04	1,6E-01	4,2E-01	5,6E-01
Liver	1,3E-01	1,3E-01	1,3E-01	2E-02	2E-02	2E-02	1,6E-01	1,1E-01	2,4E-01
Kidney	2,9E-01	3,1E-01	2,8E-01	1E-02	1E-02	1E-02	2,1E-01	1,8E-01	2,1E-01
Heart	1,6E-01	1,3E-01	1,6E-01	9E-03	7E-03	9E-03		4,3E-02	2,1E-02
Lungs	1,0E-01	1,0E-01	1,0E-01	6E-03	6E-03	6E-03	2,9E-02	7,6E-02	6,9E-02
Spleen	1,2E-01	1,2E-01	1,3E-01	5E-03	5E-03	6E-03	2,1E-02	3,4E-02	2,6E-02
RBC	3,4E-02	4,4E-02	3,4E-02	5E-03	7E-03	5E-03			5,6E-02
Brain	5,5E-02	6,5E-02	4,8E-02	3E-03	3E-03	2E-03	1,7E-02	4,5E-02	0,0E+00
FT		7,0E-02	7,0E-02		1E-03	1E-03		5,1E-02	6,7E-02
Cervix		6,0E-02	6,3E-02		1E-03	1E-03		3,3E-02	
Ovarium		7,1E-02	8,9E-02		6E-04	8E-04		3,9E-02	4,0E-02
Diaphragm	2,1E-01	1,9E-01	2,2E-01	3E-03	3E-03	4E-03	1,9E-02	3,2E-02	1,9E-02
Masseter	3,3E-01	2,6E-01	3,2E-01	5E-03	4E-03	5E-03	1,7E-02	2,4E-02	
LD	2,0E-01	2,3E-01	1,8E-01	3E-02	3E-02	3E-02	2,1E-02	2,3E-02	5,3E-02
MM	2,1E-01	2,3E-01	2,2E-01	1E-01	1E-01	1E-01	2,6E-02	1,7E-02	4,8E-02
Tongue	1,4E-01	1,0E-01	1,3E-01	7E-03	5E-03	6E-03			
Tibia							1,1E+00	1,0E+00	1,6E+00
ST	4,2E-02	3,2E-02	3,2E-02	8E-03	6E-03	6E-03	8,9E-01	1,2E+00	2,1E+00
MT	1,5E-02		1,5E-02	1E-04		1E-04	1,6E+00	1,8E+00	
Antlers	3,0E-02	1,9E-02	3,8E-02	4E-03	3E-03	6E-03	2,9E-01	4,2E-01	5,0E-01
Fur	5,6E-02			8E-03			3,0E-01	2,1E-01	2,4E-01
Hoof	2,1E-02		2,0E-02	5E-03		4E-03	3,5E-01	3,4E-01	4,2E-01
Skin	9,5E-02	8,2E-02	7,6E-02	1E-02	1E-02	1E-02	4,1E-02	6,0E-02	5,2E-02

APPENDIX F

This section contains absorbed organ dose rates unweighted for radiation quality

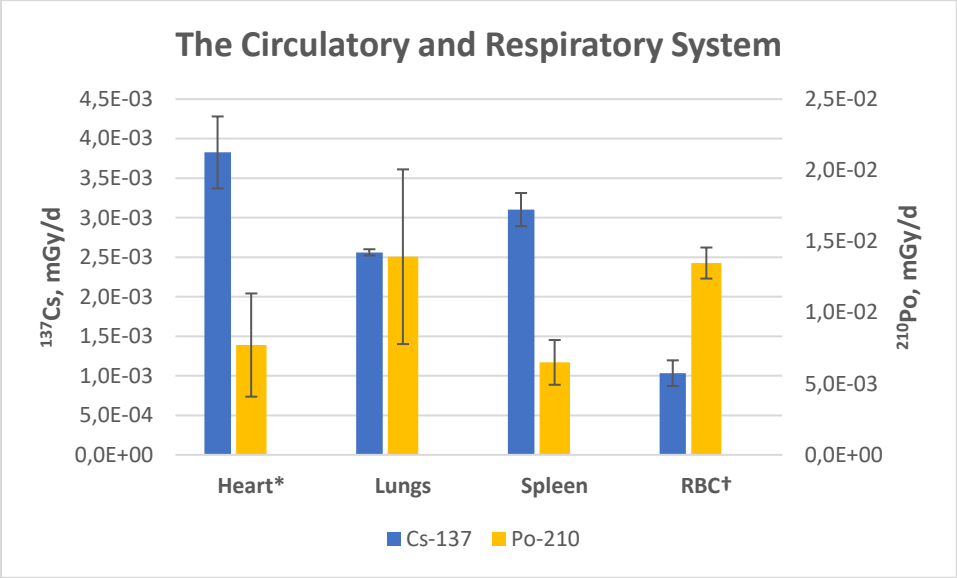

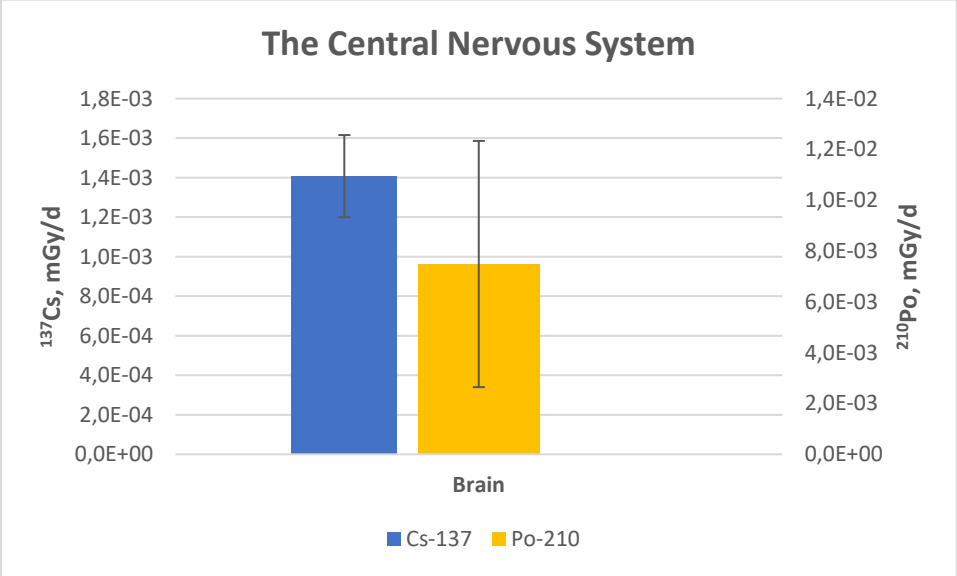

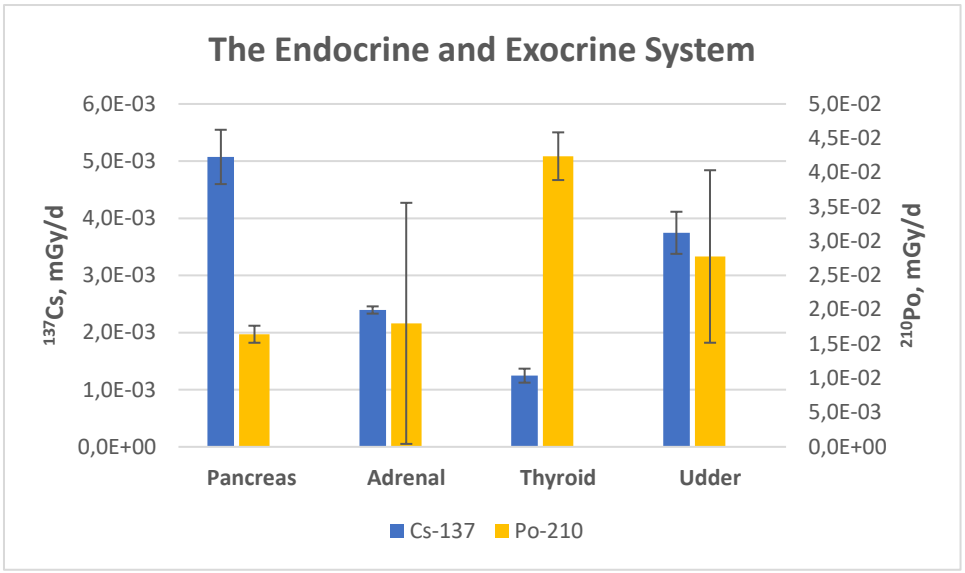
The Endocrine and Exocrine System
6,0E-03
5,0E-03
4,0E-03
3,0E-03
2,0E-03
1,0E-03
0,0E+00
137Cs, mGy/d
5,0E-02
4,5E-02
4,0E-02
3,5E-02
3,0E-02
2,5E-02
2,0E-02
1,5E-02
1,0E-02
5,0E-03
0,0E+00
210Po, mGy/d
Pancreas
Adrenal
Thyroid
Udder
Cs-137
Po-210

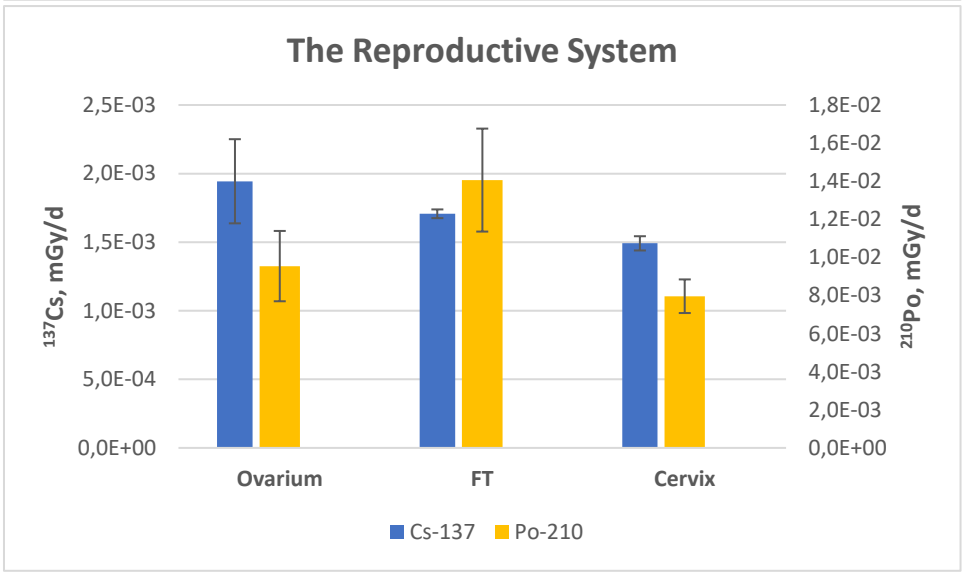
The Reproductive System
2,5E-03
2,0E-03
1,5E-03
1,0E-03
5,0E-04
0,0E+00
137Cs, mGy/d
1,8E-02
1,6E-02
1,4E-02
1,2E-02
1,0E-02
8,0E-03
6,0E-03
4,0E-03
2,0E-03
0,0E+00
210Po, mGy/d
Ovarium
FT
Cervix
Cs-137
Po-210

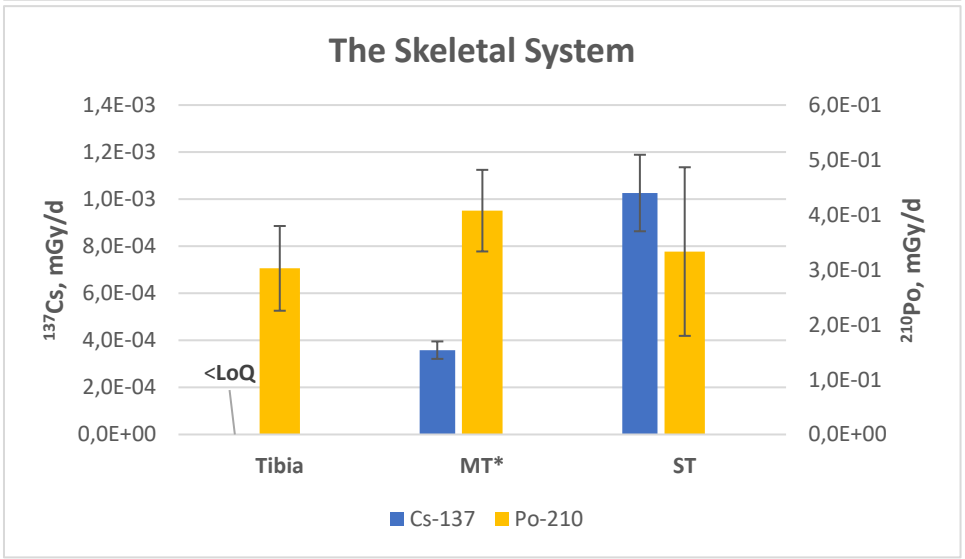
The Skeletal System
1,4E-03
1,2E-03
1,0E-03
8,0E-04
6,0E-04
4,0E-04
2,0E-04
0,0E+00
137Cs, mGy/d
6,0E-01
5,0E-01
4,0E-01
3,0E-01
2,0E-01
1,0E-01
0,0E+00
210Po, mGy/d
<LoQ
Tibia
MT*
ST
Cs-137
Po-210

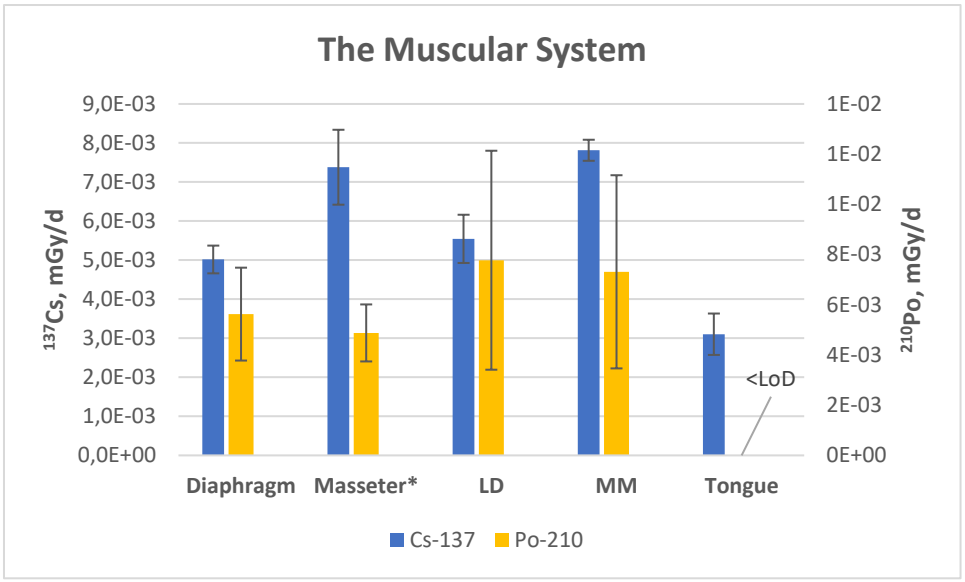
The Muscular System
9,0E-03
8,0E-03
7,0E-03
6,0E-03
5,0E-03
4,0E-03
3,0E-03
2,0E-03
1,0E-03
0,0E+00
137Cs, mGy/d
1E-02
1E-02
1E-02
8E-03
6E-03
4E-03
2E-03
0E+00
210Po, mGy/d
<LoD
Diaphragm
Masseter*
LD
MM
Tongue
Cs-137
Po-210

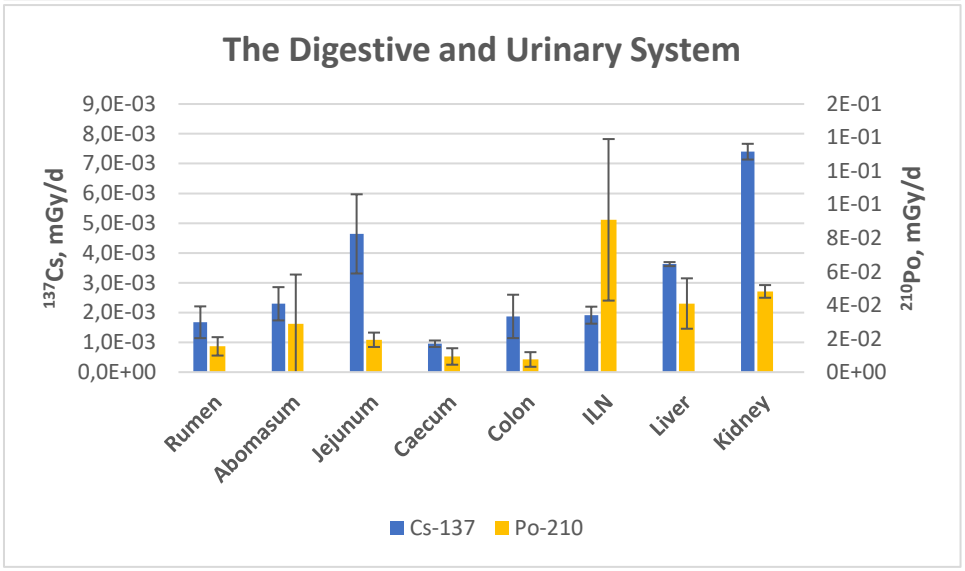
The Digestive and Urinary System
9,0E-03
8,0E-03
7,0E-03
6,0E-03
5,0E-03
4,0E-03
3,0E-03
2,0E-03
1,0E-03
0,0E+00
137Cs, mGy/d
2E-01
1E-01
1E-01
1E-01
8E-02
6E-02
4E-02
2E-02
0E+00
210Po, mGy/d
Rumen
Abomasum
Jejunum
Caecum
Colon
ILN
Liver
Kidney
Cs-137
Po-210

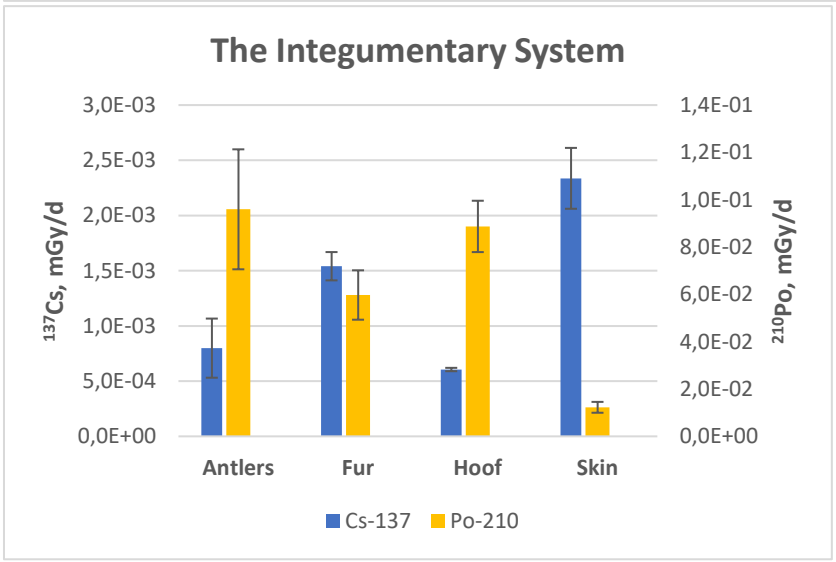
The Integumentary System
3,0E-03
2,5E-03
2,0E-03
1,5E-03
1,0E-03
5,0E-04
0,0E+00
137Cs, mGy/d
1,4E-01
1,2E-01
1,0E-01
8,0E-02
6,0E-02
4,0E-02
2,0E-02
0,0E+00
210Po, mGy/d
Antlers
Fur
Hoof
Skin
Cs-137
Po-210

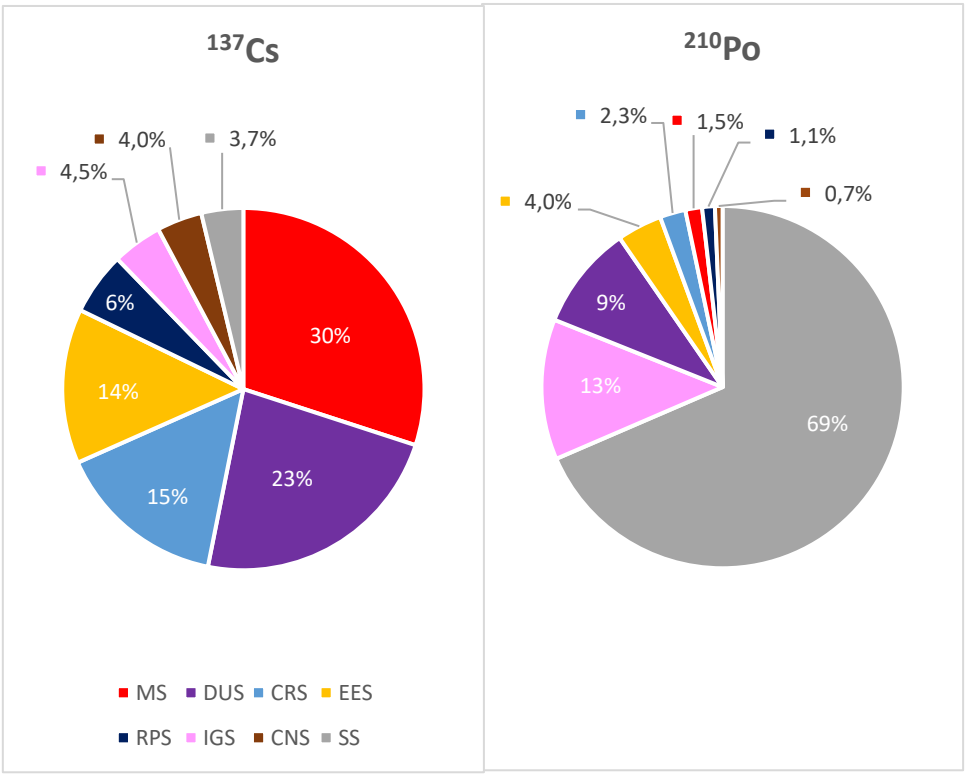

Figure E10: Pie chart showing the relative accumulation of ^{137}Cs and ^{210}Po, respectively, between various organ systems in semi-domesticated reindeer. The legend applies to both pie charts.

APPENDIX G

In this section a comparison of in vivo measurements done by the DSA and measurements done in this study of three semi-domesticated reindeer. Activity concentrations from muscular tissue associated with meat consumption, (QF, BB and LD), were averaged and abbreviated as meat. Measurements done by the DSA were abbreviated as DSAMeat.

Table D3: Comparison of measurements done in the field by DSA, 19.09.2019 Vågå, and in this study of the three semi-domesticated reindeer.

Reindeer	A	B	C
DSAMeat	1270	1760	1750
Meat	1995	2128	2021

Meat/DSAMeat	1.6	1.2	1.2

Table D4: Data on external doses from the same herd with data given by (Aramrun et al., 2019).

Integrated dose over 11 months		
	uGy	SD
Cs-137	103	93
K-40	47	19
Th232	9	6
U-238	15	9
Cosmic radiation	297	40
Total mean external absorbed dose	471	104
Estimated dose rates		
	uGy/h	SD
Cs-137	1.28E-02	1.16E-02
K-40	5.85E-03	2.36E-03
Th232	1.12E-03	7.47E-04
U-238	1.87E-03	1.12E-03
Cosmic radiation	3.70E-02	4.98E-03
Total mean external absorbed dose	5.86E-02	1.29E-02

Coefficient to relate internal Cs-137 contamination to the dosimeter:

0.028 nGy per Bq/kg

(Aramrun et al., 2019)

Norges miljø- og biovitenskapelige universitet
Noregs miljø- og biovitskapelege universitet
Norwegian University of Life Sciences

Postboks 5003
NO-1432 Ås
Norway